INTERNATIONAL HYDROLOGICAL PROGRAMME

Environmental isotopes in the hydrological cycle

Principles and applications

Edited by
W.G. Mook

Volume III

Surface water

by
Kazimierz Rozanski
University of Mining and Mettalurgy, Krakow, Poland
Klaus Froehlich
(previously) IAEA, Vienna, Austria
Willem G. Mook
Groningen University, Groningen, The Netherlands

IHP-V | Technical Documents in Hydrology | No. 39, Vol. III
UNESCO, Paris, 2001

United Nations Educational,
Scientific and Cultural Organization

International Atomic Energy Agency

(SC-2001/WS/38)

UNESCO/IAEA Series on

Environmental Isotopes in the Hydrological Cycle
Principles and Applications

÷

Volume I	**Introduction: Theory, Methods, Review**
Volume II	**Atmospheric Water**
Volume III	**Surface Water**
Volume IV	**Groundwater: Saturated and Unsaturated Zone**
Volume V	**Man's Impact on Groundwater Systems**
Volume VI	**Modelling**

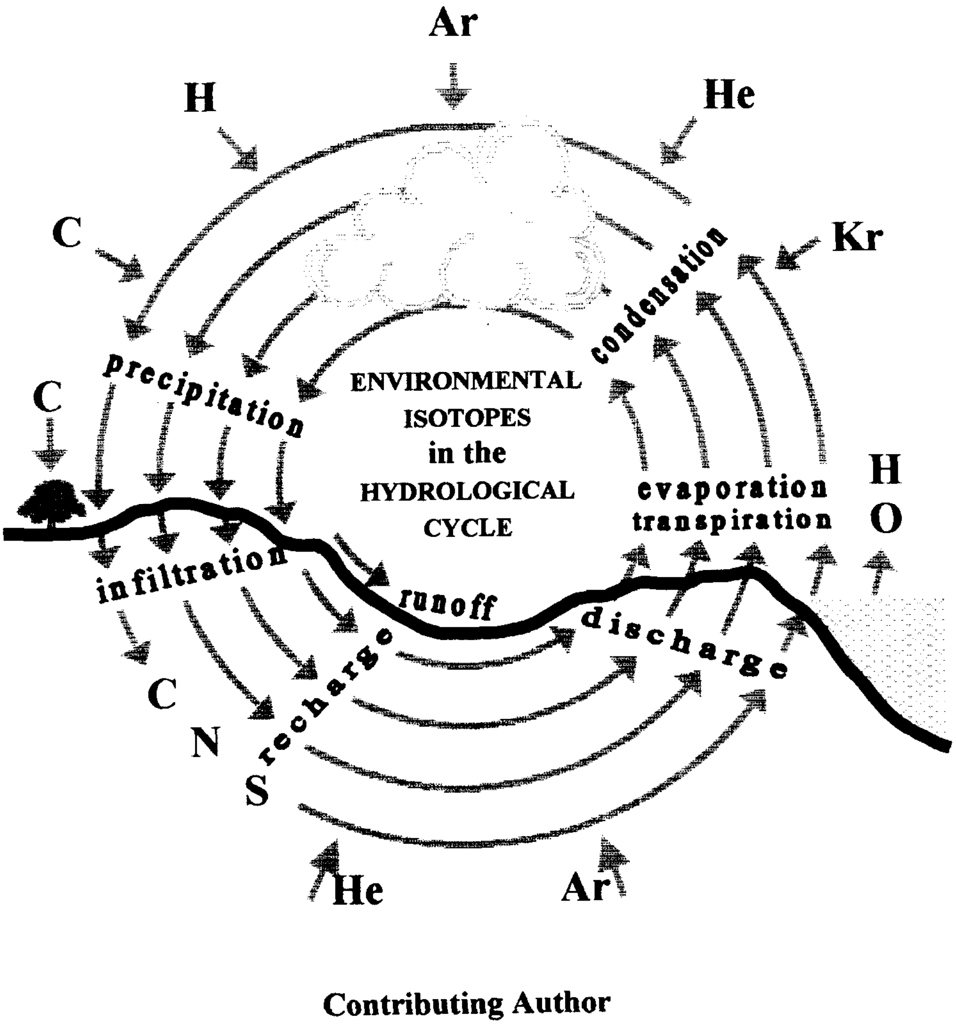

Contributing Author

W. Stichler, GSF-Institute of Hydrology, Neuherberg, Germany

PREFACE

The availability of freshwater is one of the great issues facing mankind today - in some ways the greatest, because problems associated with it affect the lives of many millions of people. It has consequently attracted a wide scale international attention of UN Agencies and related international/regional governmental and non-governmental organisations. The rapid growth of population coupled to steady increase in water requirements for agricultural and industrial development have imposed severe stress on the available freshwater resources in terms of both the quantity and quality, requiring consistent and careful assessment and management of water resources for their sustainable development.

More and better water can not be acquired without the continuation and extension of hydrological research. In this respect has the development and practical implementation of isotope methodologies in water resources assessment and management been part of the IAEA's programme in nuclear applications over the last four decades. Isotope studies applied to a wide spectrum of hydrological problems related to both surface and groundwater resources as well as environmental studies in hydro-ecological systems are presently an established scientific discipline, often referred to as "Isotope Hydrology". The IAEA contributed to this development through direct support to research and training, and to the verification of isotope methodologies through field projects implemented in Member States.

The world-wide programme of the International Hydrological Decade (1965-1974) and the subsequent long-term International Hydrological Programme (IHP) of UNESCO have been an essential part of the well recognised international frameworks for scientific research, education and training in the field of hydrology. The International Atomic Energy Agency (IAEA) and UNESCO have established a close co-operation within the framework of both the earlier IHD and the ongoing IHP in the specific aspects of scientific and methodological developments related to water resources that are of mutual interest to the programmes of both organisations.

The first benchmark publication on isotope hydrology entitled "Guidebook on Nuclear Techniques in Hydrology" was realised in 1983 through the activity of the joint IAEA/UNESCO Working Group on Nuclear Techniques established within the framework of IHP, and it has been widely used as practical guidance material in this specific field.

In view of the fact that the IHP's objectives include also a multi-disciplinary approach to the assessment and rational management of water resources and taking note of the advances made in isotope hydrology, the IAEA and UNESCO have initiated a joint activity in preparation of a series of six up-to-date textbooks, covering the entire field of hydrological applications of natural isotopes (environmental isotopes) to the overall domain of water resources and related environmental studies.

The main aim of this series is to provide a comprehensive review of basic theoretical concepts and principles of isotope hydrology methodologies and their practical applications with some illustrative examples. The volumes are designed to be self-sufficient reference material for scientists and engineers involved in research and/or practical applications of isotope hydrology as an integral part of the investigations related to water resources assessment, development and management. Furthermore, they are also expected to serve as "Teaching Material" or text books to be used in universities and teaching institutions for incorporating the study of "isotopes in water" in general into the curriculum of the earth sciences. Additionally the contents can fulfil the need for basic knowledge in other disciplines of the Earth Sciences dealing with water in general.

These six volumes have been prepared through efforts and contributions of a number of scientists involved in this specific field as cited in each volume, under the guidance and co-ordination of the main author/co-ordinating editor designated for each volume. W.G.Mook (Netherlands), J.Gat (Israel), K.Rozanski (Poland), M.Geyh (Germany), K.P.Seiler (Germany) and Y.Yurtsever (IAEA, Vienna) were involved as the main author/co-ordinating editors in preparation of these six volumes, respectively. Final editorial work on all volumes aiming to achieve consistency in the contents and layout throughout the whole series was undertaken by W.G.Mook (Netherlands).

Mr.Y. Yurtsever, Staff Member of the Isotope Hydrology Section of the IAEA; and Ms. A. Aureli, Programme Specialist, Division of Water Sciences of UNESCO, were the Scientific Officers in charge of co-ordination and providing scientific secretariat to the various meetings and activities that were undertaken throughout the preparation of these publications.

The IAEA and UNESCO thank all those who have contributed to the preparation of these volumes and fully acknowledge the efforts and achievements of the main authors and co-ordinating editors.

It is hoped that these six volumes will contribute to wider scale applications of isotope methodologies for improved assessment and management of water resources, facilitate incorporation of isotope hydrology into the curricula of teaching and education in water sciences and also foster further developments in this specific field.

Paris / Vienna, March 2000

PREFACE TO VOLUME III

The third volume in the series of textbooks on the environmental isotopes in the hydrological cycle deals with surface water. From man’s perspective, this is perhaps the most visible and most accessible part of the global hydrological cycle. Indeed, development of human civilisation over the past millennia was always intimately linked to availability of water; civilisations flourished and died in the rhythm of climatic cycles controlling availability and abundance of freshwater in many parts of the world.

The industrialised world brought new dimensions into ever-persisting relationship between man and water. Particularly this century saw dramatic impact of man’s activities on surface water systems in a form of massive and widespread pollution of these systems with numerous pollutants of various nature: organic compounds, heavy metals, oil products, agrochemicals, etc. In many instances natural cleaning capacities of those systems were surpassed with the resulting conversion of numerous rives and lakes into biologically dead sewage channels and reservoirs. Although growing concern has led in many parts of the world to gradual control of this impact, pollution of surface water systems still remains one of the central problems related to management of global water resources.

This series of 6 volumes are meant to be in first instance textbooks helping young people to apply environmental isotope methodologies in addressing various practical problems related to the hydrological cycle. Practical approach was adopted also throughout Volume III. Three core chapters of this volume (Chapter 2, 3 and 4) deal with rivers, estuaries and lake systems, respectively. Systematic presentation of possibilities offered by various isotope tracers in addressing questions related to the dynamics of surface water systems, their interaction with groundwater and vulnerability to pollution is pursued throughout those two chapters. Practical hints and suggestions are given how to carry on environmental isotope investigation. The volume closes with an outlook to future of surface water systems in the light of anticipated global warming induced by greenhouse gases.

Krakow, Vienna, Groningen

K. Rozanski
K. Froehlich
W. G. Mook

CONTENTS

2 RIVERS

1 BASIC CONCEPTS AND MODELS

1.1 INTRODUCTION

This Volume III in the series of textbooks is focused on applications of environmental isotopes in surface water hydrology. The term *environmental* means that the scope of this series and the Volume III is essentially limited to isotopes, both stable and radioactive, that are present in the natural environment, either as a result of natural processes or introduced by anthropogenic activities. Artificial isotopes and/or chemical substances, that are intentionally released in order to obtain information about a studied system, will be mentioned only marginally.

Generally, isotopes are applied in hydrology either as ***tracers*** or as ***age indicators***. An ideal tracer is defined as *a substance that behaves in the studied system exactly as the material to be traced as far as the sought parameters are concerned, but that has at least one property that distinguishes it from the traced material* (Zuber, 1986).

Using stable isotopes as tracers, this property is the molecular mass difference between the substance and its tracer. The radioactive decay of radioisotopes also offers the possibility to determine the residence time of water in a system, which, under given conditions, is called the age or transit time (see also Sect.1.4).

In Volume I the characteristics and natural occurrence of the environmental isotopes is discussed in detail. Here we present a brief summary.

In nature, there exist two stable isotopes of hydrogen (^{1}H - protium and ^{2}H - deuterium) and three stable isotopes of oxygen (^{16}O, ^{17}O, ^{18}O). Out of nine isotopically different water molecules, only three occur in nature in easily detectable concentrations: $H_2{}^{16}O$, $H_2{}^{18}O$ and $^1H^2H^{16}O$. The isotopic concentration or abundance ratios are generally referred to those of a specifically chosen standard. The internationally accepted standard for reporting the hydrogen and oxygen isotopic ratios of water is Vienna Standard Mean Ocean Water, V-SMOW (Coplen, 1996). The absolute isotopic ratios ^{2}H/^{1}H and ^{18}O/^{16}O of V-SMOW were found to be equal to

$$^2H/^1H = (155.95 \pm 0.08)\times10^{-6} \quad \text{(De Wit et al., 1980)}$$

$$^{18}O/^{16}O = (2005.20 \pm 0.45)\times10^{-6} \quad \text{(Baertschi, 1976)}$$

These values are close to the average isotopic composition of ocean water given by Craig (1961a; b). Since the ocean represents about 97% of the total water inventory on the earth's surface and the observed variations of $^2H/^1H$ and $^{18}O/^{16}O$ within the water cycle are relatively small, the heavy isotope content of water samples is usually expressed in delta (δ) values defined as the relative deviation from the adopted standard representing mean isotopic composition of the global ocean:

$$\delta_{S/R} = \frac{R_{Sample}}{R_{Reference}} - 1 \qquad \textbf{(1.1)}$$

where R_{Sample} and $R_{Reference}$ stands for the isotope ratio ($^2R = {}^2H/^1H$ and $^{18}R = {}^{18}O/^{16}O$) in the sample and the reference material (standard), respectively.

We will use the following symbols, applying the superscripts as in ^2H, ^{18}O and ^{13}C:

$$^2\delta \ (\equiv \delta^2H \equiv \delta D) = {}^2R_S/{}^2R_R - 1$$

$$^{18}\delta \ (\equiv \delta^{18}O) = {}^{18}R_S/{}^{18}R_R - 1$$

$$^{13}\delta \ (\equiv \delta^{13}C) = {}^{13}R_S/{}^{13}R_R - 1$$

As the thus defined δ values are small numbers, they are expressed in ‰ (per mill). It should be emphasised, however, that also then the δ values remain small numbers, because ‰ stands for $\times 10^{-3}$.

^2H and ^{18}O isotopic compositions of meteoric waters (precipitation, atmospheric water vapour) are strongly correlated. If $^2\delta$ is plotted versus $^{18}\delta$, the data cluster along a straight line:

$$^2\delta = 8 \cdot {}^{18}\delta + 10‰$$

This line is referred to as the *Global Meteoric Water Line* (Craig, 1961b).

The observed variations of ^2H and ^{18}O content in natural waters are closely related to the isotope fractionation occurring during evaporation and condensation (freezing) of water, where the heavy water molecules, $H_2{}^{18}O$ and $^1H^2H^{16}O$, preferentially remain in or pass into the liquid (solid) phase, respectively. This isotopic differentiation is commonly described by the fractionation factor α, which can be defined as the ratio of the two isotope ratios:

$$\alpha_{B/A} = \frac{R_B}{R_A} \qquad \textbf{(1.2)}$$

expresses the isotope ratio in phase B relative to that in phase A. If B refers to liquid water and A to water vapour in thermodynamic equilibrium, the fractionation factor α_e corresponds to the ratio of the saturation vapour pressure of normal water (H_2O) to that of "heavy" water ($^1H^2HO$ or $H_2{}^{18}O$).

Since in general isotope effects are small ($\alpha \approx 1$), the deviation of α from 1 is often used rather than α. This quantity is called isotope fractionation and defined by:

$$\varepsilon_{B/A} = \alpha_{B/A} - 1 = \frac{R_B}{R_A} - 1 \qquad \textbf{(1.3)}$$

ε is referred to as an enrichment if $\varepsilon > 0$ ($\alpha > 1$), and as a depletion if $\varepsilon < 0$ ($\alpha < 1$); generally ε values are reported in ‰, being small numbers.

Also for α and ε we apply the same superscripts:

$$^{2}\alpha_{B/A} = {}^{2}R_B/{}^{2}R_A = {}^{2}\varepsilon + 1 \text{ and } {}^{18}\alpha_{B/A} = {}^{18}R_B/{}^{18}R_A = {}^{18}\varepsilon + 1.$$

1.2 ISOTOPE EFFECTS BY EVAPORATION

Under natural conditions, thermodynamic equilibrium between liquid and vapour phase is not always established, for instance during evaporation of an open water body into an unsaturated atmosphere. In this case, slight differences in transfer of light and heavy water molecules through a viscous boundary layer at the water-air interface result in additional isotopic fractionation denoted by the so-called *kinetic fractionation factor*, α_k. This kinetic fractionation factor is controlled by molecular diffusion of the isotopically different water molecules through air, the moisture deficit (1 – h) over the evaporating surface and, to a lesser extent, by the status of the evaporating surface (Merlivat and Coantic, 1975; Merlivat and Jouzel, 1979).

The model generally adopted to describe isotope effects accompanying evaporation into an open (unsaturated) atmosphere was formulated by Craig and Gordon (1965). Its schematic description is presented in Fig.1.1. In the framework of this conceptual model, the isotopic composition of the net evaporation flux can be derived as a function of environmental parameters controlling the evaporation process (see Volume II for detailed discussion):

$$\delta_E = \frac{\alpha_{V/L}\delta_L - h_N\,\delta_A + \varepsilon_{V/L} + \varepsilon_{diff}}{1 - h_N - \varepsilon_{diff}} \qquad \textbf{(1.4)}$$

where:

δ_L	isotopic composition of the lake water
h_N	relative humidity of the atmosphere over the lake, normalised to the temperature of the lake surface
δ_A	isotopic composition of the free-atmosphere water vapour over the lake
$\alpha_{V/L}$	equilibrium isotope fractionation factor between water vapour (V) and liquid water (L), at the temperature of the lake surface
$\varepsilon_{V/L}$	$= \alpha_{V/L} - 1$ (< 0)
ε_{diff}	transport (kinetic) or diffusion fractionation $= n\,\Theta\,(1 - h)\,\Delta_{diff}$ (see Volume II).

The overall fractionation by evaporation is now: $\varepsilon_{tot} = \varepsilon_{V/L} + \varepsilon_{diff}$. All ε values are negative, as the fractionation processes cause an ^{18}O depletion of the escaping water vapour.

The α values for kinetic or transport isotope processes are defined as the "new" isotopic ratio relative to (= divided by) the "old": $\alpha_{after/before} = R_{after}/R_{before}$. For the diffusion process this means that the (kinetic) fractionation factor $\alpha_{after/before\ diffusion} < 1$, as the isotopically heavy gas diffuses more slowly. The kinetic fractionation $\varepsilon = \alpha - 1$ is then negative.

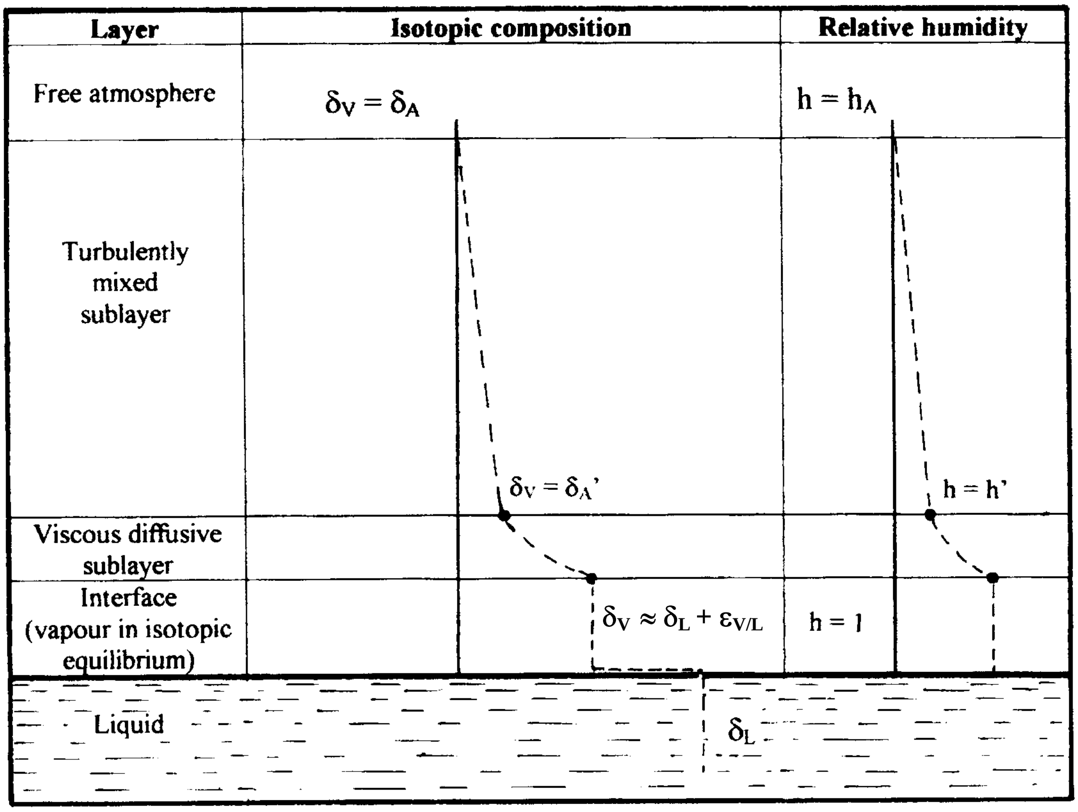

Fig.1.1 The Craig-Gordon model for isotopic fractionation during evaporation of open water body into the free atmosphere (Craig and Gordon, 1965). The boundary region between evaporating surface and free atmosphere is subdivided into several layers: (i) the interface located immediately above the evaporating surface, where isotope equilibrium is maintained between liquid and vapour phase, (ii) the viscous diffusive sublayer where molecular transport is dominating, introducing additional kinetic fractionation among various isotopic species of water vapour, and (iii) the turbulently mixed sublayer where no further isotope differentiation occurs. Schematic profiles of relative humidity and isotopic composition of water vapour across the boundary region are shown (modified from Gat, 1966).

Summarising, in the total (overall) process the first stage –the formation of water vapour in isotopic equilibrium with the water –causes isotopic depletion of the vapour with respect to the water by a fractionation $\varepsilon_{V/L}$ being negative. Also the second stage –the (partial) diffusion of vapour out of the diffusive sub-layer to the free atmosphere– causes the escaping vapour to become depleted in ^{2}H and ^{18}O by $\Delta\varepsilon$ also being negative.

ε_{diff} represents the kinetic, i.e. the diffusion part of the overall fractionation process and has the following general expression in the framework of the Craig-Gordon model (see Volume II):

$$\varepsilon_{diff} = n\,\Theta\,(1 - h)\,(1 - D_m/D_{mi}) = n\,\Theta\,(1 - h)\,\Delta_{diff} \qquad \textbf{(1.5)}$$

where Δ_{diff} presents the maximum diffusion isotope depletion of ^2H and ^{18}O in the case of a fully developed diffusive sub-layer (h = 0, Θ = 1, n = 1), which values are equal –25.1‰ for ^2H and –28.5‰ for ^{18}O (Merlivat, 1978), while the factor n varies: $0.5 \le n \le 1$. The weighting factor Θ can be assumed to be equal 1 for small water bodies whose evaporation flux does not significantly perturb the ambient moisture (cf. Volume II and Sect.3.2.1.3.4 of this volume for further discussion). For an open water body, a value of n = 0.5 seems to be most appropriate. This has been confirmed by wind-tunnel experiments (Vogt, 1978), where the following ε_{diff} values were obtained:

For ^2H: $\varepsilon_{diff} = -12.5^6(1 - h_N)$ ‰

For ^{18}O: $\varepsilon_{diff} = -14.2^4(1 - h_N)$ ‰

The temperature dependence of the equilibrium fractionation factors α for ^2H and ^{18}O of liquid water with respect to water vapour has been well established experimentally and can be calculated from (Majoube, 1971):

For ^{18}O:

$$\ln{}^{18}\alpha_{V/L} = -\ln{}^{18}\alpha_{L/V} = 2.0667\cdot 10^{-3} + \frac{0.4156}{T} - \frac{1.137\cdot 10^3}{T^2} \qquad \textbf{(1.6)}$$

For ^{2}H:

$$\ln{}^{2}\alpha_{V/L} = -\ln{}^{2}\alpha_{L/V} = -52.612\cdot 10^{-3} + \frac{76.248}{T} - \frac{24.844\cdot 10^3}{T^2} \qquad \textbf{(1.7)}$$

where T stands for the absolute water temperature in [K]. The above equations are valid for the temperature range 273.15 to 373.15 K (0°C – 100°C). More recent determinations of equilibrium fractionation factors between water and water vapour (Horita and Wesolowski, 1994) essentially confirm the validity of Eqs.1.6 and 1.7 for the above-mentioned temperature range. Table 1.1 contains numerical values of the equilibrium fractionation factors calculated according to Eqs.1.6 and 1.7 for the temperature range of 0 to 30 °C.

The relative humidity above the lake is usually reported with respect to air temperature. To normalise this quantity to the temperature of the lake surface the following equation can be used:

$$h_N = h\,\frac{p_{SAT(air)}}{p_{SAT(water)}} \qquad \textbf{(1.8)}$$

where $p_{SAT(air)}$ and $p_{SAT(water)}$ indicate saturation vapour pressure with respect to air and water temperature, respectively, h and h_N are the measured in ambient air and normalised relative humidity, respectively.

The saturation vapour pressure can be calculated from the empirical equation (e.g. Ward and Elliot, 1995):

$$p_{SAT} = \exp\left(\frac{16.78\,T - 116.9}{T + 237.3}\right) \text{ [kPa]} \tag{1.9}$$

where T is the air temperature expressed in degrees Celsius. Eq.1.9 is valid for temperatures ranging from 0 to 50^{o}C.

Table 1.1 Equilibrium fractionation factors $\alpha_{L/V}$ of liquid water relative to water vapour (Majoube, 1971), and the saturation vapour pressure p_{SAT} over liquid water (Ward and Elliot, 1995), as a function of the water temperature.

t (°C)	**$^{18}\alpha_{L/V}$**	**$^{2}\alpha_{L/V}$**	**p_{SAT} (hPa)**	**t (°C)**	**$^{18}\alpha_{L/V}$**	**$^{2}\alpha_{L/V}$**	**p_{SAT} (hPa)**
0	1.01173	1.11255	6.110	**16**	1.01015	1.09006	18.192
1	1.01162	1.11099	6.570	**17**	1.01007	1.08882	19.388
2	1.01152	1.10944	7.059	**18**	1.00998	1.08760	20.651
3	1.01141	1.10792	7.581	**19**	1.00989	1.08639	21.986
4	1.01131	1.10642	8.136	**20**	1.00980	1.08520	23.396
5	1.01121	1.10495	8.727	**21**	1.00972	1.08403	24.884
6	1.01111	1.10349	9.355	**22**	1.00963	1.08288	26.455
7	1.01101	1.10206	10.023	**23**	1.00955	1.08174	28.111
8	1.01091	1.10065	10.732	**24**	1.00946	1.08061	29.857
9	1.01081	1.09926	11.486	**25**	1.00938	1.07951	31.697
10	1.01071	1.09788	12.285	**26**	1.00930	1.07841	33.635
11	1.01062	1.09653	13.133	**27**	1.00922	1.07734	35.676
12	1.01052	1.09520	14.032	**28**	1.00914	1.07627	37.823
13	1.01043	1.09389	14.985	**29**	1.00906	1.07523	40.083
14	1.01034	1.09259	15.994	**30**	1.00898	1.07419	42.458
15	1.01025	1.09132	17.062				

The isotopic composition of atmospheric moisture over a lake, δ_A, can be directly measured in samples of atmospheric moisture collected over the studied lake system, estimated from the available isotope data for local precipitation or derived from evaporation-pan data. The approach based on the isotopic composition of local precipitation was shown to provide reasonable results for relatively small lake systems that do not significantly influence the moisture content in the local atmosphere above the lake (cf. Sect.3.2.1.3.3). In the majority of situations, the isotopic composition of monthly rainfall appears to be in isotopic equilibrium with atmospheric moisture at the ground-level temperature (Schoch-Fischer et al., 1984; Jacob and Sonntag, 1991). Thus, having information about the isotopic composition of local precipitation close to the lake, one can back-calculate the isotopic composition of atmospheric moisture:

$$\delta_A = \alpha_{V/L}\delta_P + \varepsilon_{V/L} \approx \delta_P + \varepsilon_{V/L} \qquad \mathbf{(1.10)}$$

where δ_P is the mean isotopic composition of local precipitation and $\alpha_{V/L}$ is the equilibrium fractionation factor between water vapour and liquid (the first with respect to the second) calculated from Eqs.1.6 or 1.7 for the corresponding mean local ground-level temperature.

As the evaporation process continues, the isotopic composition of an evaporating water body (δ_L) and the net evaporation flux (δ_E) define a ($^2\delta$,$^{18}\delta$) relation, that is called *evaporation line*. The slope S of this line is given by the following equation:

$$S = \frac{h_N(^2\delta_A - {}^2\delta_L) - {}^2\varepsilon_{tot}}{h_N(^{18}\delta_A - {}^{18}\delta_L) - {}^{18}\varepsilon_{tot}} \qquad \mathbf{(1.11)}$$

where $\varepsilon_{tot} = \varepsilon_{V/L} + \varepsilon_{diff}$ and the superscripts refer to ^{2}H and ^{18}O, respectively.

The initial isotopic composition of the water, the evaporated moisture, and the residual water must all plot on the same straight line because of mass balance considerations (cf. Fig.3.2b). The slope of the evaporation line is determined by the air humidity and the equilibrium and kinetic fractionations, both depending on temperature and boundary conditions.

1.3 ISOTOPE INPUT TO SURFACE WATER SYSTEMS

The observed spatial and temporal variability of the isotopic composition of precipitation stems from physical processes operating on both micro- and macro-scales. Whereas the equilibrium and kinetic isotope fractionation effects play a decisive role during phase transitions and diffusion-controlled transport, respectively, the Rayleigh mechanism contributes to the observed isotope variability during transport in macro-scale (see Vol. II).

The relationship between the isotopic composition of precipitation (input) and newly formed groundwater and surface runoff (output) is build upon processes that differentiate between rain events on a meteorological or seasonal basis, and processes that fractionate between the different isotopic water species, primarily evaporation (Gat and Tzur, 1967). These processes having the collective name of *catchment isotope effect* may encompass a wide range of temporal and spatial scales. Some occur during or immediately after the rain event on or above the ground surface. Others involve soil moisture or shallow water reservoirs. It is worth to note that the catchment effect for any given area may vary in time due to both natural (climate) and man-induced changes (Gat and Lister, 1995).

Fig.1.2 shows schematically the compartments and flow pattern across the atmosphere - land surface - soil zone interface, contributing to formation of the isotopic composition of input to surface water and groundwater systems. The residence time of water in the surface reservoirs depicted schematically in Fig.1.2 varies between minutes (the canopy) to many years in case of large lakes.

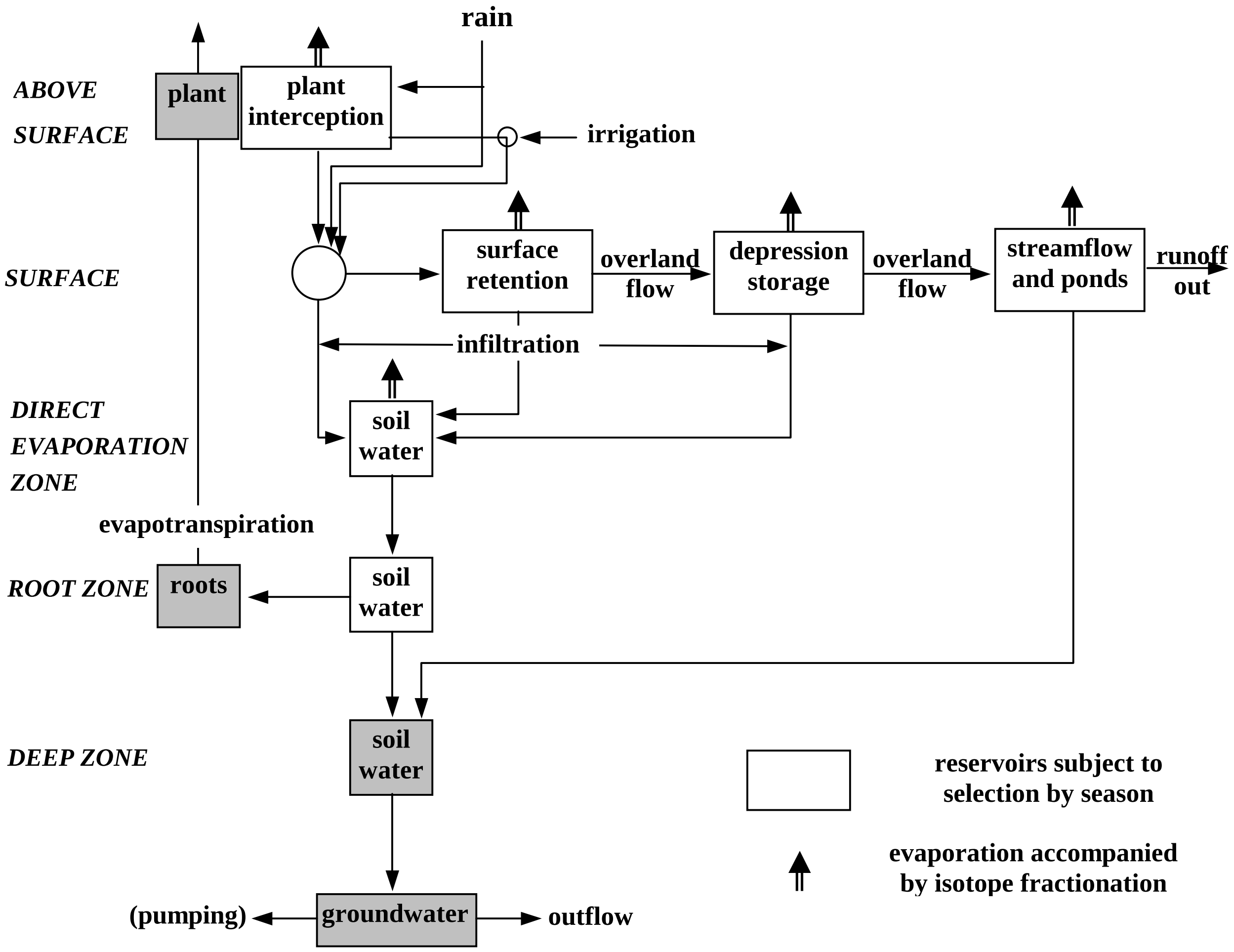

Fig.1.2 Flow patterns and processes accompanying transformation of precipitation to runoff and newly formed groundwater. Reservoirs subject to selection by season are shown as rectangular boxes. Double arrows indicate fluxes subject to isotope fractionation (cf. Volume II).

1.4 MEAN TRANSIT TIME, MIXING RELATIONSHIPS

When studying the dynamics of water flow in catchments or in surface reservoirs and lakes one often uses the term *mean transit time* or *turnover time* to describe how much time the water molecules spent in the given system before leaving it via outflow or evaporation flux. The turnover time is defined for a hydrological system which is in a steady state (e.g. Nir and Lewis, 1975; Zuber, 1986):

$$T = V_m/Q \tag{1.12}$$

where Q is the volumetric flow rate through the system and V_m is the volume of mobile water in the system. The assumption of steady state requires that V_m = const.

When a tracer is applied to obtain information about a given system, careful analysis has to be carried out with respect to the relation between the mean transit time of a tracer and that of water in the studied system, depending on the injection-detection mode and the behaviour of the tracer in the system (cf. Volume VI, see also Zuber, 1986).

In problems related to interaction of river or lake water with groundwater, or in problems related to hydrograph separation, one often deals with a mixture of two (or more) waters having different isotopic signatures. For instance, evaporated lake water mixing with local infiltration water in the adjacent groundwater system. From the mass balance considerations, the isotopic composition of the mixture can be easily derived if the end-members are fully characterised:

$$\delta_{MIX} = \frac{M_1}{M}\cdot\delta_1 + \frac{M_2}{M}\cdot\delta_2 + \ldots\ldots\ldots\ldots \frac{M_N}{M}\cdot\delta_N \tag{1.13}$$

where M_1 .... M_N are the contributions of the individual end-members to the total mass (flux) M of the system, whereas δ_1....δ_N are their respective isotopic compositions.

If plotted as $^{2}\delta$ versus $^{18}\delta$, the two-component mixtures will fall on a straight line connecting the isotopic signatures of the end-members. However, it has to be noted that mixtures of two components that have different isotope ratios (e.g. $^{13}C/^{12}C$ or $^{15}N/^{14}N$) and different concentrations of the element in question (e.g. C or N) do not form straight lines if plotted in diagrams with co-ordinates of isotope ratios (δ values) versus concentration (see, for instance, Sect.3.2.2). In such cases, linear relations could be obtained if plotting the isotope content versus the inverse of the respective concentration, e.g. $^{15}\delta$ versus 1 / (nitrate concentration), where

$$^{15}\delta = \frac{(^{15}N/^{14}N)_{nitrate}}{(^{15}N/^{14}N)_{air\,standard}} - 1$$

2 RIVERS

2.1 HYDROLOGICAL ASPECTS

2.1.1 THE GLOBAL HYDROLOGICAL CYCLE

The word *river* stands for a surface flow in a channel; *stream* emphasises the fact of flow and is synonymous with river; it is often preferred in technical writing. Small natural watercourses are sometimes called *rivulets,* but a variety of names - including *branch, brook, burn,* and *creek* - are also used.

Rivers are fed by precipitation, by direct overland runoff, through springs and seepage, or from meltwater at the edges of snowfields and glaciers. The contribution of direct precipitation on the water surface *–channel precipitation-* is usually minute, except where much of a catchment area is occupied by lakes. River water losses result from seepage and percolation into adjacent aquifers and particularly from evaporation. The difference between the water input and loss sustains surface discharge or stream flow.

The amount of water in river systems at any time is but a tiny fraction of the Earth's total water (Table 2.1). The oceans contain 97 percent of all water and about three-quarters of fresh water is stored as land ice; nearly all the remainder occurs as groundwater. Water in river channels accounts for only about 0.004 percent of the Earth's total fresh water. It should be noted that the values of the parameters listed in Tables 2.1 and 2.2 result from global estimates with varying degrees of uncertainty. Therefore, they may slightly differ from values given in literature.

Water is constantly cycled through the systems of land ice, soil, lakes, groundwater (in part), and river channels. Over the oceans, evaporation exceeds precipitation, and the net difference represents transport of water vapour over land, where it precipitates as rain and returned to the oceans as river runoff and direct groundwater discharge. About 30% of this precipitation runs off to the oceans in rivers, while direct groundwater discharge to the oceans amounts to only 6% of the total discharge. A small part of the precipitation is temporarily stored in lakes and rivers.

Considering the present-day hydrologic cycle (Fig.2.1), about 496 000 km^3 of water evaporates from the ocean (423 000 km^3) and land surface (73 000 km^3) annually. Using the values of the net evaporation (precipitation) flux and the volume of atmospheric vapour given in Fig.2.1, the *mean turnover time* of the atmospheric vapour is about 10 days. - In this context *the mean turnover time* is related to the reservoir and is defined as the amount of water in a reservoir divided by either the rate of addition of water to the reservoir or the rate of loss from it. - About 30% of the precipitation falling on land runs off to the oceans primarily in rivers while direct groundwater discharge to the oceans accounts only about 6% of the total discharge. A small part of precipitation is temporarily stored in the waters of rivers and lakes.

Table 2.1 Water masses at the Earth's surface (adopted from Berner and Berner, 1987).

Reservoir	**VOLUME** (in 10^6 km^3)
Oceans	1370
Ice caps and glaciers	29
Deep groundwater (750- 4000 metres)	5.3
Shallow groundwater (<750 metres)	4.2
Lakes	0.125
Soil moisture	0.065
Atmosphere	0.013
Rivers	0.0017
Biosphere	0.0006
TOTAL	**1408.7**

The various reservoirs in the hydrologic cycle have different (reservoir) turnover times. The large amount of water in the oceans makes their turnover time accordingly long; with the data given in Fig.2.1, a value of 3240 years is estimated. The mean turnover times of the other reservoirs of the hydrologic cycle (lakes, rivers, ice and groundwater) are between this value and the one of atmospheric water vapour.

The bases for comparing the world's great rivers include the size of the drainage area, the length of the main stem, and the mean discharge. Ranking in Table 2.2 is by drainage area. The global average of the external runoff (last column in Table 2.2) is about $0.01 m^3/s/km^2$. Great rivers with notably higher discharges are fed either by the convectional rains of equatorial regions or by monsoon rains that are usually increased by altitudinal effects. The Huang Ho (not shown in Table 2.2) averages 0.046, the Amazon 0.026 and the Ganges-Brahmaputra 0.024 $m^3/s/km^2$.

Table 2.2 The world's main rivers, ranked according to drainage area.

River	Drainage area 10^3 km^2	Length km	Mean discharge 10^3 m^3/s	m^3/s/km^2
Amazon	7 050	6 400	180	0.0255
Paraná	4 144	4 880	22	0.0052
Congo	3 457	4 700	41	0.0121
Nile	3 349	6 650	3	0.0009
Mississippi-Missouri	3 221	6 020	18	0.0057
Ob-Irtysh	2 975	5 410	15	0.0053
Yenissey	2 580	5 540	19	0.0073
Lena	2 490	4 400	16	0.0065
Yangtze	1 959	6 300	34	0.0174
Niger	1 890	4 200	6	0.0032
Amur	1 855	2 824	12	0.0066
Mackenzie	1 841	4 241	11	0.0061
Ganges-Brahmaputra	1 621	2 897	38	0.0237
St.Lawrence-G.Lakes	1 463	4 000	10	0.0069
Volga	1 360	3 530	8	0.0058
Zambezi	1 330	3 500	7	0.0053
Indus	1 166	2 900	5	0.0047
Tigris-Euphrates	1 114	2 800	1	0.0012
Nelson	1 072	2 575	2	0.0021
Murray-Darling	1 057	3 780	0.4	0.0003
Orinoco	948	2140	20	0.0210
Tocantins	906	2 699	10	0.0112
Danube	816	2 850	7	0.0088
Columbia	668	2 000	7	0.0104
Rio Grande	445	1 360	0.08	0.0001
Rhine	160	1 392	2	0.0137
Rhône	96	800	2	0.0177
Thames	10	340	0.08	0.0082

Among great rivers with mean discharges near or not far below world averages per unit area are those of Siberia, the Mackenzie, and the Yukon, all affected by low precipitation for which low evaporation rates barely compensate. The basins of the Mississippi, Niger, and Zambezi include some areas of dry climate, and the Nile, Murray-Darling, and Tigris-Euphrates experience low precipitation combined with high evaporation losses.

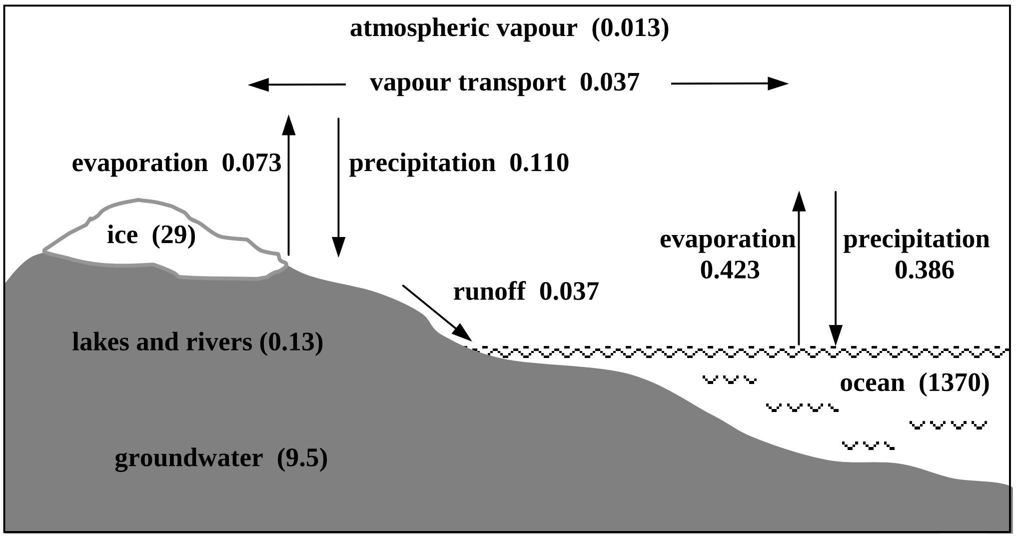

Fig.2.1 The hydrological cycle. The numbers in parentheses refer to volumes of water in 10^6 km^3, and the fluxes adjacent to the arrows are in 10^6 km^3 of water per year (adopted from Berner and Berner, 1987).

2.1.2 TEMPORAL VARIATIONS OF RIVER DISCHARGE

The temporal variations in the discharge of rivers can be classified in two groups: inter-annual variations and annual (seasonal) variations. The inter-annual variation in the discharge of many rivers and river systems are governed by climatic changes and by such climate phenomena as the *El Niño-Southern Oscillation* (ENSO). Simpson et al. (1993) have demonstrated the latter influence through studies of the River Murray and its most extensive tributary, the Darling River system. Its annual natural discharge is often inversely related to sea surface temperature (SST) anomalies in the eastern tropical Pacific Ocean. These SST variations are correlated with ENSO. The Darling and Murray river historical discharge values indicate that annual surface runoff from regions dominated by subtropical summer monsoon precipitation and annual surface runoff primarily responding to temperate winter storms, are both strongly influenced by ENSO cycles.

A prominent example of a well-established association between the El Niño phenomenon and the inter-annual variations of the river flow is the Nile river. The East African monsoon is the main rainfall-producing mechanism over the Blue Nile catchment and provides the teleconnection between El Niño and the Blue Nile flow. During the flood season, from July to October, most of the water in the main Nile is supplied by the Blue Nile. A warm SST in the Pacific ocean is associated with less rainfall over Ethiopia and drought conditions in the river flow of the Blue Nile and that of the main Nile (Eltahir, 1996; Amarasekera et al., 1997).

The seasonal variation in the discharge defines the regime of a river. Three broad classes can be distinguished for perennial streams.

1) The *megathermal* regimes are related to hot equatorial and tropical climates and occur in two main variants: (i) discharge is powerfully sustained throughout the year with a double or strong single maximum corresponding to heavy seasonal rainfall, or with slight warm-season minima; (ii) stream flow decreases markedly and may cease altogether in the warm half of the year (dry summers in mid-latitude climates).

2) The *microthermal* regimes are controlled by seasonal release of meltwater. There are winter minima and summer maxima resulting from snowmelt and convectional rain. Alternatively, spring meltwater maxima are accompanied by secondary fall maxima that are associated with late season thunder rain, or spring snowmelt maxima can be followed by a summer glacier-melt maximum, as on the Amu-Darya.

3) The *mesothermal* regimes can vary considerably along the length of a river. For example, October seasonal peak on the upper Niger becomes a December peak on the middle river; the swing from tropical-rainy through steppe climate reduces the volume by 25 percent through a 483-km stretch. The seasonal headwater flood wave travels at 0.09 metre per second, taking some four months over 2011 kilometres, but earlier seasonal peaks are re-established on the lower river by tributaries fed by hot-season rains. The great Siberian rivers, flowing northward into regions of increasingly deferred thaw, habitually cause extensive flooding in their lower reaches, which remain ice-covered when upstream reaches are already thawed and are receiving the meltwater of late spring and summer.

The streams are also classified as perennial, intermittent, or ephemeral. Intermittent streams, *inter alia*, exist in karstic areas. These streams can be spatially intermittent and temporally intermittent. In the latter case, the stream flows only when heavy rain raises the groundwater table and reactivates outlets above the usual level. Ephemeral streams often cause strong erosion and transport and deposit great amount of soil and rock materials.

2.2 HYDROCHEMICAL ASPECTS

Streams play a dominant role in the transport of inorganic and organic substances about the Earth’s surface, both as dissolved and as particulate matter.

2.2.1 DISSOLVED MATTER

River discharges constitute the main source for dissolved matter in the oceans. However, there is a marked difference between the average chemical composition of ocean and river water (Table 2.3). The oceans have a more uniform composition than river water and contain, by weight, about 3.5% dissolved salts, whereas river water contain only 0.012%. The average salt content of seawater is composed as follows: 3.0% out of 3.5% consists of sodium and chlorine, 0.4% of magnesium and sulphate. Of the remaining 0.1% of the salinity, calcium and potassium constitute 0.04% each and carbon, as carbonate and bicarbonate, about 0.015%. The nutrient elements phosphorus, nitrogen, and silicon, along with such essential micronutrient trace elements as iron, cobalt, and copper, are of important, because these elements strongly regulate the organic production of the world's oceans.

In contrast to ocean water, the average salinity of the world's rivers is low. Of the average salt content of 120 ppm (by weight), carbon as bicarbonate constitutes 58 ppm, and calcium, sulphur (as sulphate), and silicon (as dissolved monomeric silicic acid) make up a total of about 39 ppm. The remaining 23 ppm consist predominantly of chlorine, sodium, and magnesium in descending importance. In general, the composition of river water is controlled by water-rock interactions of the carbon dioxide-charged rain and soil waters with the minerals in continental rocks. The carbon dioxide content of rain and soil water is of particular importance in weathering processes. The chemical composition of rainwater changes markedly after entering the soils. The upper part of the soil is a zone of intense biochemical activity. One of the major biochemical processes of the bacteria is the oxidation of organic material, which leads to an increase of carbon dioxide in the soil gas. Above the zone of water saturation the soil gases may contain 10 to 40 times as much as carbon dioxide as the free atmosphere. This CO_2 gives rise to a variety of weathering reactions, for example the congruent dissolution of calcite ($CaCO_3$) in limestone:

$$CaCO_3 + CO_2\ (g) + H_2O = Ca^{2+} + 2HCO_3^- \qquad \mathbf{(2.1)}$$

and the incongruent reaction with K–spar ($KAlSi_3O_8$):

$$2KAlSi_3O_8 + 2CO_2 + 11H_2O = Al_2Si_2O_5(OH)_4 + 2K^+ + 2HCO_3^- + 4H_4SiO_4 \qquad \mathbf{(2.2)}$$

The amount of CO_2 dissolved according to reaction (2.1) depends mainly on the temperature and the partial pressure of the carbon dioxide. For example, for an atmospheric carbon dioxide pressure of 10^{-2} atmosphere and for a soil atmosphere of nearly pure carbon dioxide, the amount of calcium that can be dissolved (at 25°C) until saturation is 65 and 300 ppm, respectively. The calcium and bicarbonate ions released into soil water and groundwater eventually reaches the river system. The water resulting from reaction (2.2) contains bicarbonate, potassium, and dissolved silica in the ratios 1:1:2, and the new mineral, kaolinite, is the solid weathering product. The dissolved constituents of reactions (2.1) and (2.2) eventually reach the river systems. Recently, the global silicate weathering fluxes and associated CO_2 consumption fluxes have newly been estimated on the basis of data on the 60 largest rivers of the world (Gaillardet et al., 1999) (Fig.2.2). Only active physical denudation of continental rocks was found to be able to maintain high chemical weathering rates and significant CO_2 consumption rates.

In general, the dissolved load of the world's rivers comes from the following sources: 7% from beds of halite (NaCl) and salt disseminated in rocks; 10% from gypsum ($CaSO_4{\cdot}2H_2O$)

and anhydrite ($CaSO_4$) deposits and sulphate salts disseminated in rocks; 38% from limestone and dolomite; and 45% from the weathering of one silicate mineral to another.

Table 2.3 Average chemical composition in mg/l of oceans and rivers; only elements have been included with concentrations ≥ 1 μg/l (source: Garrels et al., 1975).

ELEMENT	SEAWATER	RIVERS	Element	SEAWATER	RIVERS
H	1.1×10^5	1.1×10^5	**Ar**	0.43	1)
Li	0.18	3×10^{-3}	**K**	3.8×10^2	1.4
B	4.4	0.018	**Ca**	4.12×10^2	14.7
C			**Ti**	1×10^{-3}	0.01
inorganic	28	11.6	**V**	2.5×10^{-3}	9×10^{-4}
diss. organic	0.5	10.8	**Cr**	3×10^{-4}	1×10^{-3}
N			**Mn**	2×10^{-4}	8.2×10^{-3}
inorganic	15	0.95	**Fe**	2×10^{-3}	0.04
diss. organic	0.67	0.23	**Ni**	1.7×10^{-3}	2.2×10^{-3}
O			**Cu**	1×10^{-4}	0.01
dissolved O_2	6	1)	**Zn**	5×10^{-4}	0.03
H_2O	$8.83\cdot10^5$	$8.83\cdot10^5$	**As**	3.7×10^{-3}	2×10^{-3}
F	1.3	0.1	**Br**	67	0.02
Na	1.08×10^4	7.2	**Rb**	0.12	1.5×10^{-3}
Mg	1.29×10^3	3.65	**Sr**	8	0.06
Al	2×10^{-3}	0.05	**Mo**	0.01	5×10^{-4}
Si	2	4.85	**I**	0.06	7×10^{-3}
P	0.06	0.078	**Ba**	0.02	0.06
S	0.09	3.83	U	3.2×10^{-3}	4×10^{-5}
Cl	1.9×10^4	8.25			

1) No reasonable estimates available.

2.2.2 PARTICULATE MATTER

Besides dissolved substances, rivers transport solids (bed load) and, most importantly, suspended load. The present global river-borne flux of solids to the oceans is estimated as $155\cdot10^{14}$ grams per year. Most of this flux comes from Southeast Asian rivers. The composition of this suspended material resembles soil and shale and is dominated by silicon and aluminium (Table 2.4).

Table 2.4 Estimated elemental fluxes of suspended matter (in 10^{12} g/year) transported by rivers to the ocean; POC = particulate organic carbon.

Element	Flux	Element	Flux	Element	Flux
Si	4 420	**Ca**	330	**Na**	110
Al	1 460	**K**	310	**POC**	180
Fe	740	**Mg**	210		

Rivers are 100 times more effective than coastal erosion in delivering rock debris to the sea. Their rate of sediment delivery is equivalent to an average lowering of the lands by 30 centimetres in 9 000 years, a rate that is sufficient to remove all the existing continental relief in 25 million years. Rates of erosion and transportation, and comparative amounts of solid and dissolved load, vary widely from river to river.

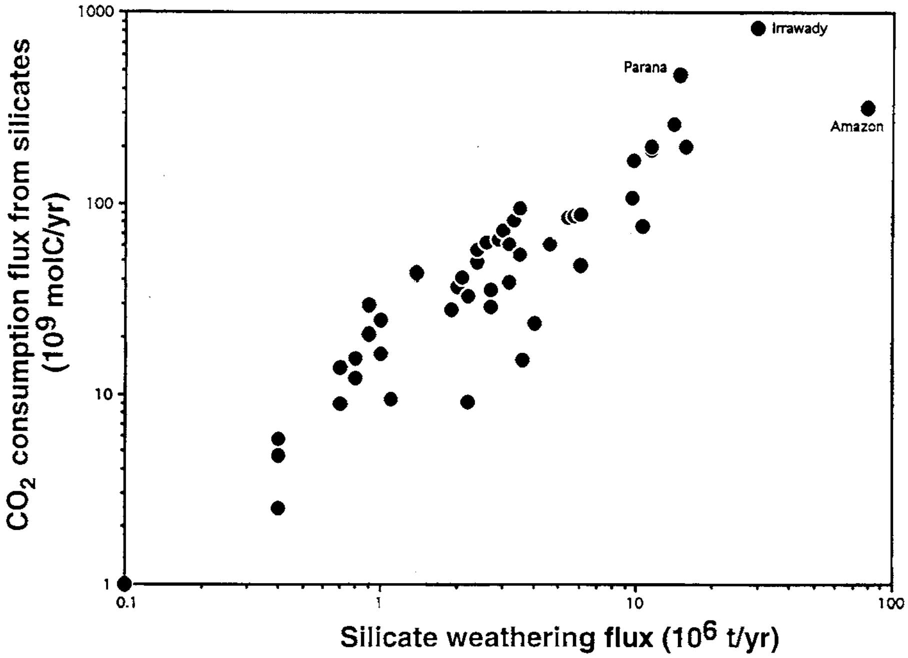

Fig.2.2 Relationship between the fluxes of material derived from the chemical weathering of silicates and the flux of CO_2 removed from the atmosphere by the weathering of alumino-silicates. The deviation of rivers such as Amazon from the main trend is due to their high silica concentration relative to cations (from Gaillardet et al., 1999).

Least is known about dissolved load, which at coastal outlets is added to oceanic salt. Its concentration in tropical rivers is not necessarily high although very high discharges can move large amount; the dissolved load of the lowermost Amazon averages about 40 ppm, whereas the Elbe and the Rio Grande, by contrast, average more than 800 ppm. Suspended load for the world in general perhaps equals two and one-half times dissolved load. Well over half of suspended load is deposited at river mouths as deltaic and estuarine sediment. About one-quarter of all suspended load is estimated to come down the Ganges-Brahmaputra and the Huang Ho (Yellow River), which together deliver some 4×10^9 ton/year; the Yangtze, Indus, Amazon, and Mississippi deliver quantities ranging from about 5×10^9 to approximately 0.35×10^9 ton/year. Suspended sediment transport on the Huang Ho equals a denudation rate of about 3090 ton/km^2/year; the corresponding rate for the Ganges-Brahmaputra is almost half as great.

2.3 ISOTOPES IN RIVERS

2.3.1 GENERAL ASPECTS

Naturally occurring stable and radioactive isotopes of the elements of the water molecule (water isotopes) and the compounds dissolved in water have increasingly been used to study hydrological, hydrochemical and environmental processes in rivers and their catchment areas. Tables 2.5 and 2.6 compile these isotopes and the principal fields of their application.

Table 2.5 Natural abundance of stable isotopes used in river studies.

Isotope	Relevant isotope ratio	Average natural abundance	Application
^{2}H	^{2}H/^{1}H	1.55×10^{-4}	Water balance & dynamics in river catchments, basins and estuaries; surface-groundwater interrelation
^{13}C	^{13}C/^{12}C	1.11×10^{-2}	Riverine carbon cycle; weathering processes; pollution; biological processes
^{15}N	^{15}N/^{14}N	3.66×10^{-3}	Pollution; biological processes
^{18}O	^{18}O/^{16}O	2.04×10^{-3}	Water balance & dynamics in river catchments, basins and estuaries; surface-groundwater interrelation
^{34}S	^{34}S/^{32}S	4.22×10^{-2}	Pollution; salt depositional processes
^{87}Sr	^{87}Sr/^{86}Sr	0.709939	Weathering of rocks and soils; anthropogenic disturbances (pollution); influence of tributaries on chemistry and pollution in rivers

In the following, natural variations of isotopes in selected rivers and catchment areas will be discussed in the context of their hydrological applications. Special emphasis will be placed to the water isotopes ^{2}H (deuterium), ^{3}H (tritium), and ^{18}O (oxygen-18) because of their specific potential in addressing water balance, dynamics and interrelationships between surface and groundwater in river basins and catchment areas. The $^{13}C/^{12}C$ and the $^{87}Sr/^{86}Sr$ ratios in runoff from catchment areas are frequently used in river and catchment hydrology investigations and are therefore discussed in some detail, whereas in the case of the other isotopes and radionuclides we refer to special publications.

Table 2.6 Typical specific activities of radioactive isotopes (radionuclides) used in river studies; *) also ^{232}Th and ^{230}Th are used in river studies, mostly combined with other uranium and thorium decay-series radionuclides (such as isotopes of Ra and ^{222}Rn) (see also Vol.I).

Nuclide	Half-life (years)	Spec. act. (Bq/l)	Application
^{3}H	12.33 a	1.55×10^{-4}	Water balance and dynamics in river catchments, basins and estuaries; surface-groundwater interrelation
^{14}C	5730 a	1.11×10^{-2}	Riverine carbon cycle; sediment dating; dating of flood events
^{238}U **^{234}U *)**	2.5×10^{9} a 2.45×10^{5} a	4×10^{-3}	Weathering, erosion and sedimentation; processes in estuaries; sedimentation

2.3.2 STABLE ISOTOPES OF HYDROGEN AND OXYGEN

The water isotopes ^{2}H or ^{18}O are very useful because of their conservative behaviour in water (constituents of the water molecule) and the large variability of their isotopic ratios $^{2}H/^{1}H$ and $^{18}O/^{16}O$. In precipitation and in river- and groundwater these are usually measured in terms of the δ values, cf. Vol.I, Chapt.4:

$$^{2}\delta = \frac{(^{2}H/^{1}H)_S}{(^{2}H/^{1}H)_R} - 1 \qquad ^{13}\delta = \frac{(^{13}C/^{12}C)_S}{(^{13}C/^{12}C)_R} - 1 \qquad ^{18}\delta = \frac{(^{18}O/^{16}O)_S}{(^{18}O/^{16}O)_R} - 1 \qquad \textbf{(2.3)}$$

where S stands for sample and R for reference or standard. Instead of these δ symbols, also $\delta^{2}H$, $\delta^{13}C$ and $\delta^{18}O$ are being used frequently. The δ values are small numbers and therefore given in ‰ (equivalent to 10^{-3}).

Seasonal variations will be larger in rivers and creeks where surface run-off from recent precipitation is the main source of flow, and smaller in streams where groundwater is the dominant source. Local precipitation events are an important component of river water in the headwaters of large basins. In the lower reaches, local additions of precipitation can be of minor importance, except during floods. In such cases, contributions from different surface and subsurface sources, each with their characteristic isotope ratio, determine the isotopic composition of the river water. Where it is possible to describe the isotopic composition of these sources, isotope analyses of river water can yield direct information about the origin and quantity of the various contributions.

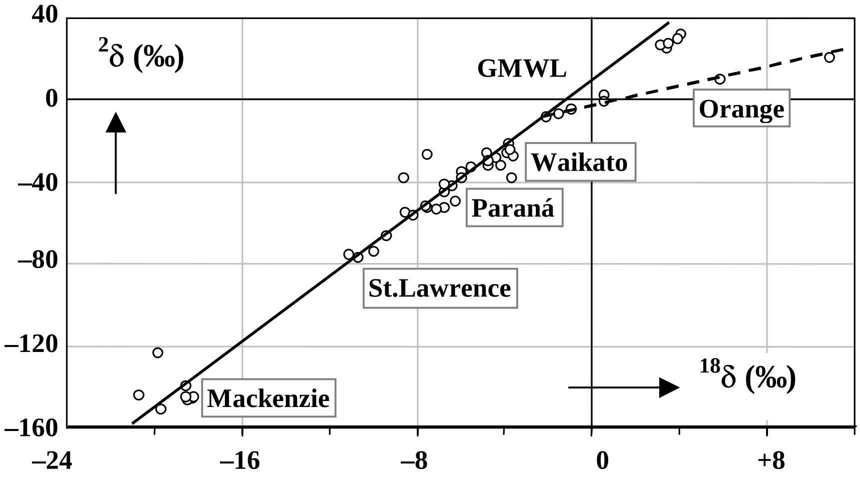

Fig.2.3 Relation between $^{18}\delta$ and $^2\delta$ for a choice of samples from a few rivers where evaporation is insignificant, contrary to the Orange river, South Africa (values along the dashed line).

This chapter presents stable isotope data of selected rivers and their application to study these rivers. It includes a discussion of isotopic variations in small watersheds as well as in larger rivers. The water isotope ^{18}O has been selected for the presentation of examples. Generally, the other water isotope, ^{2}H, would provide the same results and, thus, the measurement of only one of these isotopes is often sufficient. The oxygen and hydrogen isotopic composition of most of the world rivers was found to be close to the Global Meteoric Water Line (Fig.2.3), indicating that evaporation of river water is in most cases of insignificant influence of the isotopic composition of this water. However, in rivers and catchments of arid zones, where evaporation can be an important factor, the combined measurement of ^{18}O and ^{2}H can be used to quantify the evaporation effect and to study mixing processes between river water and adjacent groundwater. Typical applications of this type are related to the rivers Murray in Australia (Simpson and Herczeg, 1991), Nile in Africa (Vrbka et al., 1993), and Truckee in North America (McKenna et al., 1992).

2.3.2.1 VARIATIONS OF ^{2}H AND ^{18}O IN LARGE RIVERS

It is evident that the isotopic composition of riverwater is related to that of precipitation. In small drainage systems, $^{18}\delta$ of the runoff water is equal to that of the local or regional precipitation. In large rivers, transporting water over large distances, there may or may not be a significant difference in $^{18}\delta$ between the water and the average precipitation at the sampling location. Examples are given in Fig.2.4.

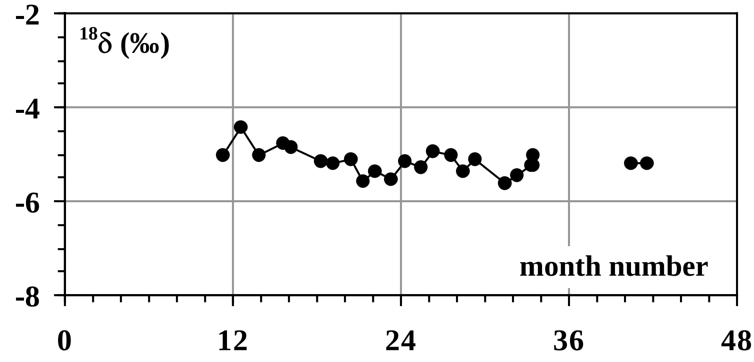

Waikato River, New Zealand
1981 – 1984.

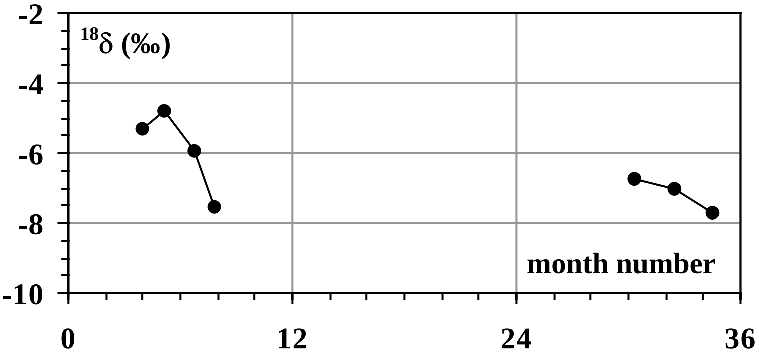

Padma (Ganges) at Kazirhat, Bangladesh
1981 – 1983

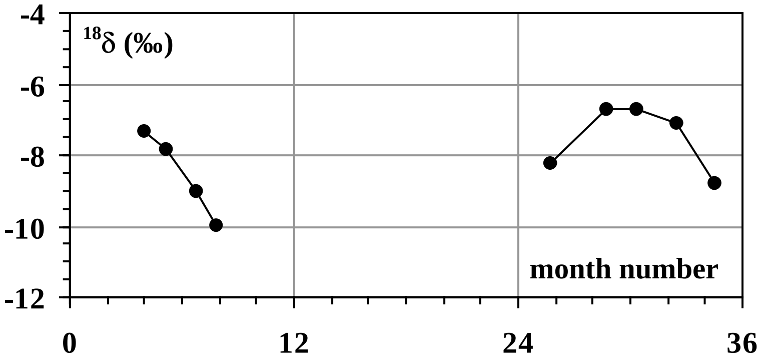

Jamuna (Brahmaputra) at Nagarbari, Bangladesh
1981 – 1983

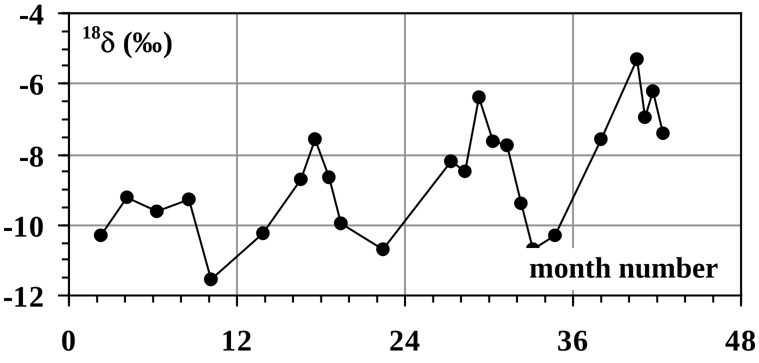

Indus at Kotri Barrage, Pakistan
1981 – 1984

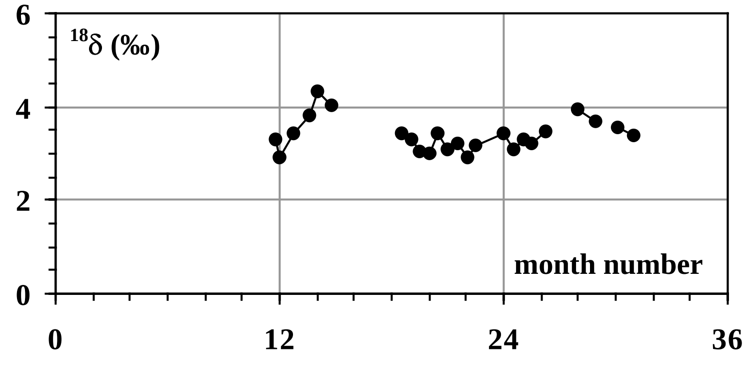

Nile River at Assiut, Egypt
1981 – 1983

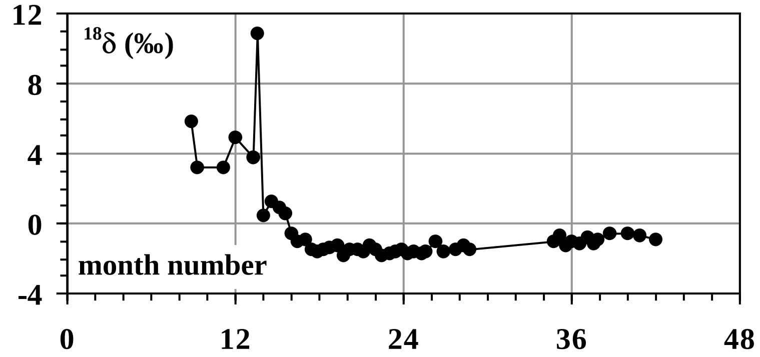

Orange River, South Africa
1981 – 1983

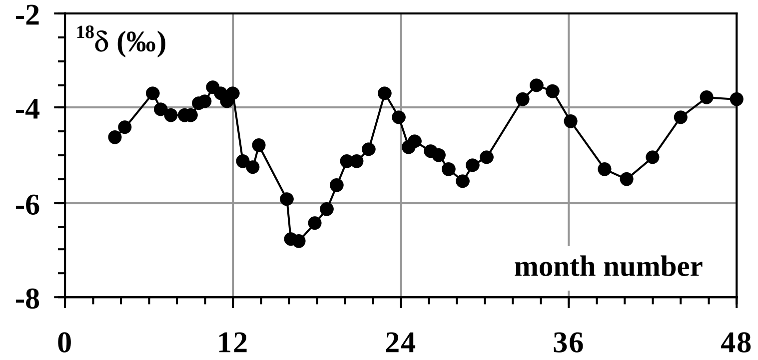

Paraná at Santa Fé,
Argentina
1981 – 1984

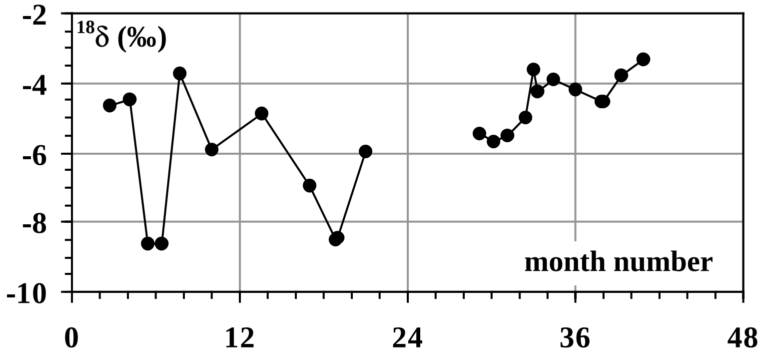

Orinoco at Soledad
Venezuela
1981 – 1984

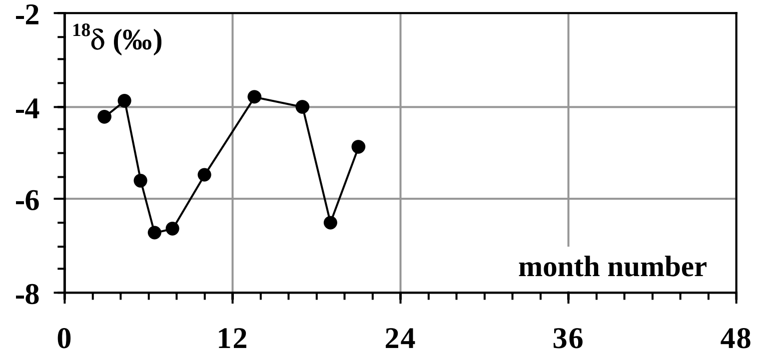

Caroni at Parque Cachamay
Venezuela
1981 – 1982

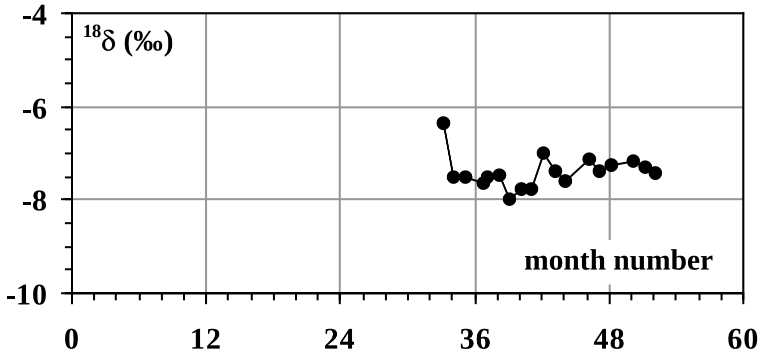

Tiber 35 km upstream
Italy
1983 – 1985

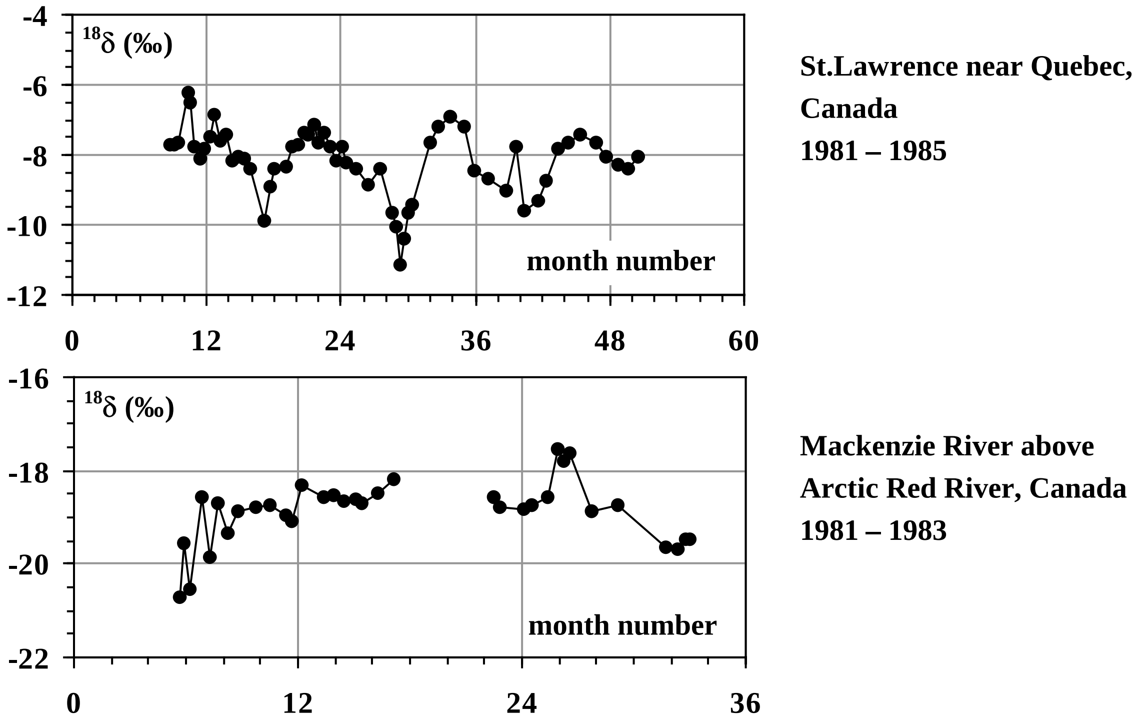

Fig.2.4 $^{18}\delta$ of some major rivers in the world. Part of the data was obtained in co-operation with participants in the SCOPE/UNEP project on Transport of Carbon and Minerals in Major World Rivers (Mook, 1982).

Apart from a possible continent effect (see Volume II), $^{18}\delta$ of the West European river Rhine is influenced by the altitude effect in precipitation: a significant part of the Rhine water is meltwater from the Swiss Alps ($^{18}\delta \approx$ -13‰) (Fig.2.5). For the same reason, differences in $^{18}\delta$ between runoff and regional precipitation is observed in, for instance, the rivers Caroni (Venezuela), Jamuna (Bangla-Desh) and Indus (Pakistan). The sharp decrease in $^{18}\delta$ of the Caroni during April 1981 is due to a large discharge of precipitation over the Andes mountains. On the other hand, the rivers Meuse (Netherlands), Mackenzie (Canada) and Paraná (Argentina) represent the average $^{18}\delta$ values of precipitation.

In most figures seasonal variations in $^{18}\delta$ are obvious, in addition to differences in average $^{18}\delta$ level. In large rivers $^{18}\delta$ increases during summer are not caused by evaporation. For instance, the $^{18}\delta$-$^{2}\delta$ relation of the rivers Rhine and Meuse follow the Global Meteoric Water Line (Vol.I: Sect.7.5; Vol.II: Sect.3.1) and do not show the lower slope typical of evaporated waters (Vol.I: Fig.7.18). The origin of the seasonal variation is therefore to be attributed to the seasonal variations in precipitation. Thus, large rivers contain not only old groundwater with a virtually constant isotopic composition, but also a relatively fast component, to be ascribed to surface runoff.

In Alpine and Nordic environments, the temporary storage of winter precipitation on ice and snow covers and their melting during summer can reverse or at least shift the isotopic cycles.

Also in the rivers Caroni, Padma, Jamuna and Indus a reverse seasonal effect is observed, caused by a relatively large meltwater component during spring and summer. For example, the ^{18}O content of the Rhine at the Dutch station (Fig. 2.5) drops from –9.5‰ in winter to about –10.5‰ in summer. If one assumes that the Rhine water at this station represents a mixture of two components, one of Alpine origin and the other from the lower part of the basin extending from Basel to the Netherlands, the fraction of each component can be estimated. Using the $^{18}\delta$ values given by Mook (1970), a simple mass balance equation:

$$^{18}\delta_{\mathrm{mixture}} = f_1\ {}^{18}\delta_{\mathrm{comp.1}} + f_2\ {}^{18}\delta_{\mathrm{comp.2}} \tag{2.4}$$

(where comp.1 and comp.2 are the mixing components and $f_1 + f_2 = 1$) shows that in summer the Alpine component of the Rhine discharge is about 50%, dropping to 20% in winter,.

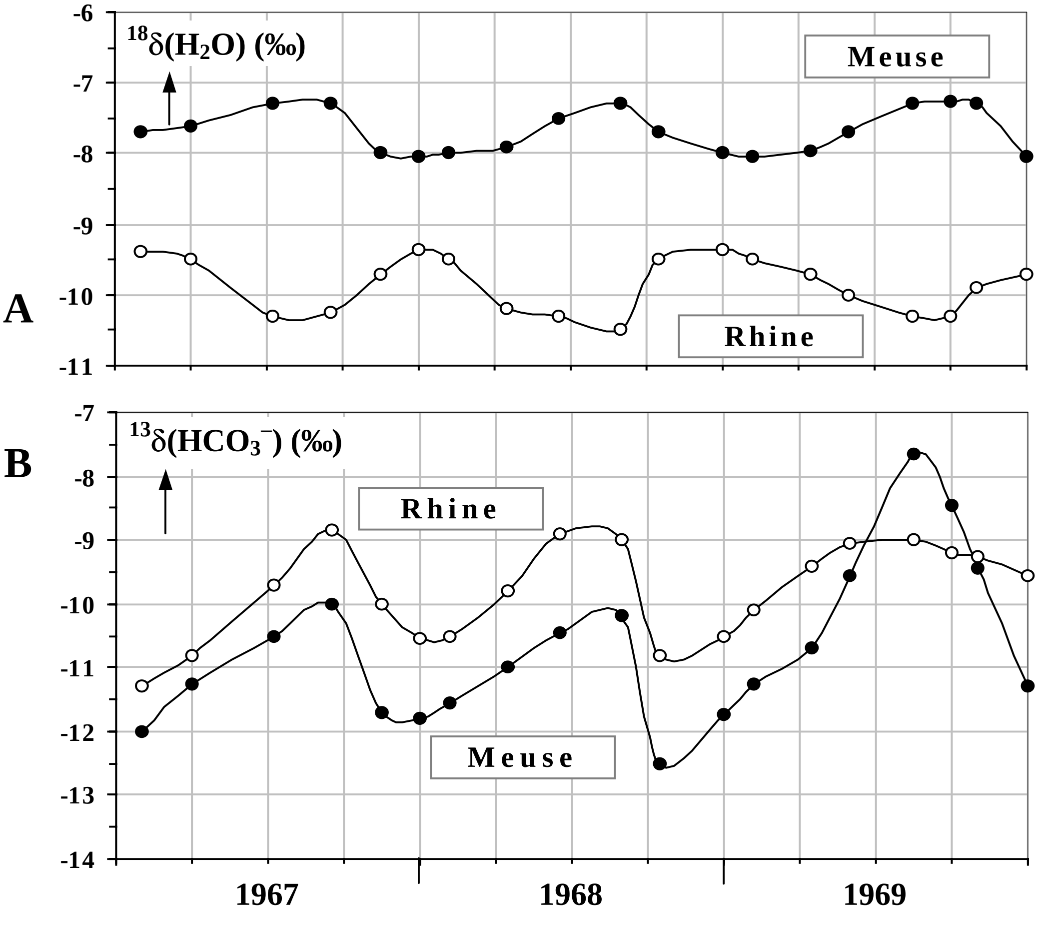

Fig. 2.5 Comparison of the isotopic composition of bimonthly samples of two rivers in the Netherlands, representing the rainwater river type (Meuse at Mook) and the meltwater river type (Rhine at Lobith, the German border). **A.** The $^{18}\delta$ values show opposite seasonal variations (Mook, 1970): $^{18}\delta$ of the Meuse reflects precipitation in the drainage area, $^{18}\delta$ of the Rhine is also controlled by the low $^{18}\delta$ values of melting snow and ice in the Swiss Alps. **B.** The $^{13}\delta$ values of the bicarbonate fraction of dissolved inorganic carbon are more or less typical for groundwater, especially in winter.

The river Danube, with a catchment area of 817 000 km^2, a length of 2857 km and a long term mean discharge at its mouth of about 6500 m^3/s, is the second largest river in Europe, after the Volga. The isotopic composition of precipitation in its catchment area is characterised by a pronounced seasonal variability (mean $^{18}\delta$ amplitude of about 8‰), which is correlated with changes in surface air temperature. Fig.2.6 presents the observed time series of $^{18}\delta$ for the Danube at Ulm (1980-1993) and at Vienna (1968-1993) and the calculated long-term trends (Rank et al., 1998). The Danube at Vienna is depleted in ^{18}O by about 1.5‰ with respect to Ulm, because of the contribution of the Alpine rivers, whose catchment areas are at higher elevations. The different flow regime of the upper Danube and the Alpine rivers is clearly reflected not only in the mean $^{18}\delta$ values but also in the different seasonal patterns of $^{18}\delta$ in the Danube at Ulm and Vienna, and in the Inn at Schärding (Figs 2.6 and 2.7).

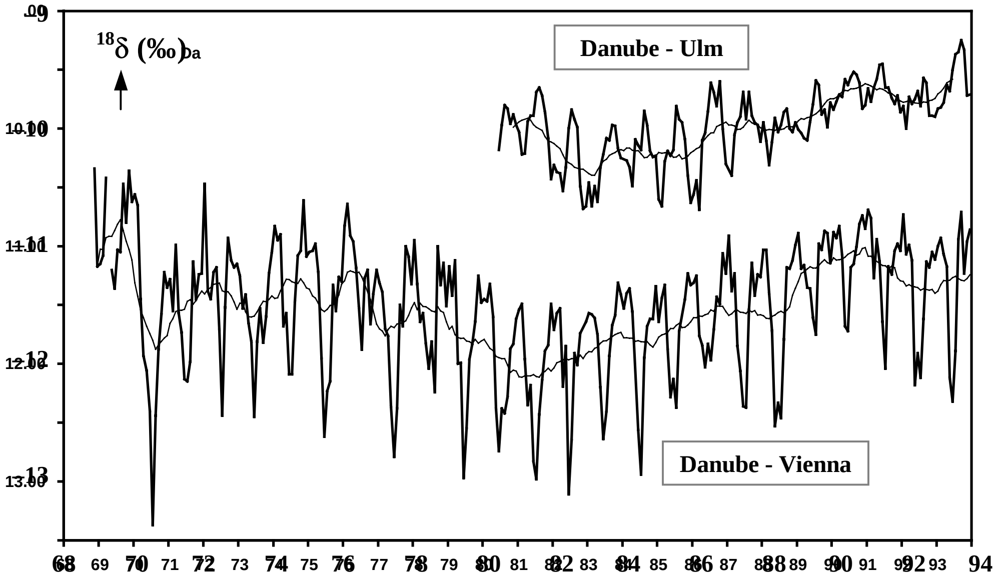

Fig.2.6 Time series of $^{18}\delta$ for the Danube at Vienna and Ulm, and trend curves for $^{18}\delta$, calculated using 12-month moving average (from Rank et al., 1998).

The mean seasonal amplitude of $^{18}\delta$ observed in Danube water at Ulm is relatively small, about 0.5‰ (from -10.2‰ in winter to -9.7‰ in summer), close to the long-term mean $^{18}\delta$ value of precipitation recorded at low-altitude stations of the catchment. This indicates a limited contribution of precipitation falling at high elevations to the flow in the initial stretches of the Danube. Precipitation in the lowlands and groundwater discharge are therefore thought to be the main contributors to the river runoff in this sector of the catchment. It is worth noting that the maximum of $^{18}\delta$ occurs in the river during the summer (Fig.2.6), in phase with the seasonality of $^{18}\delta$ observed in precipitation.

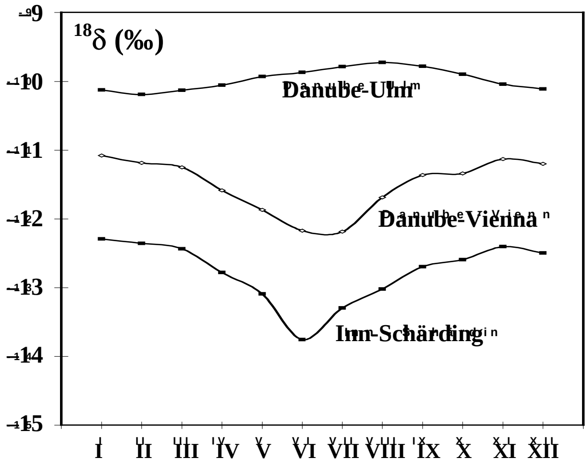

Fig.2.7 Mean monthly $^{18}\delta$ in the Danube at Vienna (1968) and at Ulm (1980-1993) and the river Inn at Schärding (1975) (from Rank et al., 1998).

Despite the difference in the absolute $^{18}\delta$ level at the two analysed sites Ulm and Vienna, the similar long-term trend at both stations indicates that a common climatic signal, visible also in the isotopic composition of precipitation, has been transferred through the upper Danube catchment (cf. Chapt.4). Similar trends were also observed in the rivers Rhône and Rhine (Schotterer et al., 1993).

The Alpine rivers are isotopically more depleted. The long-term mean $^{18}\delta$ value of the Inn River, which constitutes the most important tributary of the Danube, is -12.9‰ (Fig.2.7), indicating the contribution of precipitation produced at much higher altitudes. The difference of almost 3‰ with respect to $^{18}\delta$ observed in precipitation at Vienna or Stuttgart corresponds to an estimated elevation difference of 1500 m in the recharge areas, assuming the mean $^{18}\delta$ altitude gradient of -0.2‰ per 100 m. Since melting at high elevations occurs during late spring and summer, the seasonality of $^{18}\delta$ in the Alpine rivers does not coincide with the seasonal changes observed in precipitation. For the Inn, the amplitude of seasonal changes of $^{18}\delta$ reaches 1.5‰, with a minimum (-13.8‰) observed in June and a maximum (-12.3‰) in December. This reversed seasonal trend in $^{18}\delta$ is still visible at Vienna, although with reduced amplitude (around 1.1‰). The more negative values are observed in summer, coinciding with the higher contribution of melting water to the river runoff. The observed seasonality in Vienna is therefore mainly governed by the significant contribution (around 60%) of the Alpine rivers to the annual flow rate at Vienna. While base flow remains roughly constant throughout the year, the contribution of Alpine rivers is important during the summer, masking the contribution of isotopically enriched summer precipitation forming direct runoff.

The mean $^{18}\delta$ values of Danube water and precipitation in Vienna were used to separate the flow into three components:

1) base flow, with $^{18}\delta$ around -10.8‰ to –11.0‰
2) direct precipitation, calculated by extrapolating the observed monthly $^{18}\delta$ values in Vienna to the estimated altitude of the recharge areas of Alpine rivers (varying between -16‰ in winter and -10‰ in summer)
3) melting water, which contributes predominantly from April to September (assumed to be constant at about -16‰).

The relative proportions of the three components change significantly throughout the year. Base flow accounts for more than 90% of the total flow during the winter, with typical $^{18}\delta$ values of around –11.1‰. During summer, the base flow contribution falls to ca. 50% (Rank et al., 1998).

The headwaters of most rivers and streams will reflect the isotopic composition of local precipitation, but in the downstream areas the quantitative importance of all water sources in the river basin will control the isotope contents. This can be demonstrated by results of an environmental isotope study of the River Rhine (Buhl et al., 1991). Its drainage basin (Fig.2.8) of some 224 500 km^2 yields an average annual discharge of about 72 km^2, which ranks it as the 40th largest river in the world. The river regime is characterised by two peak periods, February – March due to lowland snowmelt, and June – July originated from snowmelt in the Alps. The latter peak diminishes below Cologne. Low discharge is prevailing from August to November.

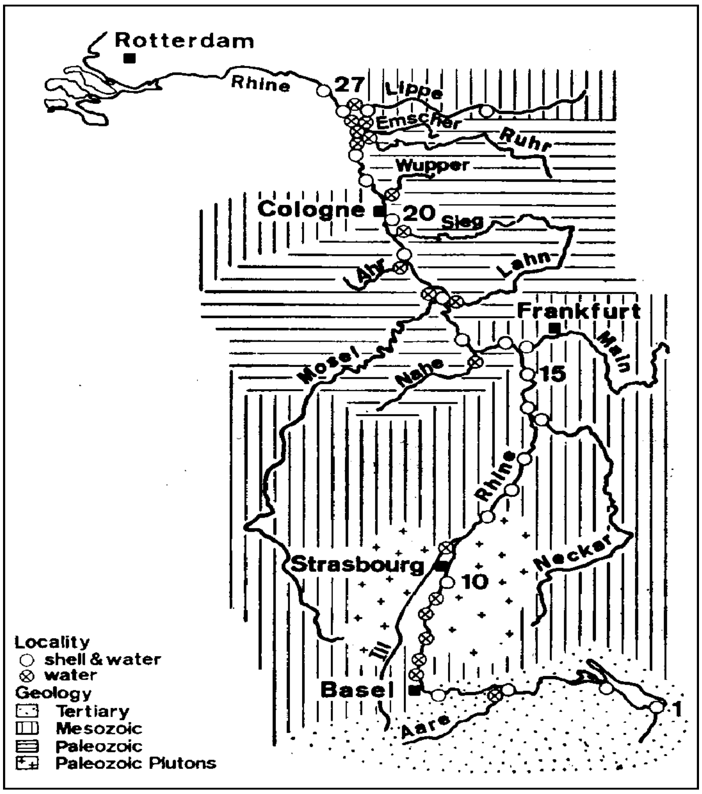

Fig.2.8 Geographic map, sampling locations, and generalized geology of the river Rhine catchment area (from Buhl et al., 1991).

Fig.2.9 demonstrates that the discharge at locality No.1 is essentially Alpine meltwater with $^{18}\delta$ of about –12.5‰. In contrast, the Rhine tributaries north of the Main river reflect the $^{18}\delta$ values of lowland precipitation (about -8‰). Using these values, balance calculations suggested that in the Lower Rhine Alpine meltwater accounts for about 50% of the total in late May and ca. 30% in late November. Since $^{18}\delta$ in the Upper Rhine at Basel is -11.5‰, the water from the Upper Rhine accounts for 57% of the total Lower Rhine discharge in the spring and 43% in the fall (Buhl et al., 1991).

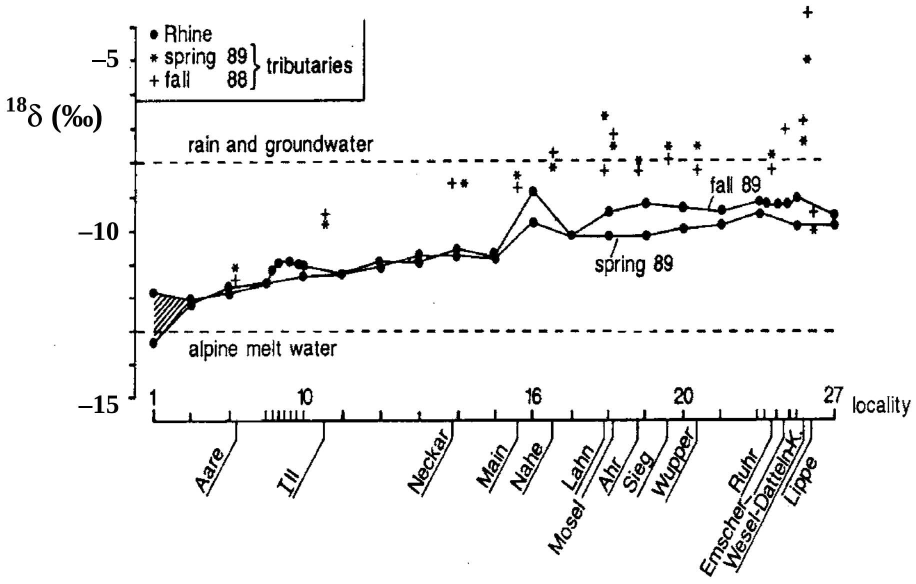

Fig.2.9 Oxygen isotopic composition of water from the river Rhine and its tributaries; the sampling locations are indicated in Fig.2.8 (from Buhl et al., 1991).

2.3.2.2 ^{18}O IN SMALL RIVERS AND STREAMS: HYDROGRAPH SEPARATION

Small rivers respond faster to changes in the isotopic composition of precipitation than do large rivers, because the surface-runoff component of the discharge will be more direct and pronounced. Fig.2.10 shows two typical examples related to runoff studies in the catchment of the Lainbach creek in the Bavarian Alps (Stichler and Herrmann, 1978). In both cases there is a quick response in the ^{18}O content of the runoff to a preceding strong rainfall. The $^{18}\delta$ value in the rainfall of 7 August was at –7.5‰, i.e. the rain was isotopically heavier than the runoff before this event. This caused a rapid increase of maximum 1‰ in $^{18}\delta$ of the runoff. Contrary to this, the rainfall of 12 August was isotopically more depleted ($^{18}\delta$ = -14‰ to -16‰) than the runoff prior to this event (Fig.2.10B). Accordingly, the δ^{18}O value of the runoff dropped by about 0.7‰.

The contributions of the surface-runoff to the total runoff in small catchment areas can be determined by the so-called *hydrograph separation*, for which hydrochemical and especially isotope data are usefully employed. The approach is often related to two-component separation of total (stream) hydrographs into surface and subsurface (groundwater) runoff for individual storm events. If the solute (conservative chemical constituent or isotope) concentrations of the components are significantly different during an individual storm event in comparison to the pre-event runoff, the mixing ratios of the two components during that event can be estimated by hydraulic continuity and simple mass balance equations.

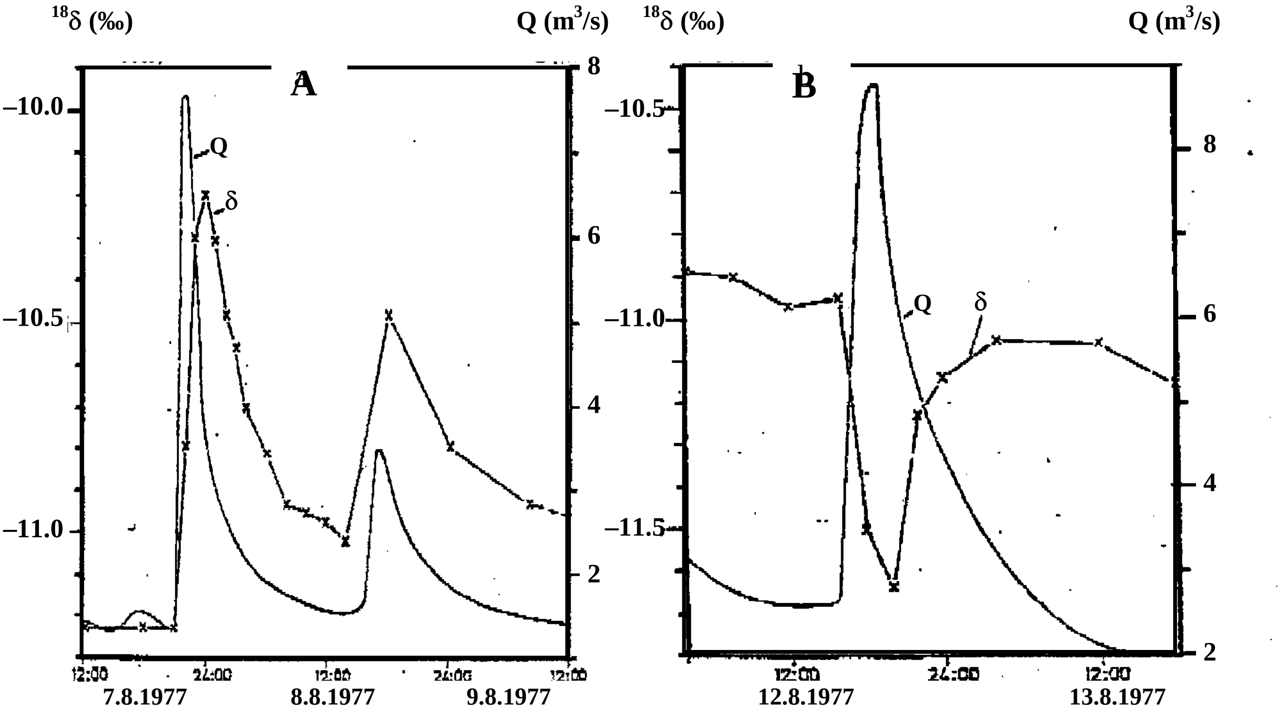

Fig.2.10 Runoff rate and ^{18}O content of the Lainbach creek (Bavarian Alps) following strong rainfall with higher (A) and lower (B) $^{18}\delta$ value in comparison to the runoff prior to the rainfall events (after Stichler and Herrmann, 1978)

To evaluate the runoff hydrograph, the following balance equations are used:

$$Q_t = Q_S + Q_0 \qquad (2.5)$$

and

$$\delta_t Q_t = \delta_S Q_S + \delta_0 Q_0 \qquad (2.6)$$

where Q_t denotes the total runoff, Q_S (Q_0) the surface runoff (base flow) component, and δ_t is derived from the individual isotope (δ_i) and run-off (Q_i) values measured during the event, by the relationship:

$$\delta_t = \frac{\Sigma\, \delta_i Q_i}{\Sigma\, Q_i} \qquad (2.7)$$

The isotopic composition of the surface runoff component is δ_S (represented by the isotopic composition of the precipitation) and the one of the base flow is δ_0 (represented by the runoff value just prior to the precipitation event).

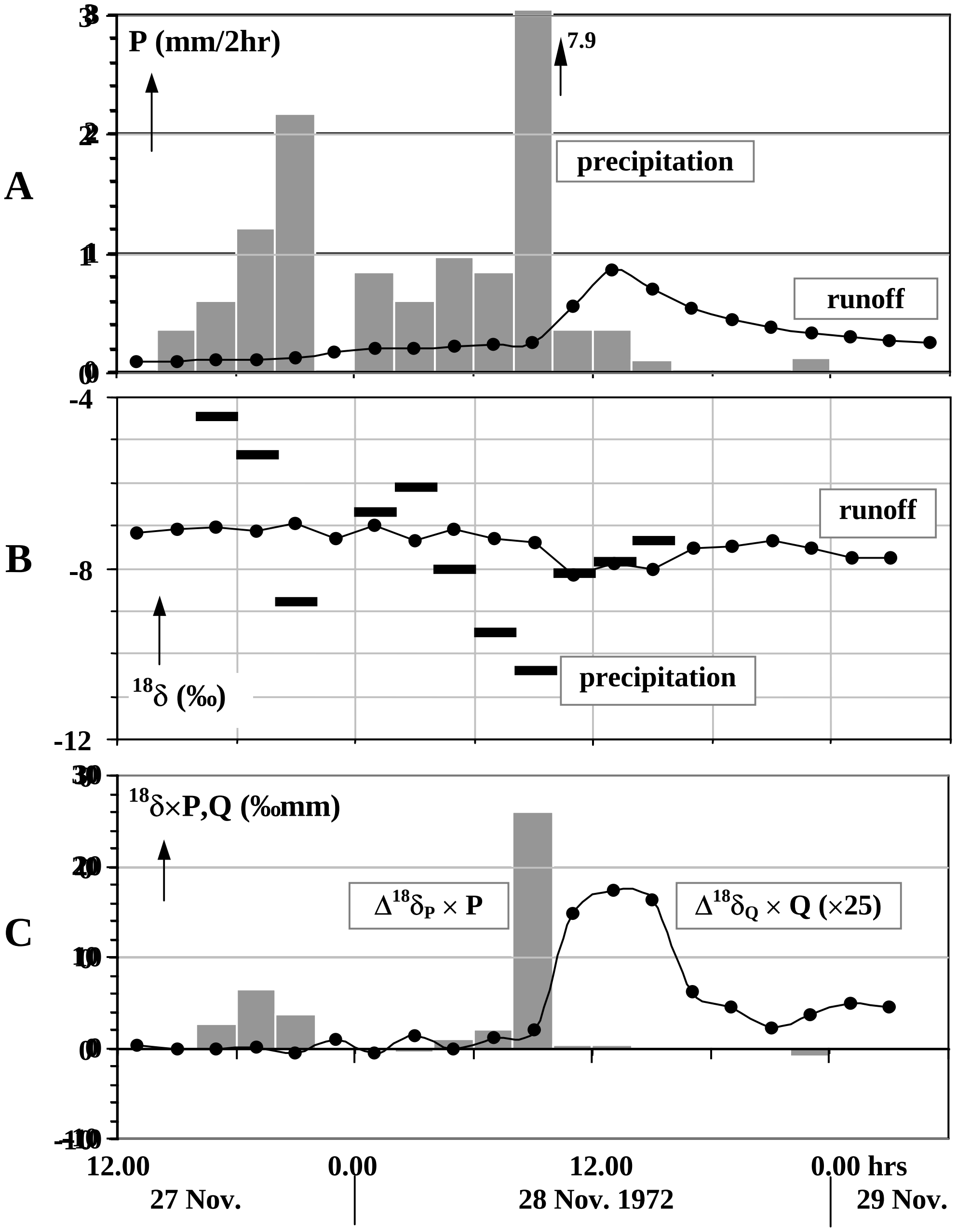

Fig.2.11 ^{18}O variations of precipitation and total runoff (B) in a small catchment area of 6 km^2, in the E. Netherlands, related to precipitation (P in mm) and runoff intensities (Q in mm over the catchment area) (A). C presents the "amount of ^{18}O" in the precipitation and runoff calculated from $(\delta_P - \delta_0)\times P = \Delta\delta_P\times P$ and $(\delta_t - \delta_0)\times Q = \Delta\delta_Q\times Q$. The base-flow value ($\delta_0$) for ^{18}O was chosen to be –7.1‰ (after Mook et al., 1974).

From Eqs.2.5 and 2.6 the relative proportion of the surface runoff Q_S/Q_t can be derived:

$$Q_S / Q_t = \frac{\delta_t - \delta_0}{\delta_S - \delta_0} \tag{2.8}$$

Another example of hydrograph separation using ^{18}O is shown in Fig.2.11. For the 28 November peak, the percentage of direct (surface) runoff was found to be 25%.

In humid mountainous catchments of small rivers and headwaters of larger rivers, that do not have significant meltwater influence, the seasonal variation of ^{18}O and ^{2}H in precipitation and riverwater often resembles a sinusoidal function. Since the river contains a mixture of water with different transit times, riverwater has an amplitude and phase that differ from those in precipitation. The amplitude of $^{18}\delta$ and $^{2}\delta$ in riverwater decreases with increasing mean transit time. Assuming that the mixing of water with different transit times t is characterised by the exponential transit time distribution function $g(t) = \exp[-t/T]/T$, the mean transit time T and the ratio f of the amplitudes in riverwater and precipitation, respectively, are related by $T = \omega^{-1} (f^{-2} - 1)^{1/2}$ where $\omega = 2\pi$/year (Maloszewski et al., 1983). In Alpine regions with rather high amplitudes in precipitation, the “dating” range is accordingly high. The upper limit of the mean transit time determination obtained by this approach is about 5 years (Ramspacher et al., 1992). An application of this method to river studies in Sweden was reported by Burgman et al. (1987).

2.3.3 ^{3}H IN RIVERS

To a varying extent, the ^{3}H content of riverwater represents that of precipitation. However, (i) the water may have been subjected to a relatively long residence time in the region, as groundwater or as surface water (lakes). Moreover, (ii) the water may have been transported over a long distance from a region with lower or higher ^{3}H content in the precipitation.

Fig.2.12 contains a few examples of large and smaller NW European rivers. It shows that there are two more aspects about the ^{3}H content of rivers, (iii) the soil often contains, at least on the northern hemisphere, ^{3}H produced by or escaped from exploding nuclear weapons, at a level exceeding the present-day ^{3}H concentration, and (iv) rivers in certain countries are likely to have, at least periodically, raised ^{3}H levels because of ^{3}H releases by nuclear power stations. The latter possibility is obviously the one that happened in the Belgian river Scheldt.

Environmental tritium (^{3}H), and especially, bomb-^{3}H has shown specific potential to determine the timescale of hydrological processes in the catchment area to be considered.

It should be noted that there are different time parameters defining the time scale of a hydrological system. Here we refer to the mean *transit time* as the time spent by a labelled element (water parcel or constituent) between its entry into, and its outflow from the hydrological system. (If the “outflow” is not the total discharge of a spring or a river, but an observation well in a groundwater system, the term *residence time* is more appropriate.)

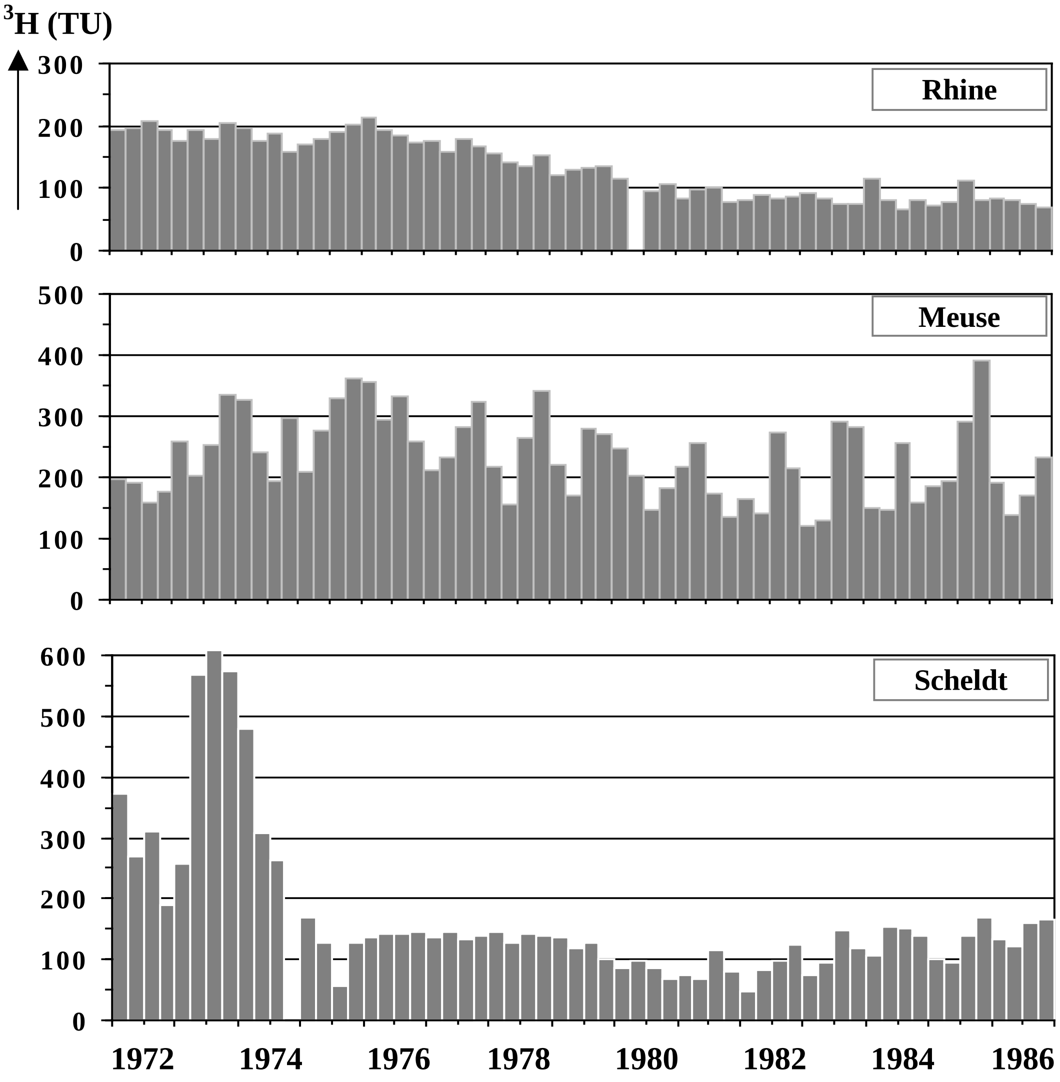

Fig.2.12 ^{3}H content (in TU) in the rivers Rhine (at Lobith), Meuse (at Eysden) and Scheldt (at Schaar van Ouden Doel), each at the point of entering Dutch territory. Each number is the average over a period of 3 months (original data from Reports on the Quality of Surface Waters in the Netherlands).

Long-term measurements of ^{3}H in river runoff can be used to estimate the mean *transit time* of the water in the catchment area. A typical example for small rivers is shown in Fig.2.13, in which long-term measurements of ^{3}H in the Lainbach creek (see also under 2.3.2.2, Fig.2.10) and respective ^{3}H measurements in precipitation are plotted against the observation time. The ^{3}H results were evaluated with conceptual hydrological models, also known as "lumped parameter models", which include the mean transit time as model parameter. In the given case, two alternative models ("exponential model" and "dispersion model") were used to estimate the mean transit time in the catchment of the Lainbach creek. The obtained values are equal to 1.6 years and 1.8 years, respectively (Maloszewski et al., 1983).

The injection of bomb-^{3}H in the global water cycle provided for the first time the possibility to trace hydrological (runoff) processes in large catchment areas. Begemann and Libby (1957) were the first who used bomb-^{3}H to establish the water balance of the North American continent, in particular the catchment area of the Mississippi river. They found a storage volume, equivalent to 7.7m water column, and a turnover time of 10 years.

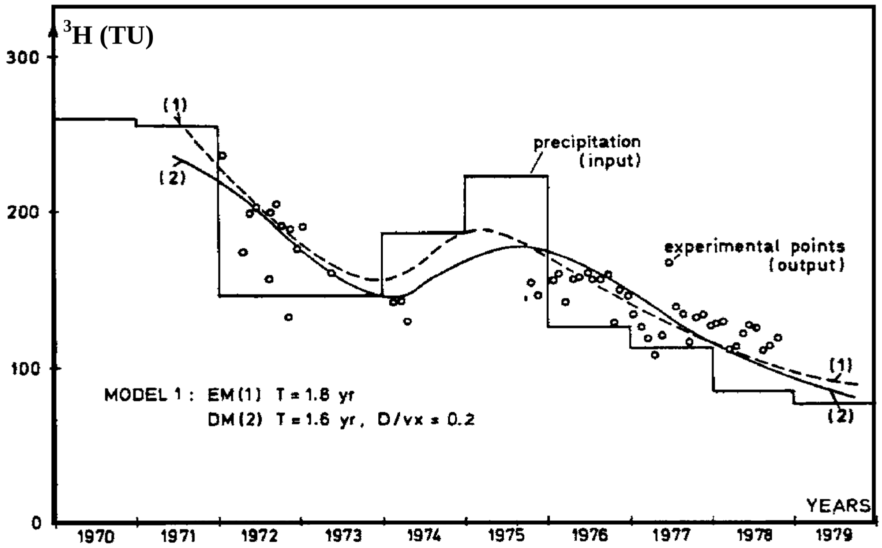

Fig.2.13 ^{3}H in precipitation and runoff in the catchment of the Lainbach creek in the Bavarian Alps at 1800m above sea level (from Maloszewski et al., 1983)

Since the early 1960s, the US Geological Survey has maintained a network of stations to collect samples for the measurement of ^{3}H concentrations in precipitation and stream flow. ^{3}H data from outflow waters of river basins draining 4500 to 75 000 km^2 have been used to determine average residence times of water within the basins (Michel et al., 1992). The basins studied include the following rivers: Colorado, Kissimmee, Mississippi, Neuse, Potomac, Sacramento and Susquehanna (Fig. 2.14).

The basins were modelled with the assumption that the outflow in the river (^{3}H concentration C_0) comes from two sources - prompt (within-year) runoff from precipitation (^{3}H concentration C_P, which is equivalent to the weighted average of the ^{3}H concentration in precipitation for the given year), and flow from the “long-term reservoirs” of the basin such as, for instance, in the case of groundwater (concentration C_G).

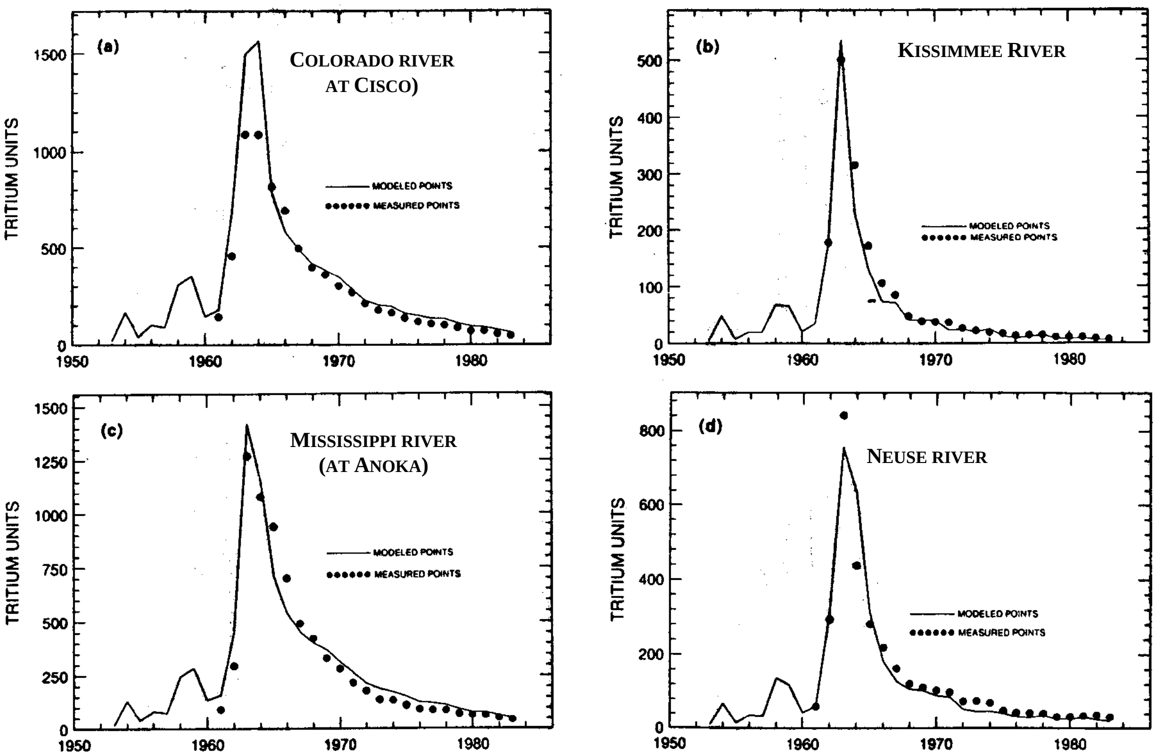

Fig.2.14 Measured and modelled ^{3}H concentrations in the outflow of the river basins of the Colorado, Mississippi, Kissimmee and Neuse river, USA (from Michel et al., 1992).

The ^{3}H concentration in the outflow from the basin, therefore, is a mixture of these two sources and is described by

$$C_0 = Q_P C_P + Q_G C_G \tag{2.9}$$

where Q_P and Q_G are the fractions of each source in the outflow ($Q_P + Q_G = 1$). Therefore, the ^{3}H concentration in the outflow water of the basin is dependent on three factors:

1) the ^{3}H concentration in runoff from the long-term reservoir, depending on the transit time for the reservoir and historical ^{3}H concentrations in precipitation

2) ^{3}H concentrations in precipitation (the within-year runoff component)

3) relative contributions of flow from the long-term and within-year components.

Predicted ^{3}H concentrations for the outflow water in the river basins (C_g) were calculated for different transit times and for different relative contributions from the two reservoirs. A box model was used to calculate ^{3}H concentrations in the long-term reservoir by the relationship:

$$\frac{dC_g}{dt} = - \lambda C_g - k(C_g - C_p) \tag{2.10}$$

where λ is the decay constant for ^{3}H (= 0.08117/year) and k is the inverse of the apparent transit time of water in the long-term reservoir of the basin. The values for the water transit time within the basins and average proportions of the outflow components are compiled in Table 2.7. The values for river basin transit times ranged from 2.5 years for the Kissimmee River basin to 20 years for the Potomac River basin. The transit times indicate the time scale in which the basin responds to anthropogenic inputs. The modelled ^{3}H concentrations for the basins also furnish input data for urban and agricultural settings where the water of these rivers is used.

Table 2.7 Results for a number of USA rivers of model calculations (Eq.2.9) of the fractions of "direct" runoff from precipitation Q_P and of "old" runoff, primarily from groundwater Q_G, as well as the reverse value of k, 1/k being the apparent transit time (Eq.2.9).

River basin	Q_P	Q_G	k year $^{-1}$	1/k year
Colorado	0.40	0.60	0.07	14
Kissimmee	0.94	0.06	0.4	2.5
Mississippi	0.64	0.36	0.1	10
Neuse	0.73	0.27	0.09	11
Potomac	0.46	0.54	0.05	20
Sacramento	0.35	0.65	0.1	10
Susquehanna	0.80	0.20	0.1	10

A similar long-term study of the temporal and spatial variation of ^{3}H in precipitation and stream flow was carried out in Germany for the mid-European rivers Rhine, Weser and Elba and their tributaries Main, Mosel and Neckar (Weiss and Roether, 1975; Esser, 1980). The measured ^{3}H values of the Rhine river are shown in Fig.2.15. The numerical model used to evaluate the measurements (Esser, 1980) divides the runoff in a surface and a groundwater component. The groundwater component has also been split into two components of different reservoir size and transit time, namely in a fast and a slow component. Moreover, the ^{3}H balance required a much higher groundwater storage volume for the fast and the slow components than the values calculated from the water balance. Consequently, each groundwater component was subdivided into a "mobile" and an "immobile" volume, between which ^{3}H is exchanged.

The model calculations were carried out for the various rivers individually (Table 2.8). Then, the water balance of the whole area of 300 000 km^2 covered by the catchments of these rivers was established using the area-weighted parameters and input data of the individual rivers. It was found that about 6% of the average annual precipitation of 780 mm flows out after a mean transit time of 2 months. The remaining precipitation infiltrates in the unsaturated zone from which 60% of the total precipitation returns to the atmosphere through evapotranspiration. Therefore, the mean groundwater recharge rate is about 270 mm, which is equally distributed to the fast groundwater reservoir (volume equivalent to a mean thickness of 400 mm, mean residence time 3 years) and the slow groundwater reservoir (mean thickness of 6000 mm, mean residence time 40 years). Adopting a transit time through the unsaturated zone of 0.5 years and using the average values for runoff and residence time values for the surface flow and the two groundwater flow components, the mean residence time of the runoff in the whole study area has been estimated to be 20 years. It should be noted that this residence time includes the tritium exchange between the mobile and immobile reservoirs, whereas the transit times listed in Table 2.8 represent the transit time of the water, which is given by the ratio (mobile volume)/ (runoff rate).

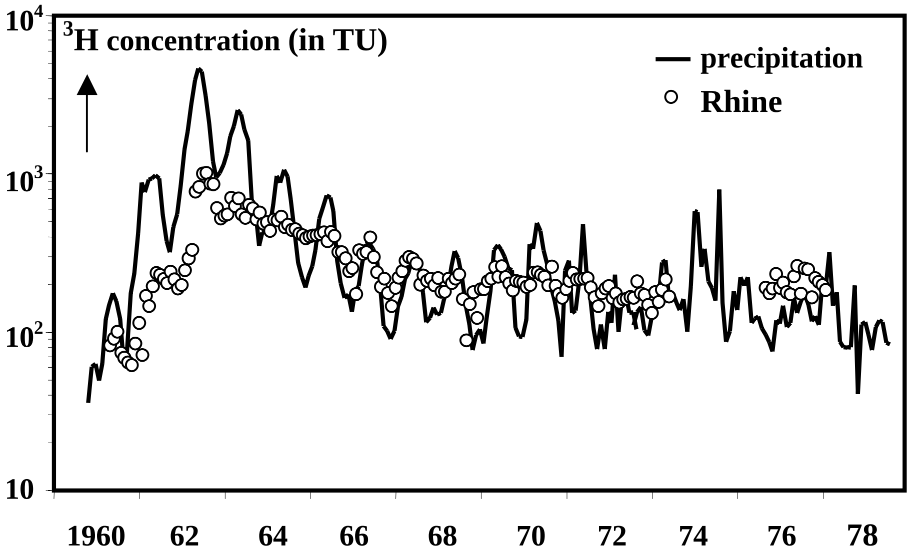

Fig.2.15 ^{3}H concentration of the river Rhine at Emmerich and in precipitation of the catchment area (cf. Fig.2.12) (after Esser, 1980).

Among the longest continuous record of ^{3}H in river water is the one of the Danube at Vienna, Austria (Fig.2.16). The basin of the Danube river extends from the Schwarzwald (Black Forest) in Germany down to the Black Sea. At Vienna, the Danube drains an area of 101 700 km^2.

A recent evaluation of the ^{3}H data (Yurtsever, 1999) considered two runoff components, a fast component (surface flow) and a slow component (groundwater discharge). The following results have been obtained for the catchment area upstream of Vienna: (i) the mean transit time of the surface runoff: 10 months; (ii) mean transit time of the groundwater runoff: 140 months; (iii) fraction of the groundwater flow in the total runoff: 36%. Thus, the average travel time (flux weighted mean transit time) of the water in the whole basin is about 57 months. The estimated subsurface flow contribution of 36% agrees quite well with the observed flow regime of the river. The mean low discharge of the Danube River at Vienna, Austria, is 804 m^3/s and the long-term average at this station is 1943 m^3/s.

Table 2.8 Water balance parameters from numerical model calculations for the mid-European rivers Elba, Weser, Rhine and Main (compiled from Esser, 1980).

Parameter	**Elba**	**Weser**	**Rhine**	**Main**	**Mosel**	**Neckar**
Transit time (years)						
• Surface runoff	0.17	0.08	0.17	0.08	0.08	0.04
• Fast groundwater runoff	0.25	0.08	0.08	0.08	0.08	0.08
• Slow groundwater runoff	1	1	1	1	1	1
• Ratio of slow to total runoff	0.47	0.45	0.51	0.38	0.31	0.35
Runoff (mm/a)						
• Surface runoff	20.4	17.0	71.2	15.1	36.5	44.0
• Fast groundwater runoff	82.2	138.0	185.9	128.5	216.5	181.0
• Slow groundwater runoff	72.0	114.0	192.0	80.4	96.0	96.0
Reservoir size (mm)						
• Surface runoff	3.4	1.4	11.9	1.3	3.0	1.8
• Fast groundwater						
Mobile volume	20.5	11.5	15.5	10.7	18.0	15.1
Total volume	320.5	411.5	515.5	310.7	318.0	1015.0
• Slow groundwater						
Mobile volume	72.0	114.0	192.0	80.4	96.0	96.0
Total volume	**7072**	**8114**	**4192**	**3080**	**2596**	**1596**

Assuming that the low discharge represents the average subsurface component, the contribution to the total runoff would be 41.4%, close to the value for the “slow component” as derived from the ^{3}H measurements. However, the ^{18}O measurements (Sect.2.3.2.1) suggest much higher “base flow” values, in winter up to 90%, in summer about 50 % of the Danube runoff at Vienna. In the latter case the runoff was separated into three components (base flow, precipitation, and meltwater). The determination/identification of the isotopic composition of these components is of critical influence on the determination of their relative proportion in the total runoff and, thus, can be considered as one reason for the higher estimates of the base flow component. In general, an exact comparison of the results from all three approaches is hardly feasible, because the runoff separation is based on different definitions of the runoff components. The “slow component” of the ^{3}H approach is not exactly equal to the "subsurface-flow component" defined by the flow-rate approach and/or the "base-flow component" of the stable-isotope approach.

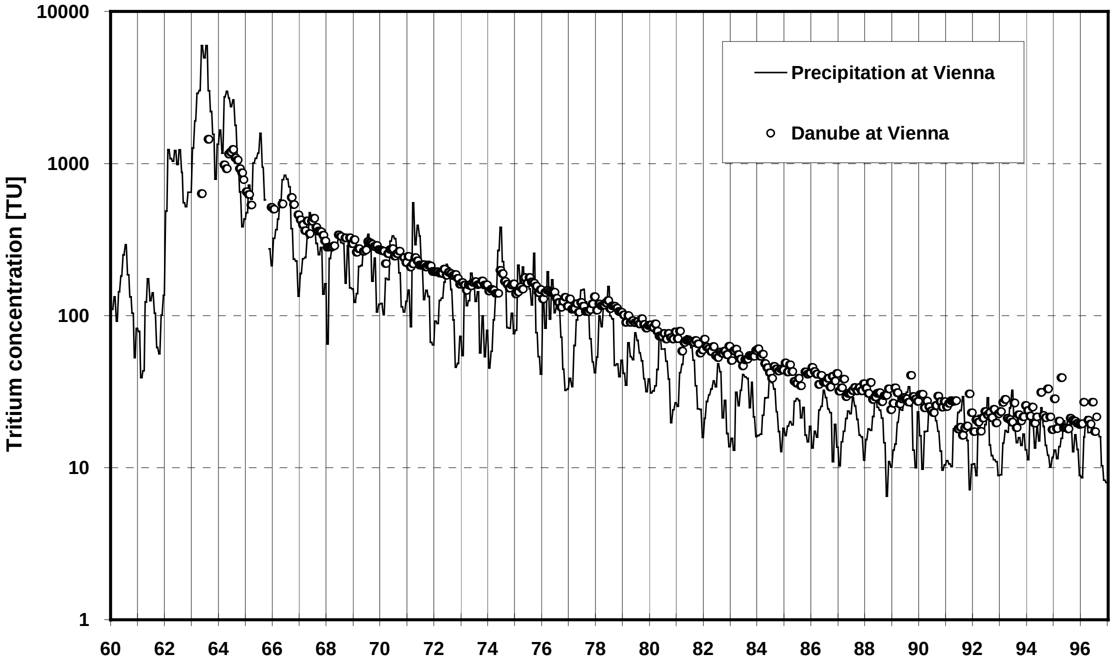

Fig.2.16 ^{3}H in precipitation and in the Danube at Vienna (from Rank et al., 1998).

Similarly to the tracer runoff application of ^{18}O (Sect.2.3.2.2), ^{3}H can in principle be used to study the runoff hydrograph. Compared to ^{18}O, the disadvantage now is that the fluctuations in ^{3}H activity in precipitation are much smaller and generally not correlated with the precipitation intensity. Only for larger streams than rivulets and longer periods of time a comparison can be made of rain and runoff intensity (Fig.2.17). The lower graph also contains a parameter that is considered to be

amount of ^{3}H in precipitation = ^{3}H concentration × amount of precipitation = $^3A \times P$

similar to Fig.2.11. The "amounts" of ^{3}H in the precipitation (blockdiagram in graph E) can be recognised in the ^{3}H runoff, however often with some delay.

2.3.4 ^{13}C IN RIVERS

Among the carbon isotopes, ^{13}C has found the greater part of applications in river studies. ^{14}C is especially suitable as dating tool; therefore it is useful for dating of river sediments and flood events. This section is concentrating on the use of ^{13}C.

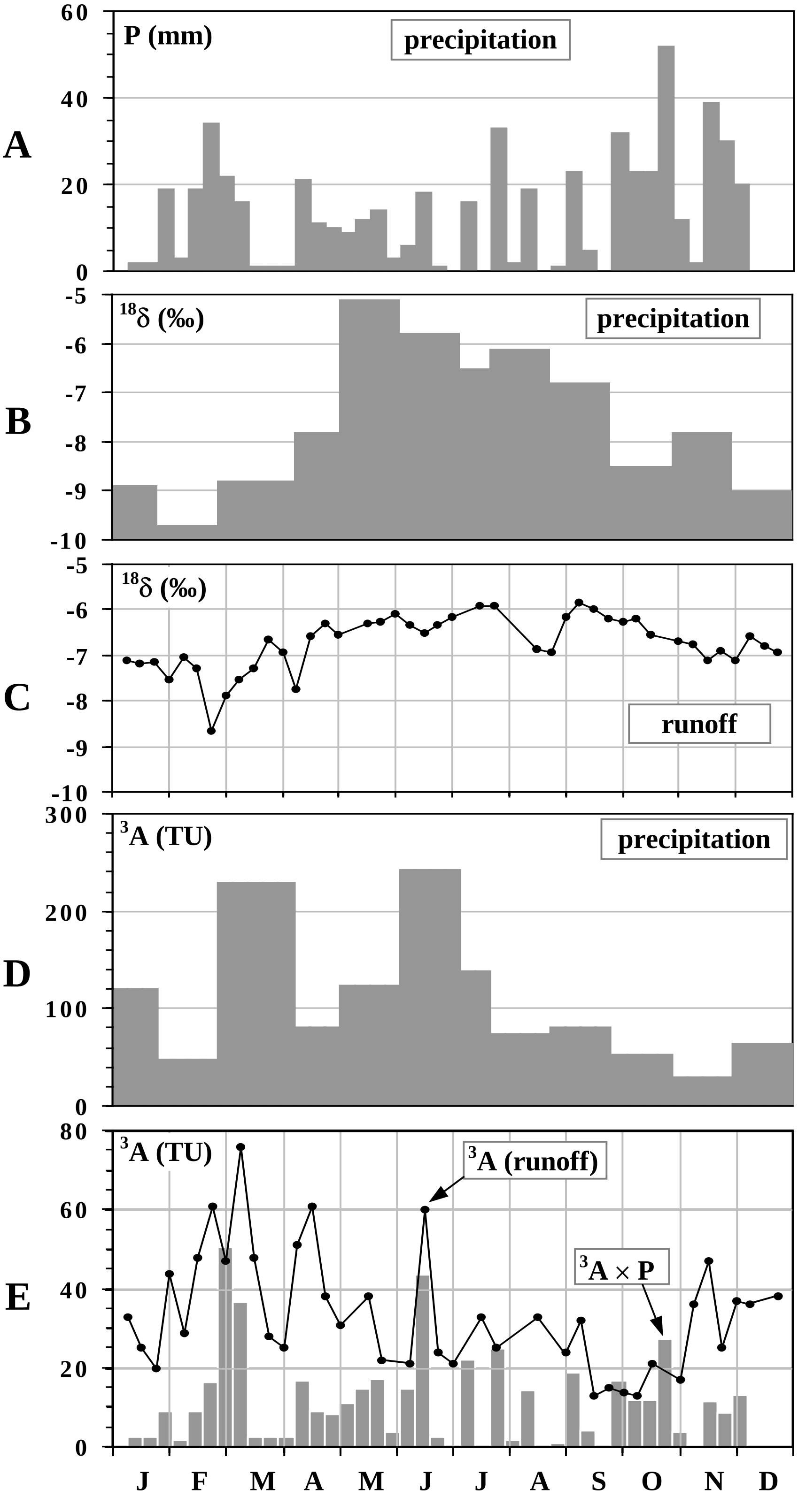

Fig.2.17 One year of weekly runoff sampling of a small river (Drentse A, the Netherlands): **A** precipitation intensity (P), **B** $^{18}\delta$ in precipitation, **C** $^{18}\delta$ in runoff, **D** ^{3}H in precipitation, **E** ^{3}H in the runoff; the block diagram in graph E indicates the "amount" of ^{3}H (= ^{3}A × P) precipitated.

Rivers, linking the terrestrial system and the ocean, transport yearly about $0.3 - 0.6 \cdot 10^{15}$ g of carbon in particulate and dissolved forms, and thus play an important role within the global carbon cycle. In general, *dissolved inorganic carbon* (DIC) and *particulate inorganic carbon* (PIC, primarily $CaCO_3$) contributions to the total carbon flux carried by rivers are globally estimated to be 45% and 15% respectively with the rest being organic matter.

A coupled study of the dissolved and particulate inorganic carbon load improves the constraints on the dissolution-precipitation processes in both the soils and the river. Of the bicarbonate ions in river water, 56 percent stems from the atmosphere, 35% from carbonate minerals, and 9 percent from the oxidative weathering of fossil organic matter. Reactions involving silicate minerals account for 30% of the riverine bicarbonate ions (cf. Sect.2.2.1).

Part of the carbon cycle, especially focussed on the carbon content of riverwater, is shown in Fig.2.18. Generally rivers contain groundwater, i.e. water that has been groundwater. Therefore, the inorganic carbon content originates from carbonate dissolution in the soil by the action of soil CO_2:

$$CaCO_3 \quad + \quad H_2CO_3 \quad \rightarrow Ca^{2+} + 2HCO_3^-$$

with $^{13}\delta$ values of the respective fractions (cf. Fig.2.18):

$$(+2‰ \text{ to } 0‰) + (-26‰ \text{ to } -22‰) = \quad (-13‰ \text{ to } -10‰)$$

Direct measurements have shown that the $^{13}\delta$ values of soil-CO_2 vary between –26 to –22‰, where the enrichment is due to diffusional processes in the soil during transport of CO_2 from the plants roots out into the atmosphere. The rate of diffusion depends largely on the moisture conditions in the soil zone: the drier, the more pronounced the CO_2 diffusion, however the lesser groundwater recharge. Soil carbonate from eroded ancient marine carbonates also varies, as indicated. The resulting groundwater bicarbonate generally has a $^{13}\delta$ of –11 to –12‰.

Riverine processes affect the isotopic composition of the dissolved inorganic carbon content, DIC (Fig.2.18) (Mook and Tan, 1991). These processes are more pronounced in stagnant surface waters as in lakes. They can be summarised as follows.

1) Exposed to the atmosphere -or rather to atmospheric CO_2-$^{13}\delta$ of the riverine DIC may change to higher values due to isotopic exchange, ultimately to values comparable to marine values which are slightly positive. This isotopic exchange proceeds hand-in-hand with chemical exchange, resulting finally in pH values of around 8.5 to 9.0.

2) Direct oxidation of organic matter produces depleted biogenic CO_2 with a $^{13}\delta$ value close to that of labile organic matter, around –26‰.

3) Photosynthesis leads to ^{13}C enrichment of riverine DIC, because of the carbon isotope fractionation of organic matter relative to dissolved HCO_3^- is –23‰, thus producing particulate organic carbon (POC) with $^{13}\delta$ values of about –35‰. On the other hand, rivers may contain terrestrial plant remnants and eroded peat with $^{13}\delta$ values of around –26‰.

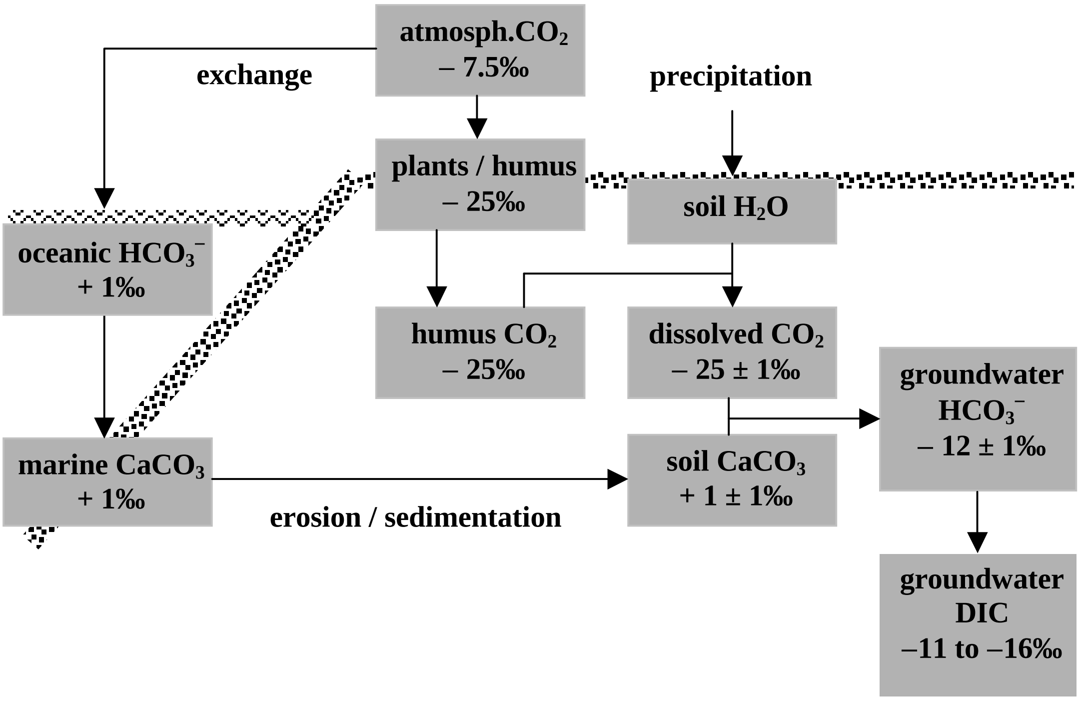

Fig.2.18 Schematic diagram of the sources of dissolved inorganic carbon (DIC) in ground– en riverwater. The $^{13}\delta$ numbers are representative averages. The carbon isotope fractionation values are given in Vol.I, Chapt.7.

As the dissolved inorganic carbon content of rivers is generally far from isotopic equilibrium with the atmosphere, isotopic identification of suspended sediments can generally distinguish between carbonate precipitated in the river versus detrital carbonate originating from the weathering and erosion of the watershed. In general, the $^{13}\delta$ values of inorganic as well as organic matter in rivers is very useful for constraining the carbon sources and processes involved in the riverine carbon cycle.

A three-year monitoring of 3 NW European rivers was carried out during 1967-1969, and its results are shown in Fig.2.5. The winter values of $^{13}\delta$ of the HCO$_3^-$ fraction closely represent $^{13}\delta$ in groundwater. During summer the above processes **1)** and **3)** especially in small and shallow streams and tributaries are considered to be responsible for the ^{13}C enrichment.

Recently, a carbon isotope study of the Rhône system was carried out (Aucour et al., 1999) including both the dissolved and particulate inorganic carbon. The objectives were to (1) understand the dynamics of inorganic carbon in the Rhône system through space and time, and (2) quantify the sources and fluxes of inorganic carbon in the Rhône system. The measurements of $^{13}\delta$ in DIC and PIC were used to trace watershed inputs and fluvial processes affecting the inorganic carbon budget. The measured DIC concentration and $^{13}\delta_{DIC}$ values varied between 1mM at -5‰ near the Rhône source and 3mM at -10‰ near its mouth, whereas tributaries draining lowland, carbonate-dominated areas showed values of 3.8mM and -11‰, respectively. Thus, an inverse relationship between the DIC concentration and $^{13}\delta_{DIC}$ in the river was found (Fig.2.19). The headwaters were characterised by high $^{13}\delta_{DIC}$ values and low DIC, indicating a minor input of respired CO_2. DIC should be mainly produced through the reaction of carbonate with atmospheric CO_2 or organic/sulphuric acids. In lowland, carbonate-dominated areas, $^{13}\delta$ values of -11‰ were consistent with production of DIC by weathering of limestone C ($^{13}\delta \approx -1‰$) with CO_2 derived from the oxidation of organic matter ($^{13}\delta \approx -21.5‰$). The evolution of the Rhône DIC concentration and $^{13}\delta$ appeared to be largely determined by mixing between the Rhône and its main tributaries. The CO_2 fluxes and DIC $^{13}\delta$ mass-balance, calculated for the different segments of the Rhône, point to a net, but very limited input of fluvial respired CO_2 from the oxidation of organic carbon (< 5%). The PIC represented a small but quite variable fraction of the inorganic carbon (< 3%), except on Alpine catchments and during floods where it appeared to be up to 10% of the DIC concentration. It was found that the carbon and oxygen isotopic composition of PIC from the Rhône during a flood and from Alpine tributaries falls within the δ-range of limestone ($^{13}\delta \geq -2‰$; $^{18}\delta \geq -6‰$); relatively light PIC isotopic composition indicate mixing of sedimentary rocks and carbonate precipitated in situ. Data for the Rhône system are typical of watersheds with high chemical weathering rates (for HCO_3), and Alpine/lowland conditions.

A comprehensive study of the carbon species and the carbon isotopic composition of DIC was also carried out in the Rhine river and its tributaries (Buhl et al., 1991). From earlier studies it was known that the Rhine is a net source of CO_2, with P_{CO2} increasing downstream by a factor of 10 to 15 above the atmospheric value of 340 ppm (Fig.2.20). The $^{13}\delta$ values measured in the DIC mirrors the trend of P_{CO2} (Fig.2.21). The $^{13}\delta$ decreases downriver from -4 to about -9‰, reaching a minimum of -10.7‰ below the confluence with the Main river. It also should be noted that the $^{13}\delta_{DIC}$ values of most of the tributaries are markedly lower than the one of the Rhine.

The evaluation of these $^{13}\delta$ results is based on the assumption that organic carbon sources yield $^{13}\delta$ values of -25‰, while dissolution of carbonates and exchange with atmospheric CO_2 introduces $^{13}\delta$ of about 0‰. Balance calculations based on these end members suggest that the proportion of DIC that is derived from organic sources increases from at least 18% in the Alpine Rhine to 43% at the confluence with the Main river.

This tributary derives about 60% of its DIC from an organic source. Note that these are minimal estimates, because of continuous equilibration with atmospheric CO_2 that tends to shift the $^{13}\delta_{DIC}$ to heavier values (Chapter 3: Vol.I, Sect.7.1.4.1). Consequently, the carbon isotope data seem to support the suggestion from a previous study that the production of excess CO_2 in the river is a result of internal microbial respiration fuelled by nutrient pollution.

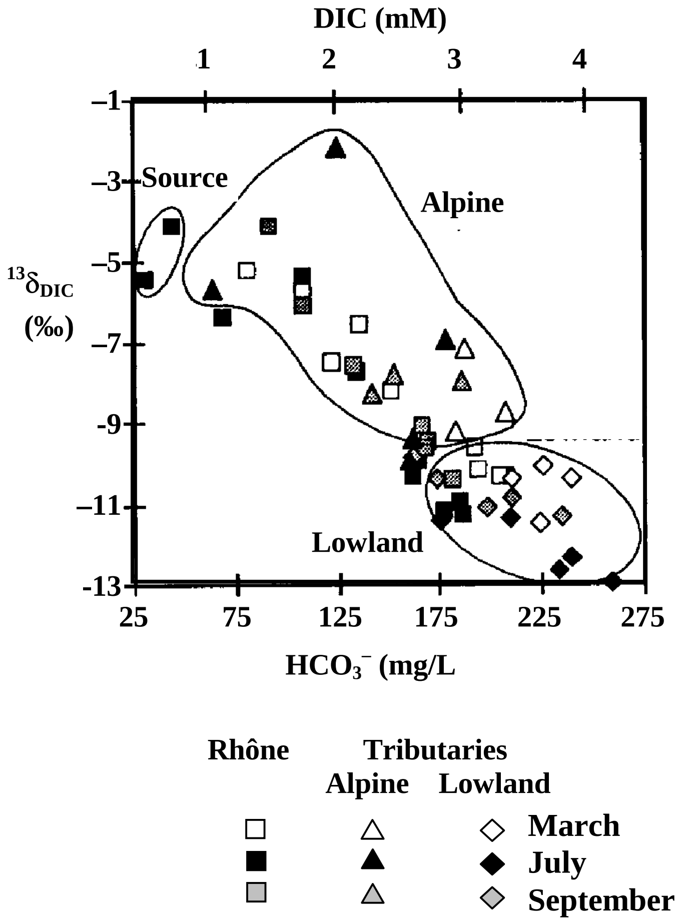

Fig.2.19 Scatter diagram of $^{13}\delta_{DIC}$ versus HCO_3^- concentration for the Rhône and tributaries, including fields for Alpine and Lowland tributaries (from Aucour et al., 1999).

Given the low $^{13}\delta_{DIC}$ values of some tributaries, it is also feasible that the tributaries control, or at least strongly influence, the CO_2 budget of the Rhine.

Yang et al. (1996) reported about an interesting finding related to the St. Lawrence system, which consists of the St. Clair, Detroit, and St. Lawrence rivers. They found that the $\delta^{13}C_{DIC}$ values in the St. Lawrence system range from –4.7‰ to +0.7‰ and are considerably heavier than the values for the tributaries, which lie between -16.5 and –6.7‰. The light values for the tributaries suggest that CO_2 from bacterial respiration plays an important role in the isotopic composition of the riverine DIC. However, in the main stem river(s), this bacterial signal is masked by isotopic equilibrium with atmospheric CO_2 due to the long residence time of the water in the Great lakes. In this connection it should be noted that the authors found δ^2H and $\delta^{18}O$ values in the St. Lawrence system (ranging from -60.9 to –44.5‰ and from –8.5 to –6.1‰ SMOW, respectively), which were much heavier than the corresponding values measured for the tributaries (–92.8 to –58.3‰ and –13.1 to –8.5). These values are compatible with isotope enrichment due to evaporation occurring in the Great Lakes system.

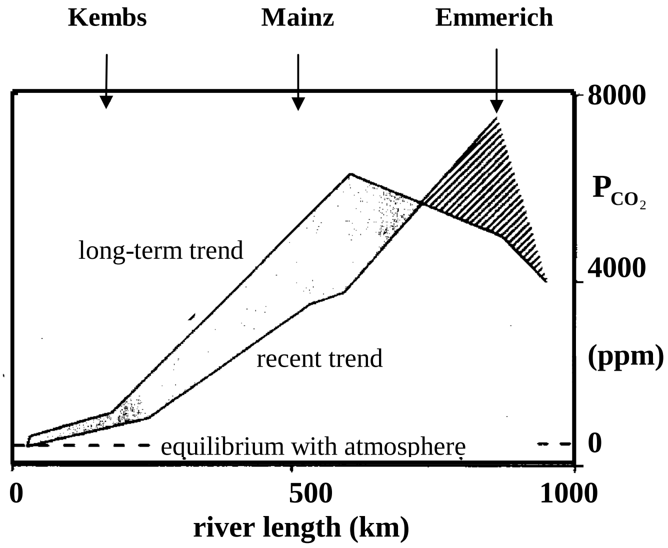

Fig.2.20 Downriver evolution of P_{CO2} for the Rhine river. The curve denoted "long-term trend" characterises the long-term anthropogenic impact to the evolution of P_{CO2}, as observed during the 1960s and the early 1970s, while the second curve represents the trend observed during the late 1980s (from Buhl et al., 1991).

2.3.5 Sr ISOTOPES IN RIVERS

The strontium isotopic composition of river water is in first instance controlled by the geology of the catchment area. The stable strontium isotope ^{87}Sr is a decay product of the primordial radionuclide ^{87}Rb (half-life = 4.8×10^{10} years, average natural abundance in the element strontium = 27.83%). Thus, the older the rocks in the catchment area and the higher the proportion of Rb-rich silicate in the rocks, the higher are the ^{87}Sr/^{86}Sr ratios of the water interacting with the rocks. In fact, Sr isotope studies of rivers have shown that variations in the ^{87}Sr/^{86}Sr ratio and Sr concentration are primarily caused by mixing of waters of various origins with different ^{87}Sr/^{86}Sr ratios and Sr contents resulting from water-rock interaction with different rock types. It was also found (Buhl et al., 1991) that natural background, controlled by geology, could be swamped by pollution, for example from salt mining activities in the catchment area.

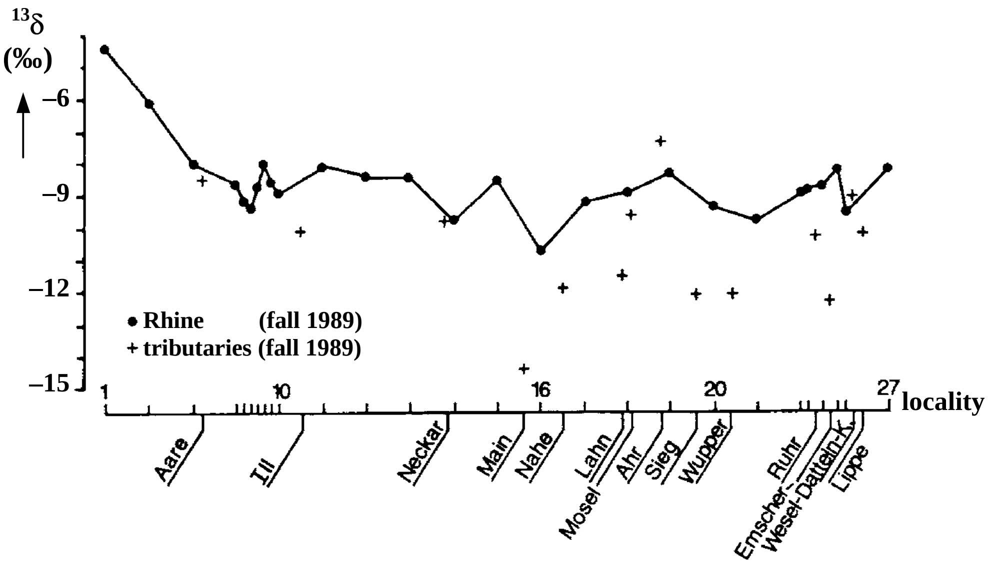

Fig.2.21 $^{13}\delta$ of DIC in the river Rhine and its tributaries (from Buhl et al., 1991).

Sr isotopes in combination with dissolved concentrations of major ions, trace elements (Rb and Sr) and stable water isotopes have been measured in a recent study of the Maroni river and its tributaries (Négrel and Lachassagne, 2000). The Maroni River drains a basin of 60 000 km^2 and flows down to the Atlantic Ocean between French Guiana and Surinam. The samples were taken during a low flow period. Plotting the measuring results of these samples in a ^{87}Sr/^{86}Sr vs. 1/Sr diagram (Fig.2.22), two mixing trends in the Maroni catchment can be discerned, which infer the existence of at least three end-members, one of which is common to both mixing lines. This end-member corresponds to the drainage of the mainly volcanic Lower Paramaca (P, basalts and amphibolites). The second end-member (highest ^{87}Sr/^{86}Sr ratio) may correspond to the drainage of the Upper Paramaca (S, schist and mica schist). The third end-member (low ^{87}Sr/^{86}Sr ratio associated with low Sr content) is considered to correspond to the drainage of granitoid intrusions.

The tributaries are scattered along the two mixing lines between the three end-members. No sample lies on a mixing line between the Upper Paramaca (S) and the granitoids. The Maroni samples plot along the mixing line between the end-members corresponding to the drainage of the Lower Paramaca (P) and that of the Upper Paramaca (S). Thus, it is the weathering of these two geological units that mainly control the ^{87}Sr/^{86}Sr ratio of the Maroni River. The shift of the points to the right of the mixing line between S and P reflect the input into the Maroni of tributaries draining weathered granitoids. Fig.2.22 shows that about 50% of the Sr in the Maroni river originates from the weathering of either P or S units.

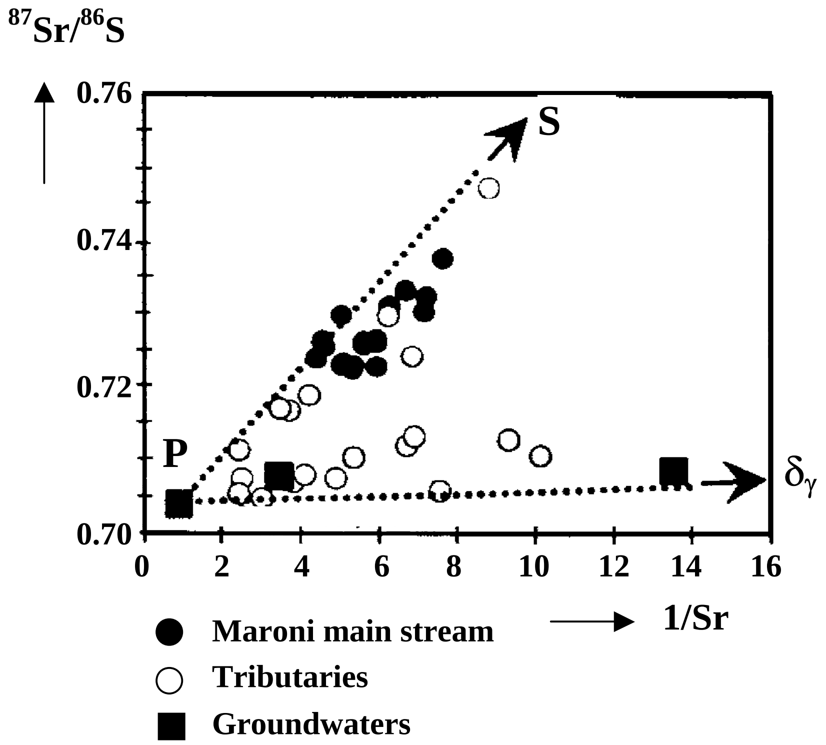

Fig.2.22 $^{87}Sr/^{86}Sr$ vs. 1/Sr of samples taken from the Maroni river and its tributaries. Note that Sr concentrations are given in µmol/L (from Négrel and Lachassagne, 2000).

3 ESTUARIES AND THE SEA

Estuaries are the regions where rivers discharge into the sea. Estuaries are therefore characterised by the mixing process of river- and seawater, resulting in *brackish* water. There are two parameters that are chosen to indicate the degree of mixing, the *brackishnes*, i.e. the percentages of fresh riverwater and salt seawater:

1) the *chlorinity*, Cl, defined as the total concentration of *halide* (chloride + bromide + iodide); this is measured by a titration procedure after which the $Cl^- + Br^- + J^-$ concentration is recalculated into NaCl and given in g/kg of water sample or in ‰; oceans have on average a chlorinity of 19.1‰

2) the *salinity*, S, defined as the salt concentration, also in g/kg or ‰; as in reality the salt content is difficult to measure, it is being calculated from the chlorinity by using the conversion equation Eq.3.1; the salinity of average seawater is 34.5‰.

The chemical composition of ocean waters is extremely constant. That is to say, the relative concentrations of the constituents, apart from dilution by pure water, is very constant throughout the world oceans. Therefore, a relation exists between the chlorinity and the salinity:

$$S = 1.80655\ Cl \qquad \textbf{(3.1)}$$

The physical method to determine the salinity of seawater is to measure the electrical conductivity and using existing tables for the conversion to salinity.

For brackish water -the word *brackish* is actually limited to water having a salinity of less than 25‰- this procedure is less accurate, as in an estuary seawater is not diluted by pure water. This means that the only accurate method is then by titration.

3.1 ISOTOPES IN THE SEA

3.1.1 ^{18}O AND ^{2}H IN THE SEA

Epstein and Mayeda (1953) were the first to analyse seawater for $^{18}O/^{16}O$. Based on their results, Craig (1961a) defined Standard Mean Ocean Water (Volume I: Sect.7.2.3). Values reported for various water masses are given in Table 3.1.

Table 3.1 Values of the hydrogen, oxygen isotopic composition and salinity in deep water of various oceans and marine basins (data from Anati and Gat. 1989; Epstein and Mayeda, 1953; Craig and Gordon, 1965; Ferronski and Brezgunov, 1989; Redfield and Friedman, 1965).

Ocean	**$^{18}\delta$ (‰)**	**$^{2}\delta$ (‰)**	**S (‰)**
Arctic		+2.2 ± 1.0	
N. Atlantic	+0.12	+1.2 ± 0.8	34.9
S. Atlantic		–1.3 ± 0.6	
Pacific	–0.2 ± 0.3	1.4 ± 0.4	34.7
Antarctic	–0.2 to –0.45	–0.9 to –1.7	34.7
Indian	–0.2 ± 0.2		34.7 ± 0.2
Mediterranean	+1.5 ± 0.2		39.0 ± 0.2
Baltic Sea	> –7 ± 1*		> 4*
Black Sea	–3.3 ± 0.2		
Red Sea	+2.5		

*Values for the freshwater component; higher values are found by admixture of seawater.

Larger variations and deviations from $^{18}\delta$ = 0‰ are found in ocean surface waters, where:

1) seawater is subject to evaporation (Persian Gulf: +2‰, equatorial surface waters: +0.7 ± 0.2‰)

2) coastal waters contain variable amounts of freshwater runoff from continental rivers; even in the Arctic Ocean the influence of the large rivers of the Siberian continent can be detected

3) polar waters contain variable amounts of meltwater (Polar Ice Sea from the Siberian rivers)

In the latter two cases $^{18}\delta$ is linearly related to the salinity, like in estuaries. In the first case evaporation causes ^{18}O enrichment, which is therefore also correlated with salinity.

During glacial periods in the past large amounts of water were withdrawn from the oceans and precipitated as vast ice sheets at the polar regions of the North American and Eurasian continents. The available estimates suggest that this ice had the ^{18}O content between -25‰ (*Laurentide ice sheet*, Remeda et al., 1993) and -23‰ (*Fennoscandian ice sheet*, Vaikmae et al., 1999). Consequently, $^{18}\delta$ of the glacial oceans must have been higher. Recent estimates suggest that $^{18}\delta$ of the global ocean during the Last Glacial Maximum was higher by 1 to 1.3‰ (Shackleton et al., 1987; Schrag, et.al., 1996).

3.1.2 ^{13}C IN THE SEA

The $^{13}\delta$ value of total dissolved inorganic carbon in seawater varies between 0 and +2.5$^{o}/_{oo}$, the majority of data between +1 and +2$^{o}/_{oo}$. The corresponding range of $^{13}\delta$ values of the largest fraction, i.e. bicarbonate, has to be calculated by correcting for the different $^{13}\delta$ values of the three constituents (CO_2, HCO_3^- and CO_3^{2-}) by about +1‰.

The isotopic composition is hardly affected by seasonal changes in temperature of in $^{13}\delta$ of atmospheric CO_2, because of the relatively low exchange rate. However, biological activity causes $^{13}\delta$ variations: growth of algae involves a fractionation of about -20 to -23$^{o}/_{oo}$, so that a consumption of 5% of C_T by algae results in a $^{13}\delta$ change of +1$^{o}/_{oo}$.

3.2 ISOTOPES IN ESTUARIES

3.2.1 ^{18}O AND ^{2}H IN ESTUARIES

In a region of mixing between freshwater (f) and seawater (m) the parameters $^{18}\delta$ and $^{2}\delta$ behave *conservatively*, i.e. $^{18}\delta$ and $^{2}\delta$ only depend on the mixing ratio of both components, as does the salinity (S) and chlorinity (Cl) (Volume I: Sect.4.3). For $^{18}\delta$ as well as:

$$\delta = \frac{f\delta_f + m\delta_m}{f+m} \tag{3.2}$$

and

$$S = \frac{f\,S_f + m\,S_m}{f+m} \qquad \text{or} \qquad Cl = \frac{f\,Cl_f + m\,Cl_m}{f+m} \tag{3.3}$$

where S = 1.80655 Cl. A linear relation between $^{18}\delta$ (and $^{2}\delta$) and the salinity can now be obtained by eliminating f and m from these equations (f + m = 1):

$$\begin{aligned}\delta &= \frac{S(\delta_m - \delta_f) + S_m\delta_f - S_f\delta_m}{S_m - S_f} = \\ &= \frac{(S - S_f)\delta_m - (S - S_m)\delta_f}{S_m - S_f} = \\ &\approx 1 - \frac{S}{35}\delta_f \qquad \text{or} \qquad \approx 1 - \frac{Cl}{19.3}\delta_f\end{aligned} \tag{3.4}$$

The salinity of freshwater can be taken 0‰, while for seawater S_m = 34.9‰ and δ_m = 0‰; δ_f is more or less specific for each river. Linear mixing is illustrated in Fig.3.1A, presenting data from the Western Scheldt estuary from the river Scheldt near Antwerp, Belgium to the North Sea.

The dependence of $^{18}\delta$ and $^{2}\delta$ on salinity is explicitly obtained by differentiating Eq.3.4:

$$\frac{d\delta}{dS} = \frac{\delta_m - \delta_f}{S_m - S_f} \approx \frac{-\delta_f}{35} \qquad \textbf{(3.5)}$$

For North-Atlantic mixing a slope of $d(^{18}\delta)/dS = 0.60$ was found. This comes to a freshwater component with $^{18}\delta \approx -21‰$, presumably representing runoff from the Siberian continent.

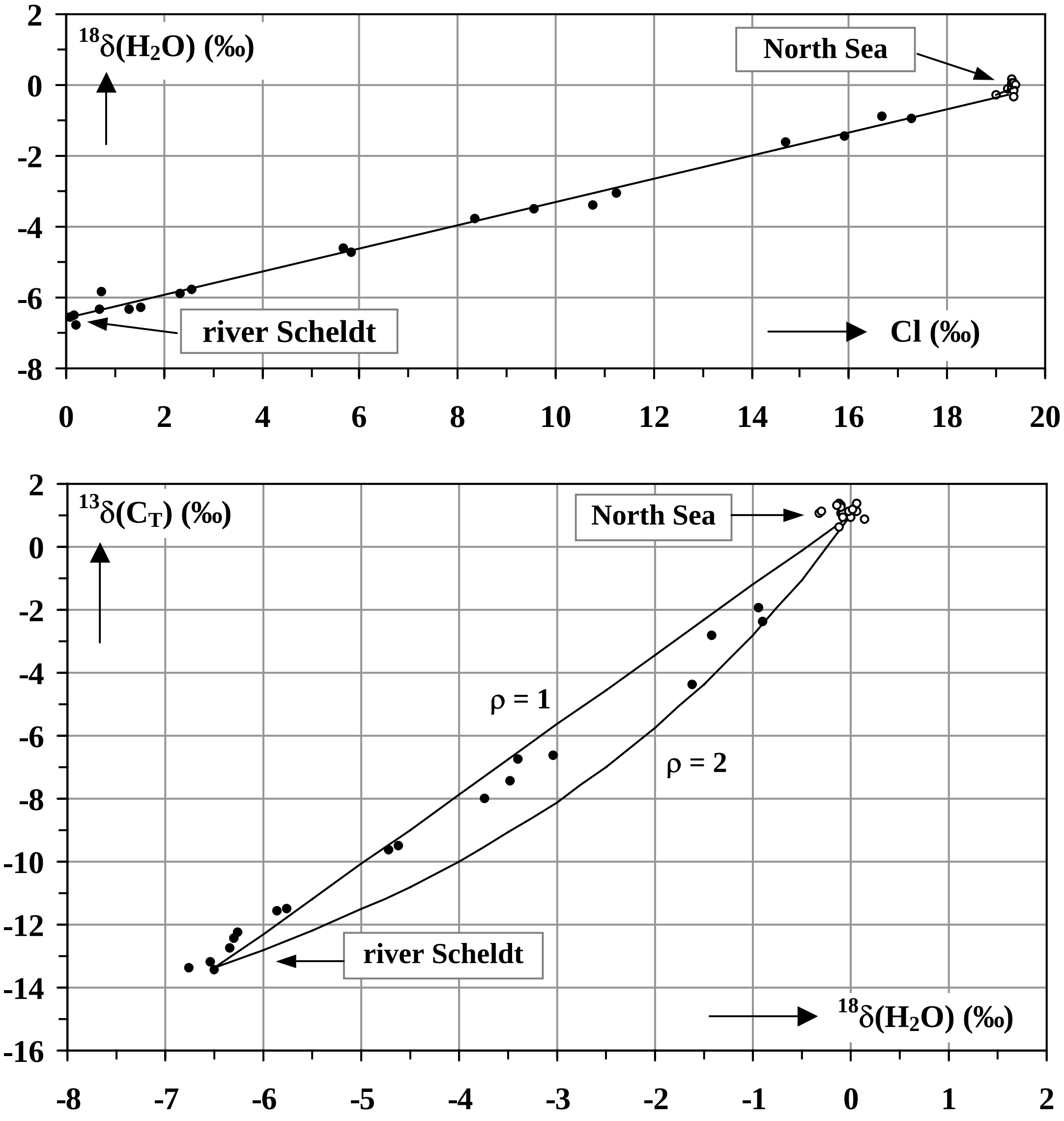

Fig.3.1 **A.** Linear relation between $^{18}\delta$ and the chlorinity (Cl) in the estuary of the Western Scheldt, the Netherlands, and coastal waters of the adjacent North Sea.

B. Relation between $^{13}\delta$ of the total inorganic carbon content (C_T) and $^{18}\delta$ of the water, the latter representing the mixing ratio of the river water and seawater. The line is calculated for two values of the C_T ratio, ρ, of the river water (f) and seawater (m): C_{Tm} = 2mmole/kg; C_{Tf} = 2 and 4mmole/kg) (Eq.3.6).

3.2.2 ^{13}C IN ESTUARIES

An overview of the carbon isotopic composition of particulate organic and inorganic carbon, and of carbonic acid in rivers on the one hand, in the sea on the other, and in estuaries as the mixing regions of the two is given in Fig.3.2.

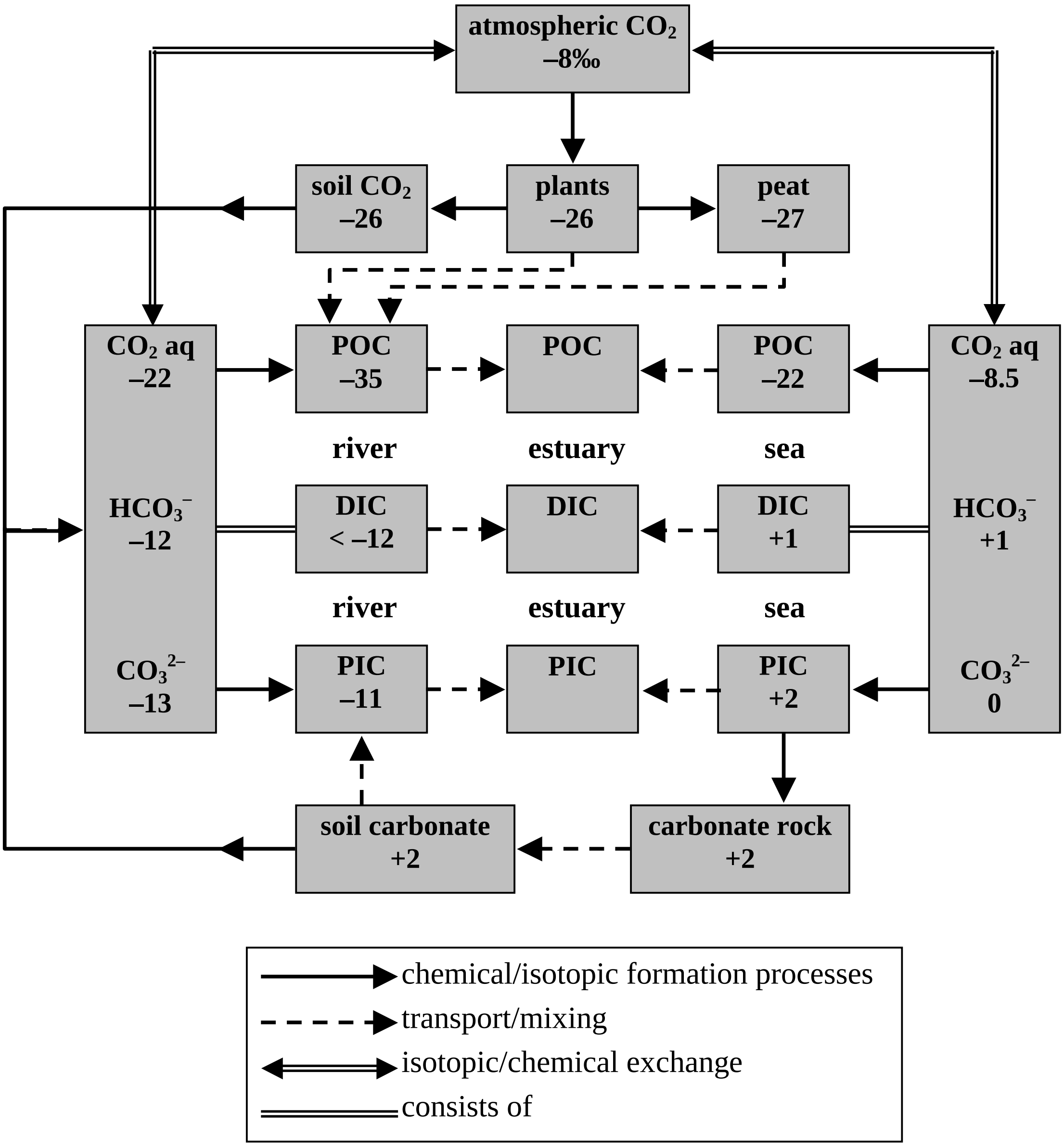

Fig.3.2 Schematic diagram of the sources of dissolved inorganic carbon (DIC), suspended particulate organic carbon (POC) and particulate inorganic carbon (PIC, primarily CaCO$_3$) in rivers, estuaries and the sea. The $^{13}\delta$ numbers are representative averages. The carbonic acid and carbonate isotope fractionation values are given in Vol.I, Ch.7 (from Mook and Tan, 1991).

Further processes affecting the $^{13}\delta$ of the DIC fractions are discussed in Sect.2.3.4 and Sect.3.3.2. The $^{13}\delta$ values shown in the diagram are more or less representative. Depending on the natural conditions deviations may occur of a few ‰, especially in the organic matter data.

The $^{13}\delta$ value of the total dissolved inorganic carbon in an estuary is determined by the mixing ratio of river- and seawater, as are $^{18}\delta(H_2O)$ and the chlorinity (Sackett & Moore, 1966; Mook, 1970) (Fig.3.1B). However, the result of a linear mixing of the two water components does not necessarily result in a linear relation between $^{13}\delta$ and the mixing ratio. The reason is that in general the C_T values of the freshwater and seawater are not equal.

The relation between the total carbon content, C_T, $^{13}\delta_T$, and $^{18}\delta$ follows from the ^{13}C mass balance:

$$^{13}\delta_T = \frac{(C_{Tf}\,{}^{13}\delta_f - C_{Tm}\,{}^{13}\delta_m)\,{}^{18}\delta + C_{Tm}\,{}^{13}\delta_m\,{}^{18}\delta_f - C_{Tf}\,{}^{13}\delta_f\,{}^{18}\delta_m}{(C_{Tf} - C_{Tm})\,{}^{18}\delta + C_{Tm}\,{}^{18}\delta_f - C_{Tf}\,{}^{18}\delta_m}$$

$$= \frac{(\rho\,{}^{13}\delta_f - {}^{13}\delta_m)\,{}^{18}\delta + {}^{13}\delta_m\,{}^{18}\delta_f - \rho\,{}^{13}\delta_f\,{}^{18}\delta_m}{(\rho - 1)\,{}^{18}\delta + {}^{18}\delta_f - \rho\,{}^{18}\delta_m} \qquad \textbf{(3.6)}$$

where f and m refer to the fresh and seawater, respectively and $\rho = C_{Tf} / C_{Tm}$, often in the range of 1 to 2. A comparison between measurements in the Western Scheldt estuary, the Netherlands, and calculated curves is shown in Fig.3.1B.

The above linear mixing of water ($^{18}\delta$) and C_T resulting in Eq.3.6 is only valid if the total dissolved carbon as well as ^{13}C are conservative, i.e. no production or consumption of carbon, and no isotopic exchange, and no additional inflow of water from another branch occurs during the course of the estuary. However, we have to emphasise that under these conditions this does result in a linear relation between $\delta^{13}C_T$ and $^{18}\delta$ (or Cl) only if C_{Tf} and C_{Tm} are equal, in other words if the total (inorganic) carbon content of the river water is equal to that of seawater (=2mmole/kg).

3.3 ESTUARINE DETAILS

3.3.1 THE RELEVANCE OF $^{13}\delta(HCO_3^-)$ VERSUS $^{13}\delta(C_T)$

In the preceding section we have seen that under certain conditions the carbon contents of seawater and riverwater is to be mixed in order to calculate the expected values of C_T and $^{13}\delta(C_T)$. However, studying processes that take place in the estuarine water requires to focus the attention to one of the fractions that constitute the dissolved carbonic acid (=CO_2aq + HCO_3^- + CO_3^{2-}). For instance, $CaCO_3$ is precipitated from CO_3^{2-}, algae consume CO_2aq. Each process has its specific (temperature dependent) isotope fractionation.

The point however is that, even if the carbon isotopic composition of the total carbon content does not change with temperature, the isotopic composition of the fraction does, because the relative concentrations of the fractions depend on temperature. The essence of this statement is that we can not speak of an isotope fractionation between $CaCO_3$ or organic carbon (such as in algae) and DIC. Therefore, when studying processes, $^{13}\delta$ of a specific fraction is to be known. For a specific temperature these can be calculated with known fractionation values(ε) and the acidity (dissociation) constants of H_2CO_3. Details are given in Volume I, Sect.9.5.4. The required constants for brackish water are given in Table 9.1.

3.3.2 LONG RESIDENCE TIME OF THE WATER

Specifically in estuaries, the distance over or/and the time during which the water components mix may be very long. Then the carbon as well as the oxygen isotopic compositions may change, because of isotopic exchange with the ambient atmospheric CO_2 and evaporation, respectively.

3.3.2.1 ISOTOPIC EXCHANGE WITH THE ATMOSPHERE

Broecker and Walton (1959) were the first to report quantitative information about the first process. The exchange rate evidently strongly depends on the turbidity of the water and thus on the wind. Fig.3.3 shows the result of a simple experiment, in which tapwater was exposed to the atmosphere at different degrees of turbidity (stirring) (Mook, 1970).

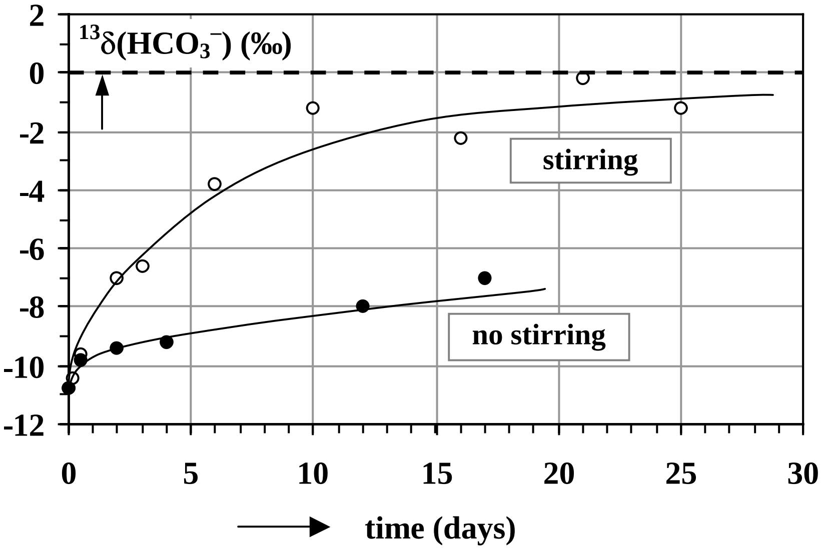

Fig.3.3 Result of a simple exchange experiment between regular tapwater and atmospheric CO_2 with $^{13}\delta$ in the range of –8 to –8.5‰ at about 20°C; $^{13}\delta$ of the HCO_3^- fraction changes towards isotopic equilibrium with atmospheric CO_2: $-8.5‰+{}^{13}\varepsilon_{b/g} \approx 0‰$. The influence of the turbidity of the water is obvious (Mook, 1970).

3.3.2.2 EVAPORATION DURING THE WATER FLOW

Fig.3.4 shows a simple model of the isotopic shift of $^{18}\delta$ because of evaporation. During its flow towards the sea the water is subjected to evaporation, changing both the oxygen and the hydrogen isotopic composition (see Volume I, Sect.4.4.5). The figure shows the Rayleigh model as well as the gradual shift of the ($^{18}\delta$,$^{2}\delta$) relation along the *evaporation line*.

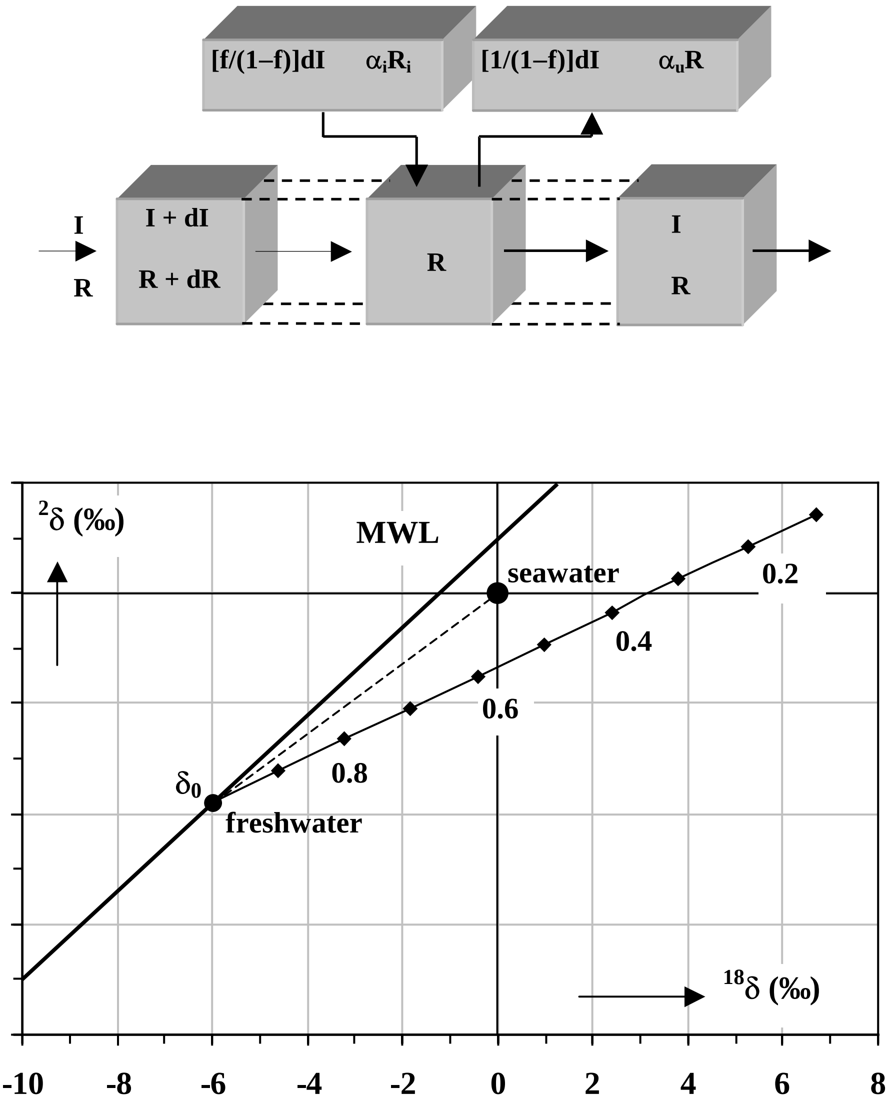

Fig.3.4 Model for calculating the shift of $^{18}\delta$ and $^{2}\delta$ of river water subjected to a relatively long residence time in its estuary (see Volume I, Sect.4.4.5). The relevant parameters are similar to the example of Fig.4.9 in Volume I. MWL denotes the Global Meteoric Water Line. The values along the "evaporation line" refer to the fractions of water remaining after evaporation. The evaporation process is quantitatively discussed in Chapter 4 of this volume. The dashed line represents estuarine mixing.

In Fig.3.4 also the "mixing line" is drawn, applicable to estuaries, i.e. the mixing between fresh riverwater and seawater. The conservative character is valid for ^{2}H as well as for ^{18}O.

4 LAKES AND RESERVOIRS

4.1 INTRODUCTION

Lakes are the most easily available water resources, extensively being used in many parts of the world. Together with other surface water bodies (wetlands, artificial surface reservoirs) they cover millions of km^2 of continental area and constitute an essential component of the regional and global water cycles. Lakes are seen nowadays as important contributors to the carbon, nitrogen and phosphorous cycles on continents through various processes such as the production of autochthonous organic matter, the sedimentation of detrital organic matter, and the precipitation of carbonates and evaporites. Lacustrine sediments also belong to the most important continental archives of climatic and environmental changes. The stored material can be used to decipher the recent climatic evolution in various parts of the globe with a resolution attainable only for ice cores.

The rapidly increasing anthropogenic impact on surface water systems in many parts of the world resulted in a heavy load of pollutants of various types such as phosphorous and nitrogen compounds, heavy metals and agrochemicals, causing rapid deterioration of the water quality. This in turn rises public concern and the realisation that this valuable resource should be preserved and protected against human activities. Some countries have meanwhile taken extensive actions, considerably improving the surface water conditions.

This chapter will focus on proven successful applications of environmental isotopes and trace substances for addressing problems related to the dynamics of lake systems. Emphasis is laid on deriving components of the water balance of these systems and quantifying interconnections with adjacent groundwater bodies. The tracers being used to address the above-mentioned problems are summarised and briefly characterised in Table 4.1. The discussion will focus on the background and application of tracer methods to lake systems, emphasising the underlying physical, chemical and mathematical aspects of the various methods, sampling strategies, etc.

The discussion that follows is by no means exhaustive. It is intended to provide a general guidance in solving most common practical problems related to the management of lakes using tracer methods. The reader interested to learn more about specific tracer methods applied to lakes and reservoirs should consult the publications listed at the end of this volume.

4.1.1 CLASSIFICATION AND DISTRIBUTION OF LAKES

According to the definition in the Encyclopaedia Britannica, a lake is "a body of slowly moving or standing water that occupies an inland basin". An operational definition for management purposes sets a lower limit to a lake volume of about 1000 m^3 (Meybeck, 1995). For lakes located in floodplains there is a continuum between lakes and other water bodies without continuous and permanent vegetation cover and wetlands. At the upper end of the volume scale, the Caspian Sea is here also considered as a lake, but not the Baltic Sea or the Black Sea, as these are in direct connection with the world ocean. Within this chapter, we will consider both *natural lakes* formed in natural depressions as well as *artificial water bodies* created by human activities, such as ponds, dredging lakes and artificial reservoirs created by dam constructions.

Table 4.1 Isotope and chemical tracers used to study lake dynamics.

Tracer	**Characteristics**	**Type of problems being addressed**	**Status**
^2H, ^{18}O	- stable isotopes of hydrogen and oxygen; - part of water molecule	- quantification of water balance - interaction with adjacent groundwater field	- often used, mostly to derive groundwater inflow/outflow rates
$^3H/^3He$	- radioactive isotope of hydrogen (^3H) and its daughter product, ^3He (noble gas)	- "dating" of lake water - intensity of vertical mixing	- proven applicability - requires sophisticated mass spectrometer
CFCs: Freon-11 Freon-12	- trace gases present in the atmosphere soluble in water	- "dating" of lake water - intensity of vertical mixing	- proven applicability - measurement by gas chromatography
SF_6	- inert gas artificially injected into a lake	- quantification of vertical and horizontal mixing	- proven applicability - measurement by gas chromatography
Dyes	- substances injected into surface inflows to lakes (rivers, canals, pipes)	- delineation of pollutant plumes - identification of stagnant zones and preferential pathways in lakes	- proven applicability

To characterise the regional and/or global distribution of lakes, two parameters are commonly used: the *lake density* and the *limnic ratio*. Lake density is simply defined as the number of lakes within a given lake-size category found in the region in question, divided by the total area of this region (number/km^2). The limnic ratio is defined as the ratio between the total area of lakes (all size categories) and the total area of the surveyed region (km^2/km^2 or %). It varies over more than two orders of magnitude: from less than 0.1% for the non-glaciated part of the United States, to more than 10% in some deglaciated shields. The limnic ratio depends on three independent factors: climate, tectonics and lithology. Table 4.2 summarises the global distribution of lakes, classified according to their origin.

Table 4.2 Global distribution of lakes (Meybeck, 1995).

Type of Lake	Area (10^3 km^2)	Volume (10^3 km^3)
Saline:		
Caspian Sea	374	78.2
Other saline lakes without contact with open ocean	204	4.2
Saline coastal lakes	40	0.1
Freshwater:		
Tectonic	424	54.6
Glacial	1247	38.4
Fluvial	218	0.6
Crater	3	0.6
Miscellaneous	88	1.0
Total	**2598**	**177.7**

Lakes are not permanent features of the Earth’s surface: they develop, gradually fill up, and disappear. The life cycle of lakes can vary in a wide range: from a few weeks for lakes caused by landslide dams that eventually break up, up to millions of years for large lakes of tectonic origin. However, the greatest part of the world's lakes is associated with the last deglaciation period and reveal ages between approximately 12 000 and 6 000 years BP.

4.1.2 MIXING PROCESSES IN LAKES

Mixing is defined as a process leading to the reduction of spatial gradients in water (Imboden and Wüest, 1995). This can result from motion at a microscopic level, controlled by molecular diffusion, and can be due to advection and turbulence phenomena operating on a macro scale. In most cases mixing processes in lakes are highly variable in both time and space. This variability mainly stems from the temporal and spatial structure of the principal driving forces, i.e. weather and climate. The topography of the lake and its surroundings may also be responsible for heterogeneous mixing.

The differences in water density induced by temperature and/or salt concentration changes are of great importance for the pattern of vertical mixing in lakes. For lakes that are vertically not well mixed because of differences in density, the upper less dense and well-mixed region is called *epilimnion* (comparable to the *mixed layer* in oceans). Typically, this region follows the regional temperature changes and is more turbulent than the deep, more dense and relatively undisturbed region, the *hypolimnion*. The intermediate region of relatively rapid change of parameters (temperature, density) is called *metalimnion*. The plane of maximum temperature change with depth is called the *thermocline*. In most lakes the latter is established during summer due to gradual warming of the upper layers of lake water. Because of a relatively stable density structure, it constitutes an efficient barrier against vertical mixing. The so-called *overturn* is the seasonal mixing process occurring in lakes in autumn when the epilimnion gradually cools down to temperatures lower than the average temperature prevailing in the hypolimnion. Some lakes are permanently stratified and are called *meromictic*. The deeper, stable region of such lakes is called *monimolimnion,* whereas the upper region through which most water flows is referred to as the *mixolimnion* (Hutchinson, 1957).

4.2 WATER BALANCE OF LAKES – TRACER APPROACH

Lakes are complex dynamic systems, interacting with the local environment and connected to the water cycle through both surface and underground inflows and outflows, as well as via precipitation/evaporation fluxes. The interaction with the local environment also includes chemical constituents and mineral phases that are transported from the catchment area to the lake via surface and underground inflows. These leave the lake together with outflowing water or accumulate in the lake sediments. Fig.4.1 schematically illustrates the major functional components of the water budget for a lake system.

All functional components of the lake system shown in Fig.4.1 usually undergo short-term fluctuations, caused by, for instance, the seasonality of the surface input and output. These fluctuations are often superimposed on the long-term trend induced by climatic changes or transformations (natural or man-induced) within the catchment area of the given lake system.

For a proper lake management it is often important to establish the water budget, quantifying all incoming and outgoing water fluxes for the specified time interval.

The water budget of lakes is based on the mass conservation law and has the form of a balance equation:

$$\frac{dV_L}{dt} = I_S + I_G + P - O_S - O_G - E \qquad \textbf{(4.1)}$$

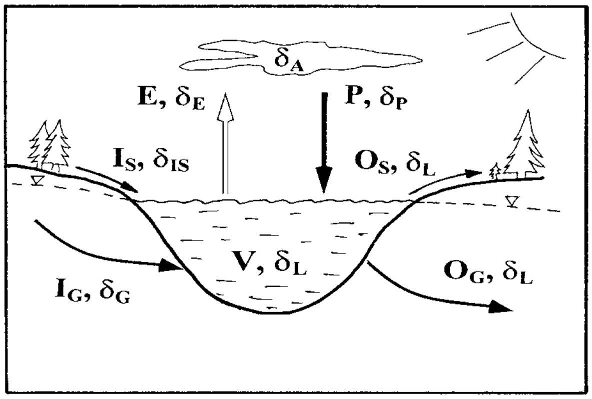

Fig.4.1 Schematic diagram depicting components of hydrological and isotope budget of a lake system. Water fluxes are labelled by capital letters whereas their isotopic composition is marked by corresponding δ values.

V_L is the lake volume, I_S, I_G, O_S and O_G represent the volumetric surface and groundwater inflow and outflow fluxes, respectively, P stands for precipitation over the lake and E is the evaporation flux from the lake. In principle all parameters listed in Eq.4.1 are functions of time. The water density is assumed constant. To derive any given component of the water budget (e.g. the rate of groundwater or evaporation) from Eq.4.1, all other parameters have to be known or to be obtained from independent estimates.

The tracer approach to establishing a lake water budget is based on the fact that the mass conservation law also applies to any trace constituent build-in within the structure of the water molecule (isotopes of hydrogen or oxygen) or dissolved in water (e.g. salts). Consequently, the mass balance equation written for the chosen tracer will have the following general form:

$$C_L \frac{dV_L}{dt} + V_L \frac{dC_L}{dt} = C_{IS}I_S + C_{IG}I_G + C_P P - C_{OS}O_S - C_{OG}O_G - C_E E - S \qquad \mathbf{(4.2)}$$

where C with the respective subscripts represent the concentration of the selected tracer in the lake as well as in all incoming and outgoing water fluxes entering or leaving the system. The last term in Eq.4.2 represents removal of a tracer from the lake by processes other than advection with water fluxes leaving the system. For instance, this can be radioactive decay (if a radioactive tracer is applied), a chemical reaction, or adsorption on sedimenting particles. If one has adequate knowledge of tracer concentrations in all functional components of the lake system as functions of time, Eqs.4.1 and 4.2 can be solved numerically for the required pair of variables.

In hydrological practice one rarely has sufficient information to directly apply Eqs.4.1 and 4.2. Moreover, usually we are not interested in short-term fluctuations but rather in the average state of the studied lake system as characterised by long-term mean values of the above parameters. If their variability is reasonably low (i.e. in the order of 10 % of their respective values) and the lake system is sufficiently "old" (cf. Sect.4.2.1.3.1), one may assume that the studied system is in a steady state, both with respect to the bulk mass of water and to the tracer applied:

$$\frac{dV_L}{dt} = 0 \quad \text{and} \quad \frac{dC_L}{dt} = 0 \qquad \textbf{(4.3)}$$

4.2.1 HYDROGEN AND OXYGEN ISOTOPES

The stable isotopes of water, ^{2}H and ^{18}O, have been shown to be the most useful tracers in establishing a lake water balance, in particular concerning the subsurface components. The stable isotope method of determining the water balance of lakes is based on the fact that the evaporation process leads to a measurable increase of $^2\delta$ and $^{18}\delta$ of the lake water. The degree of evaporative enrichment is controlled by meteorological variables such as the atmospheric relative humidity over the lake and the surface water temperature, and is correlated with the lake water balance. The isotopic composition of evaporating lake water will evolve along the ($^{18}\delta$,$^2\delta$) line which has a slope significantly smaller than eight (cf. Fig.4.2). The isotope- mass balance equation (Eq.4.2) has the following form for the ^{18}O (^{2}H) tracer:

$$\delta_L \frac{dV_L}{dt} + V_L \frac{d\delta_L}{dt} = \delta_{IS} I_S + \delta_{IG} I_G + \delta_P P - \delta_{OS} O_S - \delta_L O_G - \delta_E E \qquad \textbf{(4.4)}$$

where the δ values represent the concentrations of ^{18}O and ^{2}H in corresponding functional components of the system. It is assumed here that the isotopic composition of the groundwater outflow is identical to the isotopic composition of the lake water ($\delta_{OG} = \delta_L$). This assumption is fulfilled if the lake is well mixed. In such case also the isotopic composition of the surface outflow is equal to that of the lake water ($\delta_{OS} = \delta_L$).

Assuming that a given lake is hydrologically and isotopically in a steady state (Eq.4.3), Eqs.4.1 and 4.4 can be solved simultaneously for the required pairs of variables (e.g. groundwater inflow and outflow rates), provided that the remaining parameters are known and represented by the long-term averages:

$$I_G = I_S \left(\frac{\delta_{IS} - \delta_L}{\delta_L - \delta_{IG}} \right) + P \left(\frac{\delta_P - \delta_L}{\delta_L - \delta_{IG}} \right) + E \left(\frac{\delta_L - \delta_E}{\delta_L - \delta_{IG}} \right) \qquad \textbf{(4.5)}$$

$$O_G = I_S + I_G + P - E - O_S \qquad \textbf{(4.6)}$$

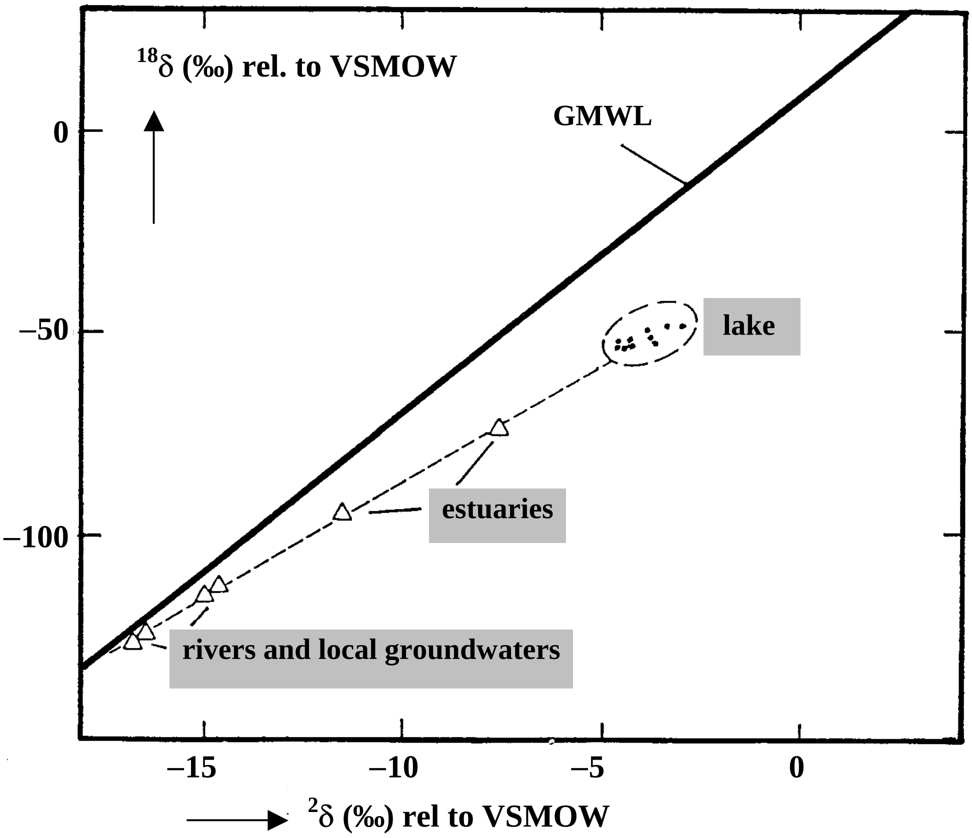

Fig.4.2 $^{2}\delta$-$^{18}\delta$ relationship for water samples collected from the Titicaca Lake and the rivers feeding the lake. Titicaca is a large tropical lake, located on the border between Bolivia and Peru, at an elevation of 3800 m above sealevel. There is a remarkable isotope enrichment of the lake water with respect to the river inflow, by more than 10‰ in $^{18}\delta$ (modified from Fontes et al., 1979).

These solutions can be further simplified, depending on the specific situation of the studied system. For instance, if the lake has no surface inflow or outflow, the first term in Eqs.4.5 and 4.6 disappears. If the system has only surface inflow and outflow and the question is what the evaporation losses are, the balance equations yield the following solutions:

$$I_S = P \cdot \left(\frac{\delta_P - \delta_E}{\delta_E - \delta_{IS}} \right) + O_S \cdot \left(\frac{\delta_E - \delta_L}{\delta_E - \delta_{IS}} \right) \qquad \textbf{(4.7)}$$

$$E = P + I_S - O_S \qquad \textbf{(4.8)}$$

The most difficult parameter to quantify in Eqs.4.5 and 4.7 is the isotopic composition of the net evaporation flux δ_E. It cannot be measured directly. Typically, the average δ_E value is calculated using Eq.1.4 and the long-term averages of the corresponding variables. In particular, the mean isotopic composition of atmospheric moisture (δ_A) is usually derived from the annual weighted mean isotopic composition of local precipitation, assuming isotopic equilibrium at the ground-level temperature. However, this way of calculating the average value for δ_E is only valid in cases where the seasonal distribution of precipitation is similar to the seasonal distribution of the evaporation flux from the lake. In general, it is recommended that the annual mean value of δ_E is calculated as the weighted average of monthly δ_E values (weighted by the monthly evaporation flux), derived using the isotopic composition of monthly precipitation and the corresponding monthly mean temperatures and relative humidities.

4.2.1.1 SAMPLING STRATEGY – GATHERING REQUIRED INFORMATION

Properly planned and implemented isotope studies aimed at quantifying the water balance of lakes or surface reservoirs require carefully designed sampling strategies, taking into account already available information, local conditions, envisaged costs, etc. Generally, regular observations should be carried out for at least one full year in order to quantify the seasonal variability of the parameters needed for isotope-mass balance calculations.

4.2.1.1.1 Precipitation (P, δ_P)

For isotope-mass balance calculations, monthly values of the amount of precipitation and the isotopic composition over the studied lake are required. Due to logistic reasons it is often not possible to obtain precipitation data for the lake itself, so that one has to rely on samples collected at near-by meteorological stations. Alternatively, regular collection of rainfall samples should be organised at selected sites close to the lake. The number of stations depends on the lake size - for relatively small lakes one station is sufficient.

Specific rules (see also the general sampling rules given in Vol.I, chapter 10) have to be observed when collecting precipitation samples for isotopic analyses. Rainfall samples should be poured from a rain gauge shortly after each precipitation event and the collected water stored in tightly closed containers. Alternatively, a small amount of paraffin oil can be added to the rain gauge to prevent evaporation of the collected water. In doing so, the water can be collected at the end of each month. Proper closing of storage bottles is essential since any evaporation will modify the isotopic composition of the stored water. The same concerns all other types of water samples being collected during sampling campaigns. At the end of each month, an aliquot of 20-50 ml should be transferred from the container into a plastic bottle with double stopcock and put aside for isotopic analyses. The collected samples should be stored in controlled conditions, away from direct sunlight and heat sources, with periodic checking of the bottles, in order to prevent evaporation losses.

If meteorological stations are located in the vicinity of a lake, it is advisable to obtain long-term statistics of precipitation in the area and compare these with actually measured values. If a regular collection of local rainfall is not feasible, samples collected from small creeks and springs in the vicinity of the lake may provide a first rough estimate of the mean isotopic composition of local rainfall.

4.2.1.1.2 Surface inflows and outflows (I_S, δ_{IS}, O_S, δ_{OS})

The isotope-mass balance approach requires adequate knowledge of both the flux of water flowing in and out of the studied lake system as well as its isotopic composition. Thus, systematic determinations of both quantities have to be arranged for major inflows/outflows. For inflows (rivers) with a distinct flow rate seasonality, discharge and isotope measurements should be carried out every month or at least during high and low flow conditions.

Although it is usually assumed that the isotopic composition of surface outflows is identical with that of the lake water ($\delta_{OS} = \delta_L$), it is recommended to collect samples of outflowing water in order to prove the validity of this assumption.

4.2.1.1.3 Isotopic composition of lake water (δ_L)

The isotope-mass balance approach assumes that the studied reservoir is well mixed. Again, this assumption has to be carefully assessed. Isotopic homogeneity of the system has to be checked in both horizontal and vertical extensions. Usually, it is sufficient to carry out two sampling campaigns: one during the dry, one during the rainy season. Sampling should include a survey of surface water as well as depth profiles in representative locations of the lake. Whenever possible, sampling for isotopic analyses should be accompanied by measurements of basic physico-chemical parameters (temperature, conductivity, dissolved oxygen).

4.2.1.1.4 Isotopic composition of groundwater inflow (δ_{IG})

A survey has to be made of existing boreholes and dug wells in the vicinity of the studied lake in the most probable directions of groundwater inflow. Since the isotopic composition of shallow groundwater usually does not reveal a significant short-term variability, it is not necessary to carry out systematic monthly observations at all accessible sites. It is usually sufficient to perform two sampling campaigns in contrasting seasons (e.g. maximum of the dry and wet period, respectively) in order to characterise the isotopic composition of the groundwater component of the total inflow to the lake. When sampling dug wells, it is important to make sure that the wells are exploited and the sampled water is not subject to evaporation.

4.2.1.1.5 Evaporation flux (E, δ_E)

For evaluating groundwater inflow/outflow rates from isotope-mass balance considerations, the evaporation rate from a lake (E) has to be known. There are several methods in use to estimate the *evaporation rate* from an open water body (see e.g. Brutsaert, 1982; Ikebuchi et al., 1988; Sene et al., 1991):

1) **by the water balance method**; this can be applied if the remaining components of the lake water balance (including changes of water storage in the lake) are known and monitored with sufficient precision; the evaporation rate for the studied period is calculated as residual of the mass balance

2) **from evaporation pans**, as operated by meteorological stations; this technique provides the most easily accessible information on the magnitude of the evaporation flux; however, since Class A pans located on a shore of a lake normally overestimate evaporation by 10 to 50% (Kohler, 1954), correction factors are needed to derive lake evaporation from pan data; the magnitude of this correction depends on local conditions such as the size of the lake, local meteorology, etc.

3) **by the energy balance method**; this is considered to be the most precise but it requires sophisticated instrumentation at the site to measure the heat balance for the evaporating surface; in cases where for logistic reasons it is not possible to install adequate instrumentation for the energy balance method, it is recommended to use an evaporation pan installed on a floating platform and submersed in the lake water; this will likely provide evaporation data which are much closer to real evaporation from the lake than Class A pans operated on the shore; moreover, such submersed pan(s) can be used to estimate δ_E (see below)

4) **from an aerodynamic profile;** this method involves measurements of wind velocity, air temperature and humidity at at least two different heights above the evaporating surface

5) **by the eddy correlation technique;** this is a direct method of assessing the evaporation flux; it relies on measurements of fluctuations with time of the vertical components of wind velocity, air temperature and wet-bulb temperature, respectively; the measurements are difficult to perform and are used only in basic experiments

6) **by the Penman approach,** based on an empirical formula derived from the energy balance and aerodynamic method.

Special studies aimed at comparing different methods of estimating E for lakes suggest that these methods are consistent within 10-20% (Sene et al., 1991; Gibson et al., 1996).

The isotopic composition of the net evaporation flux (δ_E) cannot be measured directly and, therefore, has to be calculated from Eq.1.4. It is also recommended to calculate the average δ_E as a weighted mean of monthly δ_E values (weighing by monthly values of the evaporation flux E). Calculation of δ_E using Eq.1.4 requires knowledge of the mean monthly values of four measurable parameters: isotopic composition of atmospheric moisture above the lake (δ_A), air temperature above the lake (T_{air}), water temperature of the lake surface (T_{water}) and the relative humidity above the lake (h).

The way most often applied is to calculate δ_A from monthly δ_P values assuming isotope equilibrium at groundlevel temperature. Published results of simultaneous monitoring of the isotopic composition of precipitation and atmospheric moisture suggest that for moderate climates this assumption is usually fulfilled (Rozanski, 1987; Jacob and Sonntag, 1991). Only during winter months, when snow is the dominating type of precipitation, the collected precipitation may be isotopically depleted with respect to the equilibrium value. This method of estimating δ_A does not work satisfactorily in arid or semi-arid regions or during extensive dry periods in the tropics.

An alternative method of estimating δ_A uses constant-volume Class A evaporation pans (Allison and Leaney, 1982; Gibson et al., 1999) operated on the lake shore or, preferably, submersed pans operated on a floating platform. Such constant-volume evaporation pans simulate the behaviour of a terminal lake placed under analogous climatic conditions as the studied lake. For a constant-volume pan shielded from rainfall E = I and, after reaching an isotopic steady-state, $\delta_I = \delta_E$. Consequently, from Eq.1.4 one can derive the following relation for δ_A:

$$\delta_A = \left[\alpha_{V/L}\delta_{LP} - \delta_I(1 - h_N - \varepsilon_{diff}) + \varepsilon_{tot}\right] / h_N \qquad \textbf{(4.9)}$$

where δ_{LP} is the steady-state isotopic composition of water in the evaporation pan and δ_I stands for isotopic composition of water being added to the pan to maintain constant volume. Thus, to obtain δ_A from Eq.4.9 one should know the δ value of water being added to the pan to compensate for evaporation losses. Preferably, this should be water from local inflow to the studied lake. After filling up the evapometer and allowing sufficient time for reaching isotopic steady-state (cf. Sect.4.2.1.3.1), the water in the evapometer has to be sampled and analysed periodically (e.g. weekly). Adequate instrumentation is to be installed on the site to monitor the local meteorological parameters (h_{air}, T_{air}, T_{water}). The evapometer should be operated for the entire observation period. The disadvantage of this approach is that such observation station requires daily maintenance (compensating the evaporation losses by inflow water, shielding during rainfall events, measuring the air temperature and relative humidity). Permanent shielding is not recommended, because it might create local micrometeorological conditions over the pan different from those prevailing over the lake. However, the operations can relatively easily be automated by installing temperature and humidity recorders and devices maintaining constant water level in the evapometer, and by shielding the instrument against rainfall. Monthly mean δ_A values obtained in that way can be further inserted in Eq.1.4 to calculate monthly mean values of δ_E for the studied lake.

Another way of obtaining information about δ_A with the aid of evaporation pans is recommended when daily access to installations is difficult. It can be shown (Froehlich, 2000) that when the evapometer is filled with lake water, the initial slope of the evaporation line is given by the following approximate relationship:

$$s_{LP} \approx \frac{h_N(\delta_L - \delta_A) + \varepsilon_{tot}}{1 - h_N} \qquad \textbf{(4.10)}$$

The initial slope s_{LP} is derived from the evaporation line defined by δ values of subsequent portions of water collected from the pan, plotted as a function of the remaining fraction of water F. The remaining fraction F is defined as $F = V/V_o$, where V and V_o is the actual and initial volume of water in the pan. δ_L is the isotopic composition of the lake water used to fill up the pan, δ_A is the isotopic composition of atmospheric moisture, h_N is the normalised relative humidity and ε is the total isotope fractionation.

The evaporation line can be established by filling up the evapometer with lake water, collecting daily samples of water from the pan and reading the changes of the water volume in the pan over the first few days. Such evaporation experiments should be run monthly. They can be performed in the same pan which is used to monitor the evaporation rate. One has to remember that before each evaporation experiment the pan should be emptied completely and filled again in with a new portion of the lake water. One also has to remember that Eq.4.10 is valid if there is no input of rainfall during the experiment. As in the case of the constant-volume pan method, adequate instrumentation should be installed to monitor the local meteorological parameters (h_{air}, T_{air}, T_{water}) during each evaporation experiment.

To calculate monthly mean δ_E values from Eq.1.4, in addition to δ_A also the mean monthly values of relevant meteorological parameters are required (surface air temperature, relative humidity, and surface water temperature of the lake). Usually, the mean air-based temperature and relative humidity data can be obtained from meteorological station(s) situated in the vicinity of the lake. However, information about mean monthly temperatures of the lake surface are generally not available. Thus, it is recommended to perform regular surveys of water temperature and air temperature on the lake with portable instruments. Whenever possible, the relative humidity over the lake should also be measured. Measuring campaigns on the lake, carried out at least once a month during the entire observation period, should help to identify possible differences between the mean monthly air and water temperature. Such spot measurements, however, cannot provide precise data. Therefore, whenever possible and logistically feasible, adequate instruments should be installed on the lake site (on a floating platform) to monitor the required parameters. With today’s available sensor technology and data acquisition techniques such solution is within reach of a typical project budget.

Still another method of evaluating δ_E can be applied if in the vicinity of the studied lake another lake is located, that has no outflow (surface or underground). Such lake is called a *terminal lake*. The isotope enrichment of a terminal lake with respect to the isotopic composition of the total inflow can be expressed by the following approximate equation (Gat and Bowser, 1991):

$$\Delta\delta = \delta_{LS} - \delta_{IN} \approx h_N (\delta_A - \delta_{IN}) - \varepsilon_{tot} \qquad \textbf{(4.11)}$$

where δ_{LS} is the steady-state isotopic composition of the terminal lake, δ_{IN} is the isotopic composition of the total inflow to the terminal lake, h_N is the normalised relative humidity over the lake and ε is total isotope fractionation as defined in Eq.1.4. From Eq.4.11 one can derive the δ_A value and insert it into Eq.1.4 defining δ_E for the studied lake. Such approach was adopted for the first time by Dinçer (1968) for several lakes in Turkey.

4.2.1.1.6 Simplified approach

In case of not easily accessible lakes or due to other logistic reasons it is sometimes not possible to carry out a complete observation and measurement programme as outlined above. However, even reconnaissance sampling of the investigated lake system and other waters in the study area (rivers, springs, dug wells, etc.) may provide a first rough estimate of the investigated components of the water balance. In order to use the isotope-mass balance equations, several simplifying assumptions have to be made:

1) the system is in hydrologic and isotope steady-state

2) the mean annual temperature of the surface water in the lake is identical to the mean annual surface air temperature in the area

3) the weighted mean annual isotopic composition of local rainfall is equal to the isotopic composition of the shallow groundwater in the area

4) the mean isotopic composition of the atmospheric water vapour above the lake is in isotopic equilibrium with the local precipitation.

The mean annual relative humidity and surface air temperature in the area can be assessed from the data obtained at the nearest meteorological station. If the annual evaporation rate can be estimated independently (evaporation pan data from the nearest meteorological station and/or other estimates), the isotope-mass balance equations can be used to derive the required components of the water balance. If no information is available on the magnitude of the evaporation flux, the ratio of the total inflow to the evaporation flux for the studied lake system can be derived from the following approximate relationship, valid for the hydrologic and isotopic steady state of the system (Gat and Bowser, 1991):

$$\delta_{LS} - \delta_{IT} \approx \frac{\delta_A - \delta_{IT} - \varepsilon_{tot} / h_N}{1 + \frac{I_{tot}}{E} \frac{1 - h_N}{h_N}} \tag{4.12}$$

where:

I_{tot}	total inflow to the lake (surface and underground components plus rainfall)
E	evaporation rate
h_N	relative humidity over the lake
δ_A	isotopic composition of atmospheric moisture over the lake. It can be calculated from Eq.4.13 assuming that isotopic composition of local rainfall is represented by springs and rivers in the vicinity of the lake
δ_{LS}	measured isotopic composition of the lake
δ_{IT}	estimated isotopic composition of total inflow, based on isotopic composition of sampled rivers, springs, dug wells and rainfall
ε_{tot}	$= \varepsilon_{V/L} + \varepsilon_{diff}$ = the total effective isotope fractionation as defined in Eq.1.4.

If it can be assumed that the isotopic composition of atmospheric water vapour is in isotopic equilibrium with the total inflow, Eq.4.12 can be further simplified (Gat and Bowser, 1991):

$$\delta_{LS} - \delta_{IT} \approx \frac{-(1 - h_N)\,\varepsilon_{V/L} - \varepsilon_{diff}}{h_N + (1 - h_N)\frac{I_{tot}}{E}} \tag{4.13}$$

where $\varepsilon_{L/V}$ stands for equilibrium fractionation factor between liquid water and water vapour, whereas ε_{diff} represents the kinetic (diffusion) effect defined by Eq.1.5.

Using Eq.4.12 or 4.13 it is possible to gain first insight into the dynamics of the studied system even with limited number of samples analysed. Such rough assessment based on reconnaissance sampling will provide a basis for further decisions with respect to eventual full-scale investigation.

Fig.4.3a illustrates how the isotopic enrichment of lake water depends on the hydrology of the system and on local climate. The isotope enrichment for ^{18}O, $^{18}\delta = \delta_{LS} - \delta_{IT}$, is plotted as a function of humidity deficit, for different ratios of the total inflow to evaporation rate (I_{tot}/E). This figure may serve as a quick reference for identifying the type of water balance of the studied system (evaporation-controlled or through-flow system). Eq.4.13 can be re-arranged to derive the steady-state isotopic composition of a lake, as a function of the isotopic composition of the total inflow and the hydrology of the system. If $^{2}\delta$ is plotted versus $^{18}\delta$, the steady-state isotopic composition of lake water (δ_{LS}) and of the net evaporative flux (δ_E) move with a changing hydrology (I_{tot}/E ratio) along the line that is called the *evaporation line* (Fig.4.3b).

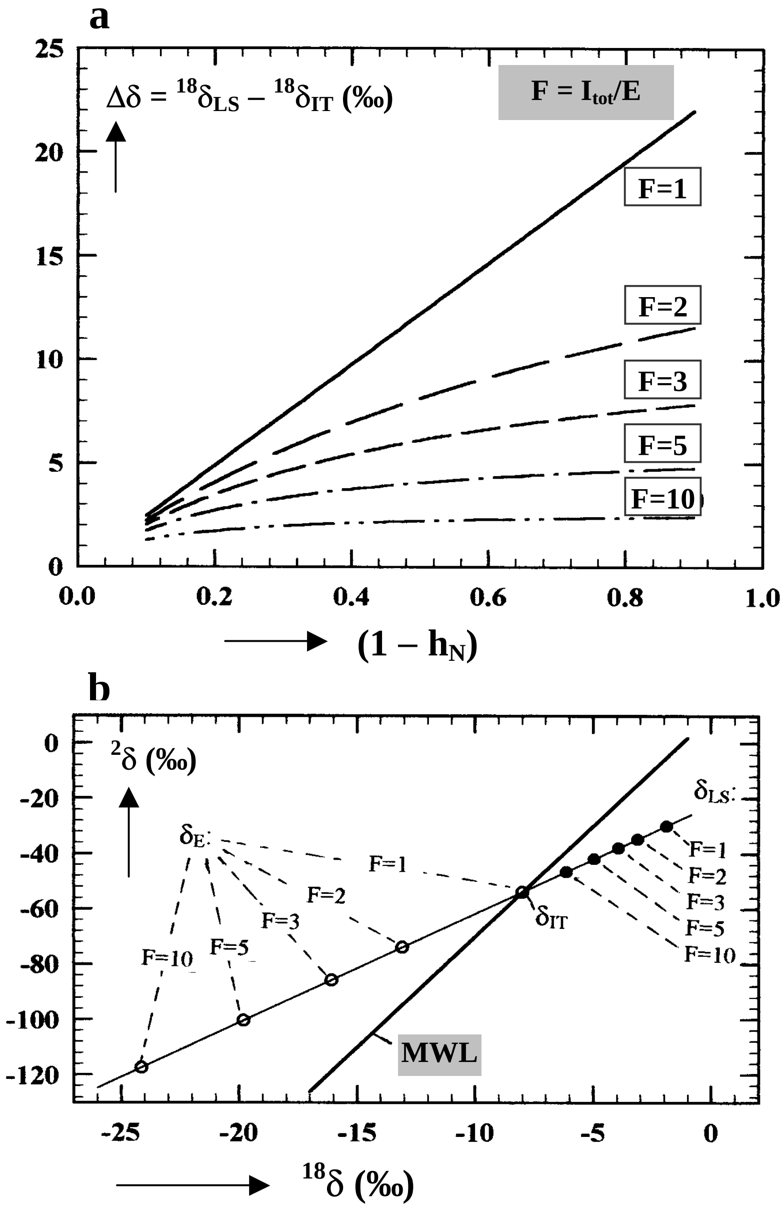

Fig.4.3 **a)** The steady-state ^{18}O isotopic enrichment of a lake water ($\Delta^{18}\delta = {}^{18}\delta_{LS} - {}^{18}\delta_{IT}$) as a function of humidity deficit ($1 - h_N$) and the ratio of total inflow to evaporation rate ($F=I_{tot}/E$). It was assumed that atmospheric water vapour is in isotopic equilibrium with the total inflow.

b) Evolution of the isotopic composition of lake water and the net evaporation flux with changing hydrology of the system (varying ratio of the total inflow to evaporation). It is assumed that atmospheric water vapour is in isotopic equilibrium with the total inflow. Calculations were performed using Eq.4.13, with the isotopic composition of total inflow located on Global Meteoric Water Line ($^{18}\delta_{IT}$ = -8‰ and $^{2}\delta_{IT}$ = -54‰) and relative humidity h_N = 0.75.

4.2.1.1.7 Tracer selection: ^{18}O or ^{2}H

As indicated above, $^{18}\delta$ and $^{2}\delta$ of meteoric waters are strongly correlated, clustering along the so-called meteoric water line when $^{2}\delta$ is plotted versus $^{18}\delta$. Also, isotope enrichments for both isotopes resulting from evaporation are linearly related (cf. Fig.4.3). Consequently, isotope-mass balance calculations based on ^{18}O or ^{2}H should yield identical results and the choice of a tracer should depend only on analytical constraints or preferences.

Already the first applications of the isotope-mass balance approach revealed persisting difficulties in reconciliation the water balance of lakes, derived independently from $^{18}\delta$ and $^{2}\delta$ data. The reason for this apparent discrepancy between ^{18}O and ^{2}H balances remains unclear. The discrepancy is particularly visible for evaporation-dominated systems (Zuber, 1983). Practical experience gathered so far suggests that ^{18}O provides much more reliable results than ^{2}H. Also, comparison of isotope-based estimates of evaporation fluxes from lakes with direct measurements (Gibson et al., 1996) point to ^{18}O as the tracer to be preferred. However, it is strongly recommended to carry out both analyses for all collected samples, even if the water balance will after all be constructed from ^{18}O data only.

4.2.1.2 UNCERTAINTIES OF THE ISOTOPE–MASS BALANCE APPROACH

It is important for practical applications to estimate the accuracy of the water balance components derived from isotope data and to assess their sensitivity to changes in the measured parameters. Using the *law of error propagation* (see Volume I, chapter 13), a comprehensive evaluation of the overall standard uncertainty of the calculated water balance components often appears to be difficult due to incomplete knowledge of the uncertainties involved. Moreover, uncertainties introduced by assumptions made in the process of formulating the isotope-mass balance equations are often difficult to quantify.

In practice, a simplified approach based on a sensitivity analysis is often sufficient to provide the required insight into the uncertainty of the derived component. In such approach, the derived water balance component is being calculated for a selected range of measured parameters, using the isotope mass balance equations. The range of investigated variables should be realistic for the studied system. Both higher and lower values are to be tested as well, since their impact on the calculated parameter is often highly asymmetric. Such procedure identifies the key variables controlling the uncertainty of the derived parameter and contributes to assessing the magnitude of this uncertainty. Table 4.3. illustrates this approach for the case of a small groundwater-fed lake in Austria, created as a result of gravel excavation (cf. Fig.4.9).

Table 4.3 The percentage changes of the groundwater inflow to small dredging lake in Austria, derived from isotope mass balance calculations (^{18}O), for the changes of the respective input parameters by ±10% (Yehdegho et al., 1997).

Parameter	Change of the calculated groundwater inflow rate (%) [a]
Precipitation	–2.0/ +2.0
Water temperature	–2.1/ +2.1
Normalised relative humidity	–9.1/ +6.5
Evaporation	+13.1/ –13.1
Seepage from the upstream lake	–1.8/ +1.8
^{18}O content of precipitation	+17.4/ –17.4
^{18}O content of lake water	–52.4/ +111.9
^{18}O content of seepage from the upstream lake	+24.1/ –24.1
^{18}O content of the groundwater inflow	+86.0/ –31.6

[a]) the number in the columns correspond to the increase/decrease by 10% of the respective input parameter

In literature one can find attempts to quantify the actual uncertainty of water balance components derived from the isotope mass balance. For instance, Zimmerman and Ehhalt (1970) report that δ_E calculated according to Eq.1.4 becomes more uncertain if the relative humidity over the lake approaches 80%. According to their calculations, for typical uncertainties of other parameters involved in water balance calculations the evaporation flux cannot be estimated with an accuracy better than about 30%. On the other hand, in a recent study Gibson et al. (1996) have demonstrated that ^{18}O-based estimates of the evaporation fluxes from small lakes situated in the continental Arctic of Canada were within ±10% of the values derived by other methods (the energy balance method and aerodynamic profile method). For small through-flow lakes showing relatively small evaporative enrichment, the critical parameter controlling the overall accuracy of the isotope mass balance method is the isotopic composition of the lake and of the total inflow (cf. Table 4.3). The subsurface components of the water balance of such lakes can be estimated using ^{18}O-based balance equations with an accuracy in the order of 10-20% (Yehdegho et al. 1997).

4.2.1.3 SPECIAL CASES

The methodological approach outlined in Sect.4.2.1.1 was based on a number of simplifying assumptions such as a hydrologic/isotopic steady-state and perfect mixing of the lake. The discussion below will focus on such situations if one or more of those assumptions are not fulfilled in the studied system.

4.2.1.3.1 Non steady-state systems

The volume and isotopic composition of most lakes and surface water reservoirs undergo seasonal fluctuations imposed by seasonality of climatic parameters such as temperature and relative humidity or by fluctuations of incoming/outgoing fluxes of water. Usually, we are interested in the long-term behaviour of a system; the steady-state approach based on proper averaging of those seasonal fluctuations then provides a meaningful solution.

However, in situations when the system is evolving in time, both hydrologically and isotopically, the steady-state version of the isotope-mass balance equations cannot be used. The lake created by exploitation of construction materials (gravel, sand) may represent such evolving system. Typically, such lakes have no surface inflow and outflow and are linked to the local groundwater system. Another example of this type of system is presented by ephemeral lakes and ponds in arid regions, filled up during flood season and gradually loosing water during the dry season.

When both the volume and the isotopic composition of the studied system are changing in time ($dV/dt \neq 0$ and $d\delta_L/dt \neq 0$), the differential equations Eq.4.1 and 4.4 can be solved numerically for the required pair of variables, provided that for the adopted time steps the changes of all other parameters in these equations are known.

In literature one can find analytical expressions for the temporal evolution of the isotopic composition of a lake, derived by solving Eqs.4.1 and 4.4. under certain simplifying assumptions. For instance, Zimmermann (1978, 1979), Gonfiantini (1986) and Gibson et al. (1996) provide analytical expressions for δ_L if changes of the lake volume are negligible. Gonfiantini (1986) and Phillips et al. (1986) provide also analytical expressions for δ_L in cases where $dV/dt \neq 0$.

Integrating the differential equation (Eq.4.4) over the limits $t_o \rightarrow t$, using the mean values of other parameters in this equation and assuming that $dV/dt = 0$, yields the following general equation for the isotopic composition of lake water as a function of time:

$$\delta_{L(t)} = \delta_{LS} - (\delta_{LS} - \delta_{LO})e^{-t/\tau} \qquad \mathbf{(4.14)}$$

Where δ_{LO} and δ_{LS} is the initial and the steady-state isotopic composition of the lake, respectively, whereas τ stands for the time constant describing the rate of temporal changes of the isotopic composition of lake water:

$$\tau = \frac{V/E}{h_N/(1-h_N) + I_{tot}/E} \qquad \mathbf{(4.15)}$$

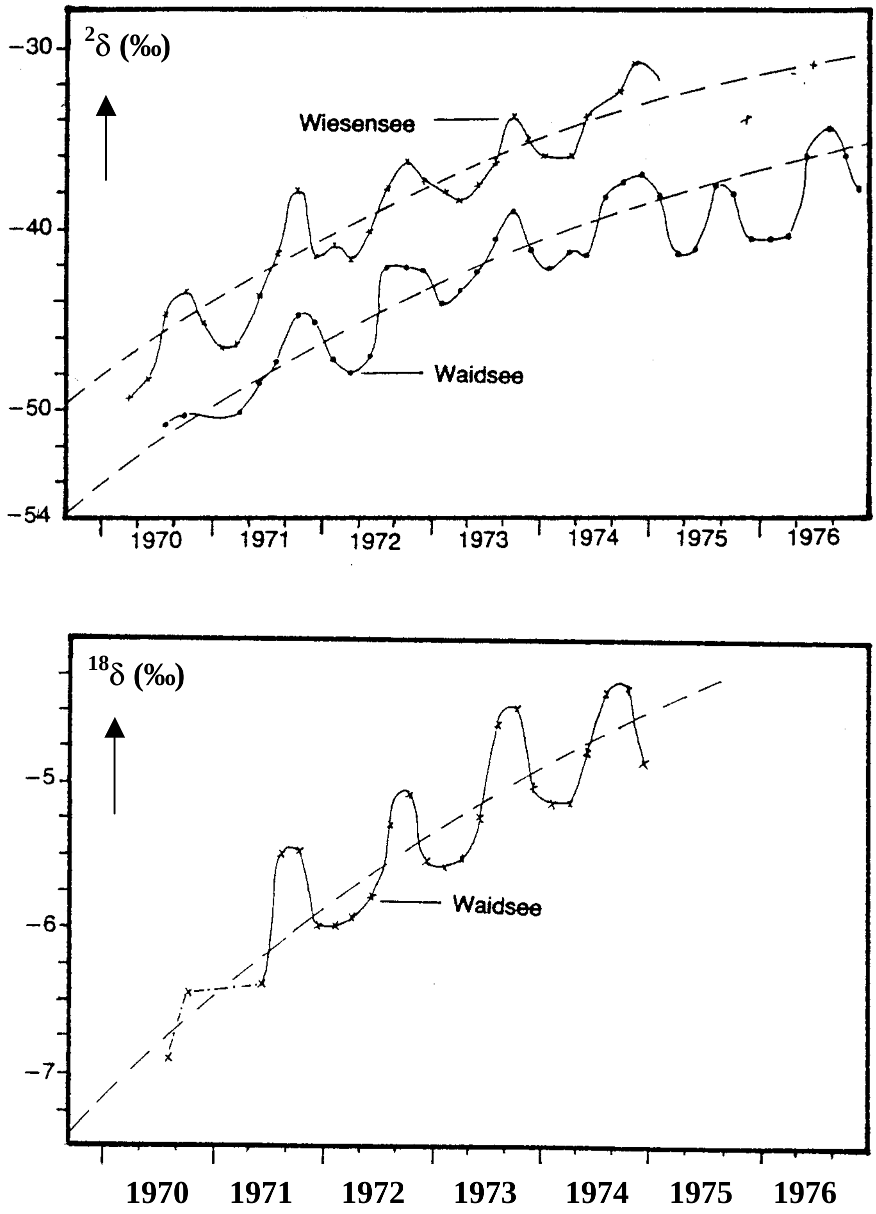

Fig. 4.4 Temporal evolution of $^2\delta$ and $^{18}\delta$ in two newly created dredging lakes in Germany (modified from Zimmermann, 1978).

For a terminal lake with $I_{tot}/E = 1$, Eq.4.15 simplifies to:

$$\tau = (1 - h_N)\cdot V/E \qquad \textbf{(4.16)}$$

It is apparent from Eq.4.16 that the isotopic time constant is $(1 - h_N)$ times the hydrological turnover time of the lake.

The following approximate equation holds for the steady state isotopic composition of the lake water (cf. Eq.4.12):

$$\delta_{LS} = \frac{h_N \delta_A - \varepsilon_{tot} + \delta_{IN}(1 - h_N)(I_{tot}/E)}{h_N + (1 - h_N)(I_{tot}/E)} \qquad \textbf{(4.17)}$$

If the evolving lake system is monitored in regular time intervals (e.g. every month), the quantities of interest, for instance the total inflow and outflow rates, can be derived for each time interval by solving Eqs.4.14, 4.15 and 4.17 with respect to the unknown quantity $X=I_{tot}/E$ and using Eq.4.6 to derive the total outflow: $O_{tot} = I_{tot} - E$ for the given time interval.

4.2.1.3.2 Stratified lakes

Stratification in lakes is induced by a density gradient, preventing the free exchange of matter between the mixed upper layer (epilimnion) and the deeper part of the lake (hypolimnion). As indicated in chapter 4.1.2, most of lakes undergo distinct seasonal cycle of vertical mixing with a period of thermal stratification (summer) and overturn events (late autumn, spring), when the entire system becomes well mixed. Some very deep lakes and especially saline lakes may show long-term (permanent) stratification (Gonfiantini et al., 1979).

If the investigation is aimed at resolving short-term fluctuations of water balance parameters in a seasonally stratified lake, the balance equations should be modified accordingly (Gat, 1970; 1995). For the period of thermal stratification, the epilimnion can be treated as a separate sub-system with a volume V_E and a dynamic boundary with the hypolimnion defined by the actual position of the thermocline. The dynamic character of this boundary results from the fact that, as the thermocline builds up and dissipates, deeper water layers will be incorporated into the epilimnion, changing its volume and isotopic composition. To account for this process, an additional term should be introduced to the balance equations for the epilimnion. This term should represent the water flux entering or leaving the epilimnion as a result of thermocline movement. In order to assess these fluxes, regular and frequent observations of the thermocline position are required. Also, it is necessary to monitor the vertical distribution of $^{18}\delta$ ($^{2}\delta$) in the lake, in order to assign appropriate isotopic compositions to the exchange fluxes.

4.2.1.3.3 Interconnected lakes

The discussion so far was focused on single, small, isolated lake systems. However, in practical applications one is often dealing with a system of interconnected lakes or surface reservoirs. A comprehensive discussion of such systems can be found in Gat and Bowser (1991). A string of lakes where the outflow of one lake at least partly serves as the hydrological input to other lake is perhaps the most commonly encountered type of this interconnection. The river system from which water is lost by evaporation along its flow path can be considered as an extreme example of the "string-of-lakes" system (Fritz, 1981).

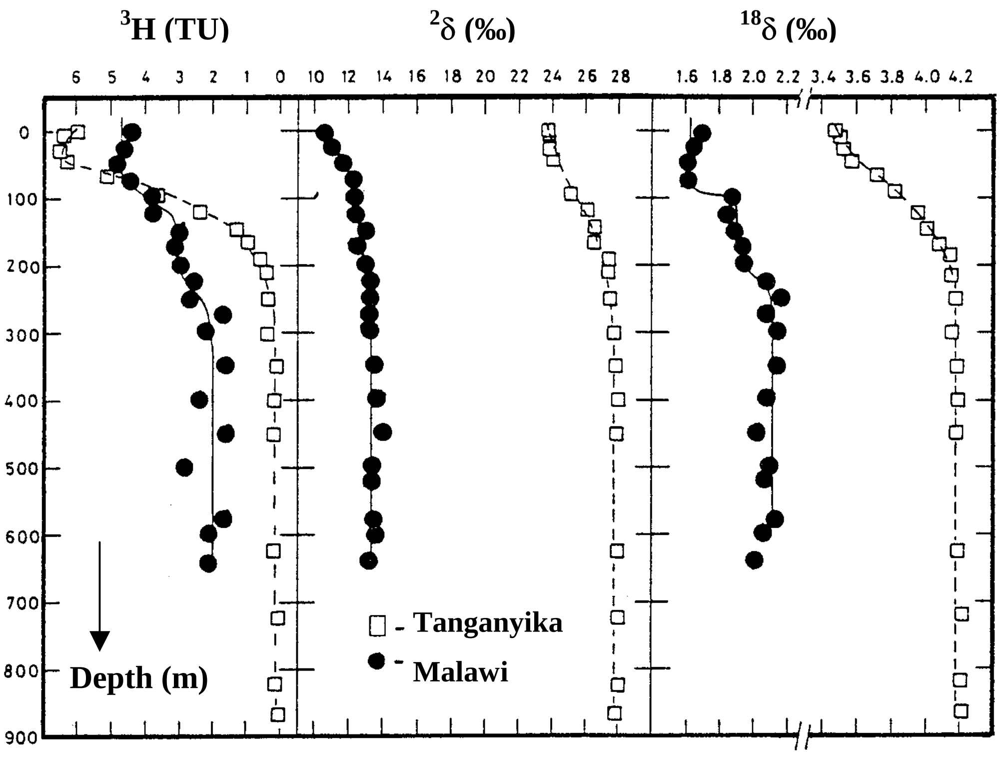

Fig. 4.5 Depth profiles of $^{18}\delta$, $^2\delta$ and ^3H content in Lake Malawi and Lake Tanganyika, East Africa. The samples were collected in 1973 for Tanganyika (Craig, 1975) and in 1976 for Malawi (Gonfiantini et al., 1979). The vertical mixing in Tanganyika lake is extremely slow, as indicated by absence of ^3H in the hypolimnion. More positive $^{18}\delta$ and $^2\delta$ values at depth, recorded also in Malawi lake, most probably reflect past climatic changes in the region leading to reduced ratio of the total inflow to evaporation rate for the studied lakes (cf. Fig.4.3b).

The water balance of a lake with the surface inflow or underground seepage from upstream lake can be treated in an analogous way as the isolated lake system, using appropriate isotope mass balance equations discussed above. The only difference is that the surface or underground inflow, controlled by the upstream lake, necessarily has the isotopic composition of this lake instead of local precipitation. Consequently, if there is a possibility that the near-by lake may "leak" into the studied system, the sampling programme should also involve this lake.

Fig.4.6 shows ^{18}O evaporative enrichment in a two-lake system, calculated for a wide range of boundary conditions (Gat, 1995).

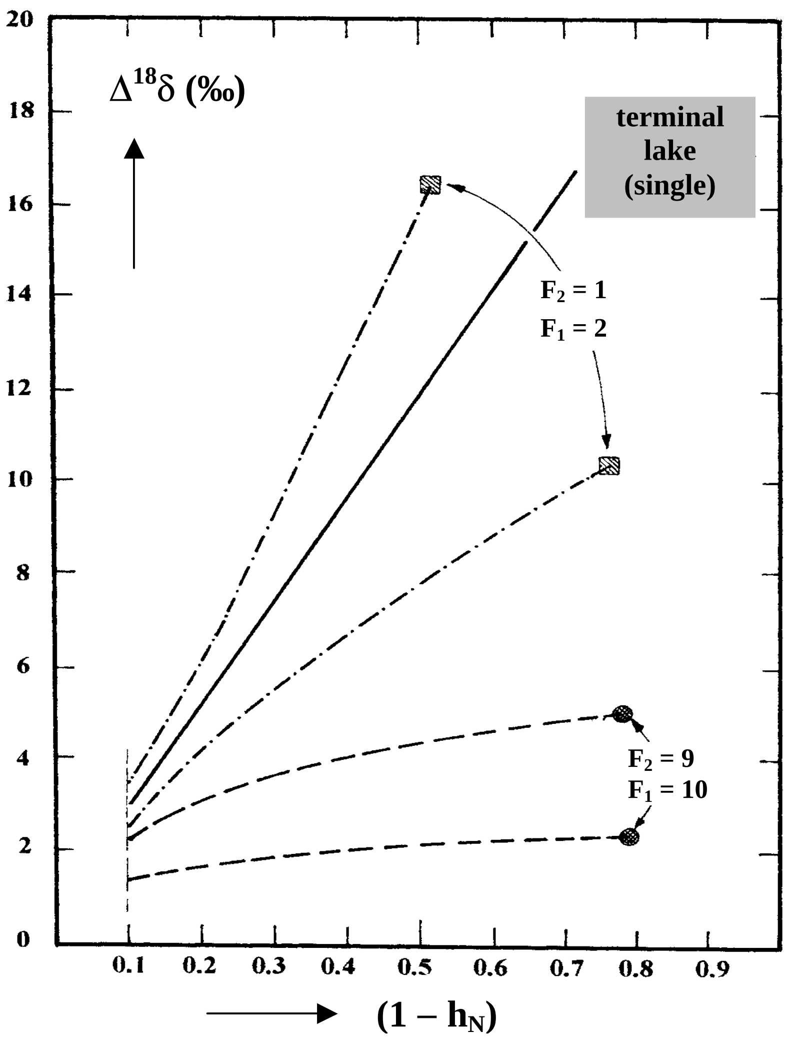

Fig.4.6 The steady-state isotope evaporative ^{18}O enrichment ($\Delta^{18}\delta$ = $^{18}\delta_{LS}$ - $^{18}\delta_{IT}$) for a two-lake system and one-lake system, drawn as a function of humidity deficit for different ratios of the total inflow to evaporation rate ($F=I_{tot}/E$). It is assumed that one-lake system has the evaporation rate equal to the total evaporation rate from the two-lake system. A state of isotopic equilibrium is assumed between δ_A and δ_I (modified from Gat, 1995).

It is apparent that the isotope enrichment in a coupled lake system exceeds that of a single lake with comparable hydrologic characteristics. However, it can be shown that if the number of interconnected lakes grows, the isotope enrichment does not increase indefinitely; due to isotopic exchange with atmospheric moisture there is an “ultimate” isotopic build-up beyond which no further isotopic enrichment occurs (Gat and Bowser, 1991). It is also evident from Fig.4.6 that the relative humidity plays major role in controlling the isotope enrichment, particularly for evaporation-dominated systems.

4.2.1.3.4 Large lakes

The formulation of isotope mass balance equations for small lakes involved several assumptions which have to be carefully re-assessed if large systems are considered. In particular, two questions have to be addressed: (i) to which extent the studied system can still considered to be homogeneous, and (ii) the moisture build-up over large water bodies.

Open water bodies constitute a continuous source of water entering the atmosphere as a result of evaporation. If the horizontal dimensions of the evaporating surface are large enough, the effect of moisture build-up over the lake can be significant. The moisture build-up over the lake depends critically on the degree of turbulent mixing in the atmosphere above the lake, which in turn is controlled by meteorological parameters (local insulation, wind direction and speed, etc.) and morphology of the surroundings (mountains or flat area). If the contribution of the lake evaporative flux to the local budget of atmospheric moisture is significant, the isotopic composition of atmospheric water vapour above the lake will be modified with respect to the free atmospheric value. Thus, large water bodies under steady-state conditions, will create their own "atmosphere" with average δ_A and relative humidity values that may deviate substantially from those recorded on the ground in the vicinity of the lake (Fontes and Gonfiantini, 1970). If these two quantities are known (measured) over the studied system, the isotope-mass balance equations and in particular the expression for δ_E (Eq.1.4) can still be used.

The sampling strategy for isotopic investigations of a large surface water system should focus on two problems outlined above, viz. checking the degree of isotopic homogeneity of the system and obtaining relevant parameters of the atmosphere above the studied lake (δ_A, h, T_{air}). In practice, the most reasonable way of "probing" the atmosphere above the lake is to install sampling and measurement stations on small islands. They should collect monthly precipitation and monitor air temperature and relative humidity. Additional advantage of this approach lies in providing also realistic numbers for monthly precipitation rates over the studied lake. For large lakes precipitation often differs significantly from that recorded around the lake. The isotopic composition of precipitation collected on islands should be used to evaluate the isotopic composition of atmospheric moisture over the lake using Eq.1.10. Alternatively, one can use the constant-volume evapometers located on islands or submersed evapometer(s) located on floating platform(s) to derive δ_A in the way discussed in Sect.4.2.1.1.5. If the above approach is not feasible (e.g. lack of islands), there are still two possible ways of handling the problem.

First, one can use the value of δ_A calculated from isotopic composition of local rainfall collected in the stations around the lake, provided that the term describing kinetic enrichment will be modified accordingly to account for humidity build-up above the lake. For large water bodies the parameter Θ in Eq.1.5, accounting for humidity build-up over the lake, can no longer be assumed as equal one. It can be estimated from the following equation (Gat, 1995):

$$\Theta = \frac{1 - h'_N}{1 - h_N} \tag{4.18}$$

where h'_N is the relative humidity, measured close to the lake surface (several cm above the evaporating surface) and normalised to the lake surface temperature, whereas h_N is the normalised relative humidity measured at some distance from the surface (several meters). In Eq.1.4 the h'_N value is to be used.

Another approach relies on direct measurements of relative humidity and isotopic composition of water vapour above the studied lake. Basically, two methods can be applied to collect atmospheric moisture over a lake for isotope analyses.

1) Spot samples of air are collected in special, commercially available inflatable sampling bags equipped with valves. In the laboratory, the moisture is extracted from the collected air samples using an appropriate vacuum line and cryogenic trapping. The size of air samples should be adjusted according to the temperature and relative humidity prevailing over the studied lake and the minimum size of water sample that can be analysed. For instance, 50 litres of air at 85% relative humidity and 25°C contain approximately one mL of water.

2) Air is pumped through a portable sampling unit consisting of a membrane pump, flow meter and a special glass trap cooled to approximately –70°C by a dry ice–alcohol mixture. Such sampling system can be located onboard a small boat or on a floating platform. The flow rate should be adjusted to the required water volume. The system should be tested in advance in order to assure complete removal of moisture from the pumped air stream, for the expected range of temperature and relative humidity values.

Although in this way samples of atmospheric moisture can be obtained from several different localities, both methods provide essentially spot samples; several sampling campaigns should be carried out during contrasting seasons and in different parts of the lake in order to characterise sufficiently well the average isotopic composition of atmospheric moisture over the studied system.

4.2.1.3.5 Saline lakes

The isotopic fractionation and the isotope-mass balance equations are not much affected by the salinity in brackish and moderately saline lakes. However, when concentrations of dissolved salts in lake water exceed those typically encountered in seawater, certain modifications are required. There are two major effects of dissolved salts on the isotopic composition of an evaporating water body: (i) dissolved salt decreases the thermodynamic activity of the water and its evaporation rate, and (ii) the ions in the solution attract in their hydration sphere water molecules with an isotopic composition and evaporation rate different from those in the free water of the bulk solution. This effect is different for each salt.

The dissolved salts decrease the thermodynamic activity of water, directly linked to the saturated vapour concentration p_{SAT}, becoming equal to $a_w \cdot p_{SAT}$, where $a_w<1$ is the activity coefficient of the water. The relative humidity of air, $h = p/p_{SAT}$, normalised to the temperature and activity of water, becomes equal h_N/a_w. In all equations discussed above h is to be replaced by the term h_N/a_w to account for the occurrence of dissolved salts. The activity coefficient for seawater is equal to about 0.98. Therefore, the salt effect on evaporating water becomes important only for saline lakes and sabkhas, and for a drying-up lake in the final evaporation stages. Water activity coefficients for the most common salts are tabulated by Robinson and Stokes (1959). If evaporation is the only process removing water from the system, the activity coefficient can be represented by the following empirical relation (Gonfiantini, 1986):

$$a_w = A \cdot f^{-2} + B \cdot f^{-1} + C \qquad \textbf{(4.19)}$$

where A, B and C are empirical constants and f is the remaining water fraction in the system (V/V_o), also equal to the ratio of the actual to the initial molality of the solution, M/M_o. For a sodium chloride solution having an initial activity corresponding to that of seawater, the water activity is:

$$a_w = -0.000543 \cdot f^{-2} - 0.018521 \cdot f^{-1} + 0.99931 \qquad \textbf{(4.20)}$$

The effect associated with hydration spheres of dissolved ions results in modification of the isotopic composition of free water in the salt solution and consequently influences the equilibrium isotope fractionation between liquid and vapour phase:

$$\alpha_{(S,T)} = \Gamma_{(S,T)} \cdot \alpha_{(T)} \qquad \textbf{(4.21)}$$

Where $\Gamma_{(S,T)}$ stands for the empirically derived correction factor that is a function of the molality and temperature of the solution as well as the type of dissolved ions. Numerous attempts have been made to determine the magnitude of this equilibrium salt effect (Sofer and Gat, 1972; 1975; Truesdell, 1974). The most comprehensive study has been carried out by Horita et al. (1993) who determined Γ values in single salt solutions for both ^{18}O and ^{2}H, in a wide range of temperatures and molalities. In multicomponent brines the equilibrium salt effect is considered to be additive (Sofer and Gat, 1975).

To account for the equilibrium salt effect in isotope mass balance equations, the equilibrium fractionation factor for pure water (α) is to be replaced by the corrected fractionation factor (Eq.4.21) whenever it relates to the saline solution (lake water). Also, the isotope-mass balance approach requires the measured δ values to properly represent the concentration of the isotopic tracers. For ^{18}O the common measurement technique, based on an exchange reaction between water and CO_2, yields $^{18}\delta$ values proportional to the activity rather than to the concentration. It is then necessary to apply the appropriate correction equation (Sofer and Gat, 1975; Horita et al., 1993):

$$\Delta\delta = -\sum_i \ln\Gamma_i \qquad \textbf{(4.22)}$$

where Γ_i is the correction factor for ion i in the solution.

The additional effect related to salinity becomes important only in the last stages of evaporation, when dissolved salts reach saturation concentrations and start to crystallise. Some deposited salts contain crystallisation water of which the isotopic composition might deviate from that of the bulk solution. The crystallisation process constitutes an additional channel for the removal of the isotopic tracer (^{18}O or ^{2}H) from the evaporating solution (c.f. last term in Eq.4.2). Isotope fractionation factors between crystallisation water and the bulk solution water have been summarised by Gonfiantini (1986).

4.2.2 OTHER TRACERS IN WATER BALANCE STUDIES OF LAKES

Stable isotopes as constituents of the water molecule, particularly ^{18}O, turned out to be the best suitable tracers for most practical applications of the tracer method in water balance studies of lakes. However, the tracer balance (Eq.4.2) is in principle valid for any type of tracer, provided that temporal changes of tracer fluxes entering and leaving the studied lake system, as well as temporal evolution of tracer concentration within the studied system, are sufficiently well characterised.

4.2.2.1 RADIOACTIVE ISOTOPES

The radioactive isotope of hydrogen, ^{3}H (tritium), build-in within the structure of water molecule, is a natural candidate for an almost ideal water tracer. It has a half-life of $T_{1/2}$ = 12.32 years and can be effectively measured at very low concentrations in water using well-established techniques (see Volume I for details). ^{3}H has been applied in the past in water balance studies of lakes in two ways.

1) ^{3}H introduced into the environment by the thermonuclear test explosions in the atmosphere during the early sixties was used as a "natural" tracer to investigate the water balance and mixing patterns of lakes. This approach was effective in the sixties and early seventies, when there was a large contrast in the environmental ^{3}H concentration between rainfall and other components of the water cycle (Gat, 1970; Gonfiantini et al., 1979; Weiss, 1979). Nowadays, this approach has become impractical, as it requires long-term observations of ^{3}H in all essential components of the studied lake system. These data are usually not available. Nevertheless, such approach has recently been attempted in combination with other tracers to Lake Bajkal (Peeters et al., 1997) and Lake Van (Dirican et al., 1999).

2) Artificial ^{3}H was used to make whole-body tracing of the studied lake system. In such tracer experiment, ^{3}H is injected into the studied lake, thus creating large initial contrast between the ^{3}H concentration in the lake water and other components of the water balance. Observing the decrease of ^3H concentration in the lake water with time and knowing other parameters of the system such as the lake volume, the evaporation flux and the relative humidity over the lake, one can in principle derive the total inflow and outflow rates from the system (Payne, 1970). The system should be observed over several years in order to reach acceptable precision of the derived parameters. Although this approach might be useful, particularly for assessing underground components of the water balance of small lakes, it is practically not employed nowadays, mostly due to restrictions in releasing radioactive isotopes to the environment.

Also attempts have been made to use other long-lived radioactive isotopes in water balance studies of lakes (Zuber, 1983). However, these failed due to problems with quantifying large tracer losses (^{60}Co in the form of $K_3Co(CN)_6$) by processes other than radioactive decay. Also in this case, the existing environmental concerns practically stopped further studies with this type of tracers.

4.2.2.2 DISSOLVED SALTS

The general form of the tracer balance (Eq.4.2) is also valid for dissolved salts. Therefore, if sufficient knowledge is on hand with respect to the ionic compositions of the particular components of the studied lake system, appropriate balance equation(s) can be set up for the chosen ion(s). Typical assumptions made are that $C_E = 0$ (no removal of salts from the system by evaporation flux) and, for saline systems, $C_P = 0$ (rainfall deposition flux negligibly small). The key question for the salt balance in lakes is to which extent the selected ion(s) in the system can be considered conservative. In many cases chloride would be the right choice but other major ions like calcium or magnesium can also be employed, depending on the characteristics of the system (see e.g. Stauffer, 1985; Krabbenhoft and Webster, 1995). In studies aimed at determining the water balance components of lakes one should always consider a possibility of a combined approach i.e. simultaneous use of different tracers, for instance ^{18}O and dissolved salts, to better constrain the studied system (Assouline, 1993).

4.3 TRACING OF WATER AND POLLUTANT MOVEMENT IN LAKES AND RESERVOIRS

As pointed out in Sect.4.1.2, mixing in lakes is controlled by both internal and external forces, highly variable in time and space. Shallow lakes and swamps are in general well mixed vertically, but poorly mixed horizontally. In such lakes, the isotopic composition of inflowing water is gradually modified by evaporation and exchange with atmospheric moisture. In deep lakes, the horizontal mixing within the upper layer (epilimnion) is generally rather fast due to the wind stirring action. The mixing rate decreases substantially with increasing depth; it has been shown that in the epilimnion the horizontal eddy diffusion coefficient is typically two orders of magnitude higher than at the thermocline and in the hypolimnion (Quay et al., 1980). Vertical mixing in deep lakes is rather slow, with the exception of the overturn period.

The vertical density stratification induced by temperature and/or salt concentration represents an efficient barrier, hampering mass transport between epilimnion and hypolimnion. In permanently stratified lakes or in very deep lake systems, water may stay in the hypolimnion for prolonged periods of time.

4.3.1 QUANTIFYING VENTILATION RATES IN DEEP LAKES

Studies focused on the dynamics of water circulation in lakes are driven not only by purely scientific interest, but also by questions of practical importance. Particularly for large lake systems, that constitute a valuable resource of potable water, often intensively exploited, the question asked in this context is how fast pollutants of various nature being released into surface layers will be distributed throughout the water column.

Quantification of vertical mixing in large, deep lakes is usually accomplished through solving appropriate mass balance equations describing the studied system in a framework of a chosen conceptual model. In the simplest case, this can be a two-box model where epilimnion and hypolimnion are treated as well-mixed reservoirs, connected by exchange fluxes. To solve the mass balance equations and quantify the exchange fluxes between the shallow and deep part of the studied system, several tracers can be applied simultaneously, depending on the complexity of the system and available data. For instance, Peeters et al. (1997) used four tracers simultaneously (CFC-11, CFC-12, ^{3}H and ^{3}He) to quantify deep-water renewal in Lake Bajkal, the world's largest and deepest freshwater body. In this case, a six-box model was applied. Within the box-model approach, the mean residence time of water in the deep-water layer can be calculated by dividing the volume of this layer by the corresponding total exchange flux with the surface layer.

Another way of quantifying the degree of vertical mixing is to calculate the *age* of the given water parcel using ^{3}H and its daughter product, ^{3}He (Torgersen et al., 1977; 1978). This age is calculated based on the assumption that all excess ^{3}He (above the equilibrium value with the atmosphere) in a given water parcel has been produced by ^{3}H decay. If a given water parcel is not subject to mixing with water of different ages, the relation between its ^{3}He and ^{3}H content (helium/tritium age, τ_{He}) defines the time (age) elapsed since the last "contact" with the atmosphere. This is expressed by the following equation:

$$\tau_{He} = \frac{1}{\lambda} \ln\left(1 + \frac{^3He_T}{^3H}\right) \qquad \textbf{(4.23)}$$

where ^3He_T is the tritiogenic ^{3}He concentration (i.e. the measured ^{3}He minus the atmospheric equilibrium concentration), ^{3}H is the measured ^{3}H concentration and λ stands for the decay constant of ^{3}H (λ = 0.05626 yr^{-1}, according to the half-life of 12.32 yr).

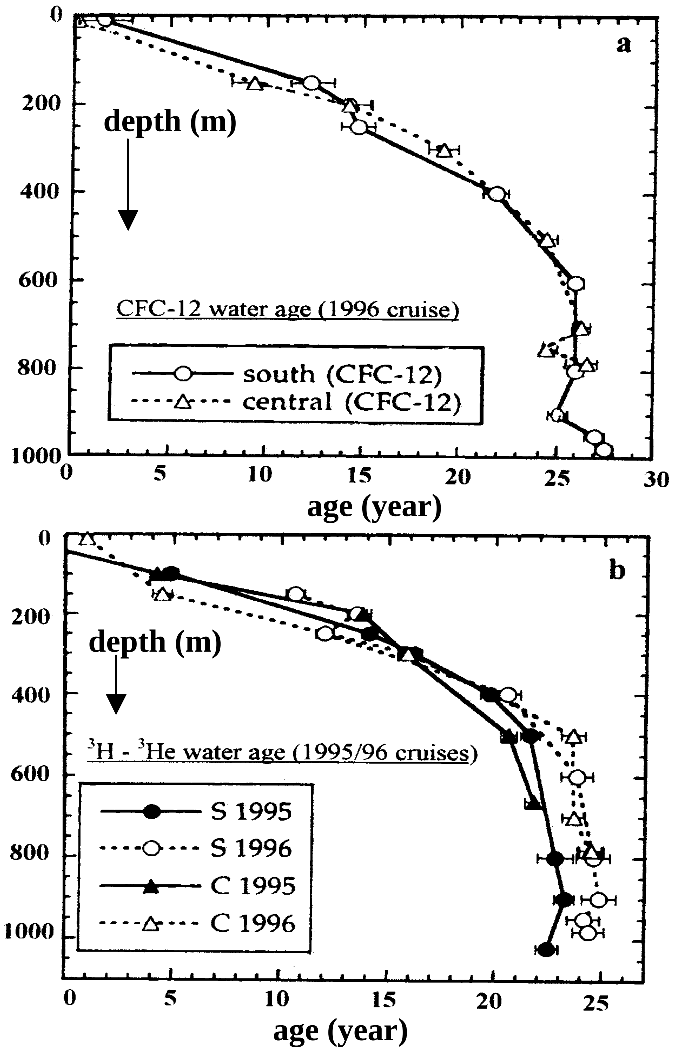

Fig.4.7 Vertical distribution of apparent ages of water in the Caspian Sea, derived from **(a)** freon concentrations and **(b)** ^{3}H-^{3}He ratios. The data represent two major basins of the system (Southern and Central Basin) and two consecutive sampling campaigns in September 1995 and 1996 (Froehlich et al., 1999; Peeters et al., 2000).

The *age* of a given water parcel can also be obtained by comparing the concentration of freons (CFC-11 and CFC-12) measured in the water with their known time histories in the atmosphere (see e.g. Katz al. 1995; Oster et al. 1996; Solomon et al. 1998; Schlosser et al., 1998; Solomon and Cook, 2000).

Fig.4.7 shows the vertical structure of ^{3}H – ^{3}He and freon-derived ages obtained for the Caspian Sea (Froehlich et al., 1999; Peeters et al., 2000). The Caspian Sea is the world's largest inland water body with a surface area of 379 000 km^2, a drainage area of approximately 3.5 million km^2, and a volume of 78 000 km^3. The ^{3}H – ^{3}He ages (Fig.4.7b) obtained for the two major basins of the system (Southern Basin and Central Basin) exhibit the same vertical structure characterised by gradual increase of the age down to about 600 m followed by a roughly constant age of about 20 to 25 years in the deeper layers. It is worth noting that *aging* of water masses at depth is clearly seen from comparing the 1995 and 1996 data. The distribution of water ages derived from freon data (Fig.4.7a) is practically identical. The calculated mean residence times of deep water yield exchange rates of approximately 7% per year for each of the two major basins (Peeters et al., 2000).

4.3.2 IDENTIFYING LEAKAGES FROM DAMS AND SURFACE RESERVOIRS

The fact that a surface water body subject to evaporation is changing its isotopic composition in a characteristic way (cf. Fig.4.2) makes it possible to distinguish between groundwater recharged under typical conditions and waters with an "evaporation history". This distinction becomes obvious when plotting the $^{2}\delta$ and $^{18}\delta$ data. The evaporated waters plot on the right-hand side of the global (local) meteoric water line.

This simple tool is of great practical importance for studies focusing on leakages from dams and surface reservoirs. Springs and leakages occurring downstream of dams always present a potential thread for these big engineering constructions. In this context the question is asked whether the given leakage (spring) carries water from the reservoir behind the dam or whether it is simply a manifestation of the local hydrological system. Identification of the first possibility often means very costly engineering measures to detect the leaking part of the construction.

Fig.4.8 presents the results of a study carried out in the northwestern region of Brazil, undertaken with the main aim of identifying the origin of leakages under a dike built in connection with the construction of a hydroelectric plant (Roldão et al., 1989). Several tracers were used simultaneously (fluorescent dyes, artificial ^{3}H , stable isotopes). Since the volume of the reservoir had fluctuated significantly with season (filling-up during the rainy period and gradual drying-up during the dry season), the isotopic composition of reservoir water was also changing systematically. This temporal evolution of the δ value of reservoir water could be traced in a number of observation wells behind the dike, thus providing an additional opportunity to assess the mean transit time of water from the reservoir to the observation points.

In some cases water originating from a dam reservoir can be distinguished from local infiltration water by environmental ^{3}H and/or the $^{13}\delta$ of the dissolved inorganic carbon (DIC, i.e. dissolved $CO_2 + HCO_3^{-} + CO_3^{2-}$). Due to exchange with atmospheric CO_2 (see Volume I) and biological activity in the reservoir (production of phytoplankton with a fractionation of $^{13}\varepsilon_{\text{organic matter relative to HCO3}} \approx -23‰$), the $^{13}\delta$ of DIC is usually significantly higher than that of river inflow and local groundwater. Significantly lower or higher ^{3}H values in the leakages, as compared to the characteristic reservoir value, also suggest a different origin of the water. Also the chemical composition of the water may provide an additional set of parameters for comparison. In some cases the use of dye tracers (Rhodamine WT) proves to be efficient. Typically, one should attempt to apply as many different tracers as possible.

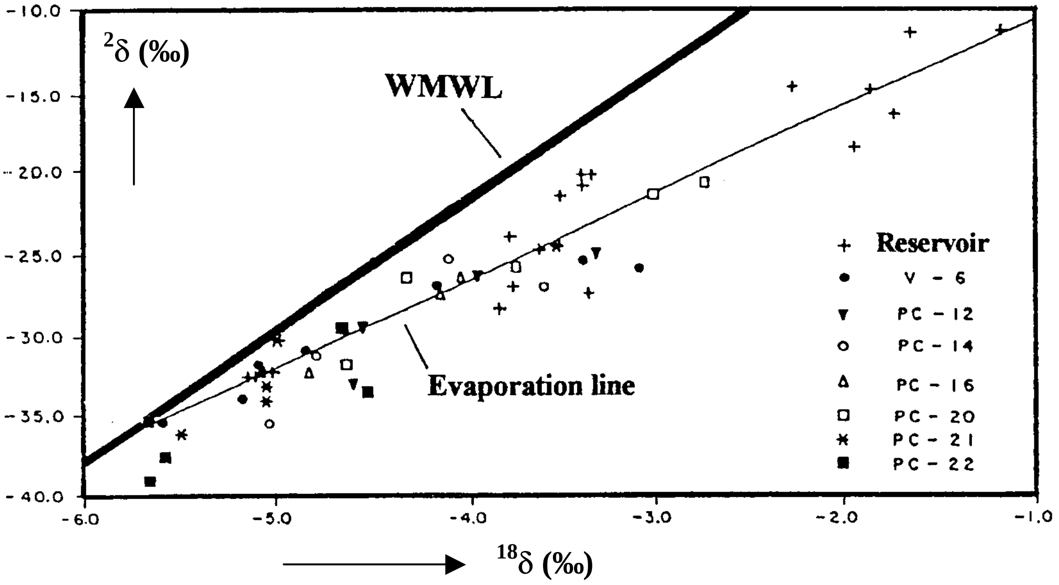

Fig.4.8 Stable isotopic composition of reservoir water and seven observation wells in the vicinity of a dike built in connection with the construction of a hydroelectric plant in the northwestern region of Brazil (modified from Roldão et al., 1989).

Often springs appearing downstream of newly filled reservoirs do not represent real leaks through the dam or dike structure, but are caused by increased hydrostatic pressure that squeezes out the older water from underlying sediments. Environmental isotopes, both stable and radioactive, can be helpful in identifying the origin of these new occurrences of water in the vicinity of the given reservoir.

Implementation of a tracer study of dam leakage should involve a survey of water occurrences in the proximity of a dam in order to obtain a comprehensive characterisation of the spatial variability in the isotopic characteristics of the groundwater (springs, boreholes, piezometers). If necessary, meteorological station(s) should be established in the area in order to collect monthly precipitation and characterise its isotopic composition. Several sampling campaigns, including the reservoir behind the dam, should be performed in contrasting seasons in order to quantify temporal variability of chemical and isotope characteristics of the reservoir water and the local groundwater system. Recent examples of tracer studies of dam leakages can be found in (IAEA, 2001).

4.3.3 QUANTIFYING LAKE WATER – GROUNDWATER INTERACTIONS

Often, it is of interest to determine the extent of interaction between a lake and the adjacent groundwater field. This can be done through delineation of the mixing zone downgradient from the lake reflecting the mixing of local recharge and the lake water outflow. Adequate characterisation of the mixing zone is of particular importance for aquifers being exploited for water supply. In such cases the vulnerability of the wells to accidental pollution originating in the lake needs to be assessed. The physico-chemical parameters of lake water (e.g. conductivity, temperature) cannot be used as the only tools for this purpose, as they are usually not sufficiently well preserved in the downstream aquifer.

Heavy isotope build-up in lakes can be substantial, depending on climatic parameters and hydrology of the system. The difference between the isotopic composition of total inflow and the lake water may reach in some cases even 10‰ for $^{18}\delta$ (cf. Fig.4.2). In those cases the lake water entering adjacent groundwater systems can easily be distinguished from local infiltration. Knowing the isotopic composition of the two end-members (lake water and local groundwater), one can calculate the percentage of lake water in the wells located downgradient from the lake. Fig.4.9. illustrates the use of stable isotope enrichment of lake water to delineate the mixing zone in the near-by aquifer system, in the case of small dredging lakes in Austria (Yehdegho et al. 1997). The influence of the lake could be traced several kilometres downgradient.

The development of a stable isotope plum downgradient from a lake also provides a means of calibrating a groundwater flow and solute transport. By employing both flow and transport models in the calibration process, assumed flow model parameters can be checked by calibration of the transport model, thus improving the confidence in the flow model results (Krabbenhoft et al., 1990a; 1990b; Stichler et al., 1999). In situations where flow and isotopic composition of lake water can be assumed constant in time, the plume will approach a steady state configuration. The time necessary to reach steady state depends on the assumed flow and transport parameters and the point of interest within the aquifer. For most natural systems except freshly created dredging lakes, this is usually the case. However, seasonal fluctuations in the inflow and outflow rates, as well as fluctuations of the isotopic composition of the lake water will perturb the plume. The seasonal signal in isotopic composition of lake water propagates downgradient and can be used as an additional means to calibrate the flow model. Fig.4.10 shows an example of such study performed on a small lake in Germany (Stichler et al., 1999). Distinct seasonal changes of $^{18}\delta$ of lake water, reaching around 1.2‰ in the studied system, were traced in a pumping well about hundred meters from the lake shore. The authors used the lumped-parameter approach to find the velocity and proportion of lake water in the pumping wells located near the lake. They also showed that without making use of isotope data it is possible to calibrate the numerical flow model in such a way that no lake water flows to the pumping wells.

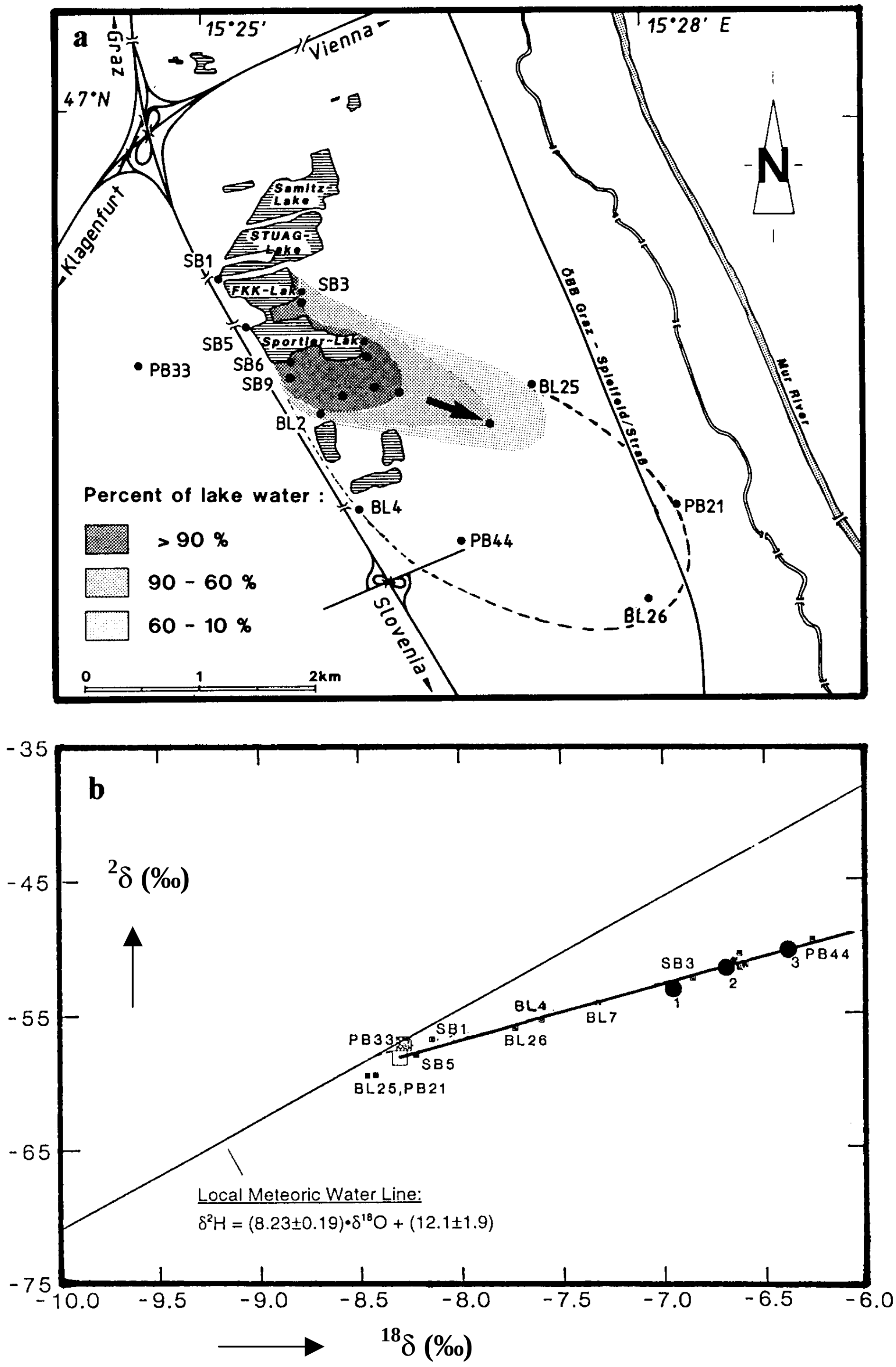

Fig.4.9 The use of stable isotope enrichment of lake water to delineate the mixing zone in the near-by aquifer system, for a group of small dredging lakes in Austria. **(a)** sketch map showing the mixing zone between lake water and local groundwater, delineated on the basis of isotopic data. **(b)** The ($^{18}\delta$,$^{2}\delta$) diagram for the investigated lake system. Heavy dots labelled by (1,2,3) represent the mean isotopic composition of three consecutive lakes (Samitz lake, Stuag lake, FKK-Sportler lake) (modified from Yehdegho et al., 1997).

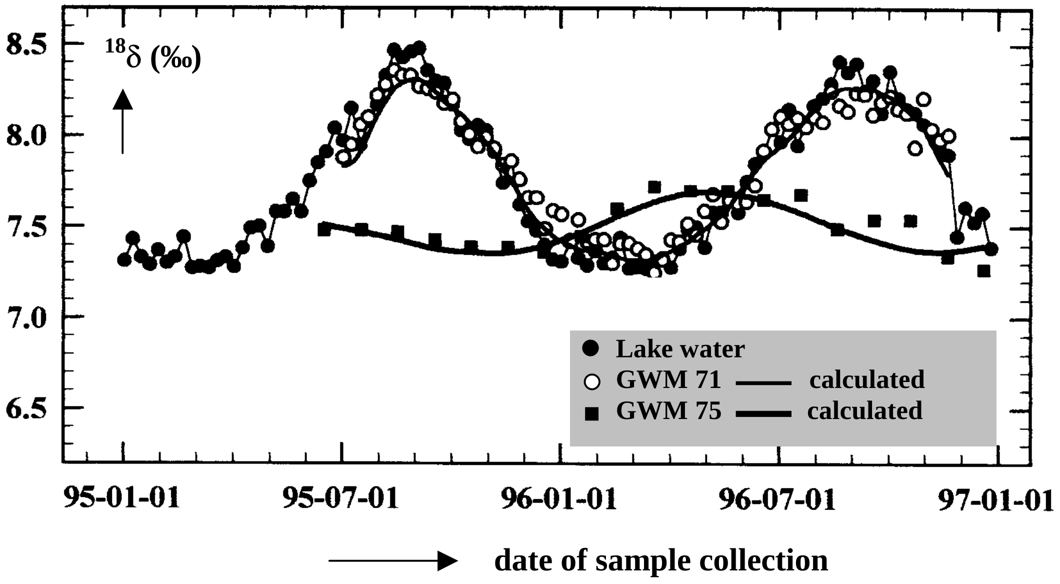

Fig.4.10 Propagation of seasonal fluctuations of $^{18}\delta$ in lake water downgradient in the adjacent aquifer. The values calculated for the observation wells were obtained using a lump-parameter modeling approach (modified from Stichler et al., 1999).

5 RESPONSE OF SURFACE WATER SYSTEMS TO CLIMATIC CHANGES

Among the most important issues related to man's impact on climate is the question of how the anticipated global warming, due to increasing concentrations of greenhouse gases in the atmosphere, will influence the water cycle on both regional and global scales. Surface water systems on continents are likely to be particularly affected by climatic changes. Due to the intimate link between isotopic composition of precipitation and climatic parameters, it is expected that long-term fluctuations of isotope characteristics of regional precipitation, induced by climatic changes, will be transferred to surface water systems, providing an early warning as to the direction and possible magnitude of those changes.

5.1 IMPACT OF CLIMATIC CHANGES ON THE ISOTOPIC COMPOSITION OF PRECIPITATION

The data gathered over the last few decades, mainly through operation of the global IAEA/WMO network (GNIP), provide a fairly detailed picture of the spatial and temporal variability of the isotopic composition of meteoric waters world-wide (Rozanski et al., 1993). This variability appears to be controlled by numerous, mutually related factors like surface air temperature, relative humidity of the atmosphere, amount of precipitation, latitude, distance from the coast and the elevation of the given area above sea level (see Volume II of this series). It also became apparent that, like many other atmospheric properties, the isotopic composition of atmospheric water vapour and, consequently, of precipitation exhibits a broad spectrum of temporal variations.

It has been demonstrated that spatial and temporal variations of $^{2}\delta$ and $^{18}\delta$ of meteoric waters have their origin in isotope fractionation effects accompanying evaporation from the ocean and subsequent condensation during the atmospheric transport of the vapour. It has also become apparent that the isotopic composition of local precipitation, in particular at mid- and high latitudes, is controlled by regional-scale processes such as:

1) the evaporation conditions at the source regions of the atmospheric moisture and

2) the average water vapour transport patterns into the continents and the resulting "rain-out history" of the air masses (Dansgaard, 1964; Craig and Gordon, 1965; Merlivat and Jouzel, 1979; Rozanski et al., 1982; Siegenthaler and Matter, 1983; Johnsen et al., 1989).

The link between the isotopic composition of precipitation and climatic changes on time scales exceeding instrumental records can be investigated in two ways:

1) through the application of Global Circulation Models (GCMs) which simulate the changes in isotopic water cycles induced by major climatic shifts (e.g. Hoffmann and Heimann, 1993; Joussaume and Jouzel, 1993; Cole et al. 1999; Hoffmann et al., 2000), and

2) by exploring environmental archives in which variations of ^{2}H/^{1}H and ^{18}O/^{16}O isotope ratios and climatic parameters (e.g. temperature) are independently recorded. In most cases surface water systems are an intermediate step between precipitation and the given archive, such as lacustrine sediments, groundwater or organic matter.

5.2 CLIMATIC CHANGES OF THE INPUT FUNCTION

As pointed out in Sect.1.3, the apparent relationship between isotopic composition of precipitation and newly formed groundwater and surface runoff in a given area stems from a fairly complex array of selection processes having the collective name: *catchment isotope effect*. On time scales relevant to climatic shifts one may consider several mechanisms that can modify the average isotopic signature of rainfall after it reaches the plant-soil system. For mid latitudes, a change associated with the seasonal selection of rainfall will probably be one the most important. Since at mid latitudes both $^{18}\delta$ and $^{2}\delta$ exhibit large seasonal fluctuations, climatically-induced changes in the relative contribution of summer and winter precipitation to newly formed groundwater may lead to substantial shifts in its average isotopic characteristics. The varying rates of infiltration during summer and winter may result either from shifts in the seasonality of rainfall and/or temperature, or from climatically-induced changes in the plant cover (e.g. transition from tundra to forest or from forest to savanna). Those effects are superimposed on the climatic signal imprinted in regional precipitation.

Fig.5.1 shows time series of monthly $^{18}\delta$ values for the Danube river in Ulm (Germany) and in Vienna (Austria), for the time period 1969 - 1994 (Rank et al., 1998). These data are compared with the record of $^{18}\delta$ in precipitation available for the Vienna district. The distinct seasonality in $^{18}\delta$ of the Danube river, with most negative δ values occurring during late spring and summer, results from snow and ice melting in the Alps. It is interesting to note that long-term changes of the isotopic composition of precipitation over the European continent, apparent in the Vienna record, are transmitted with ca. one year delay through the catchment of the Danube river, without substantial demping (cf. Fig.5.1b).

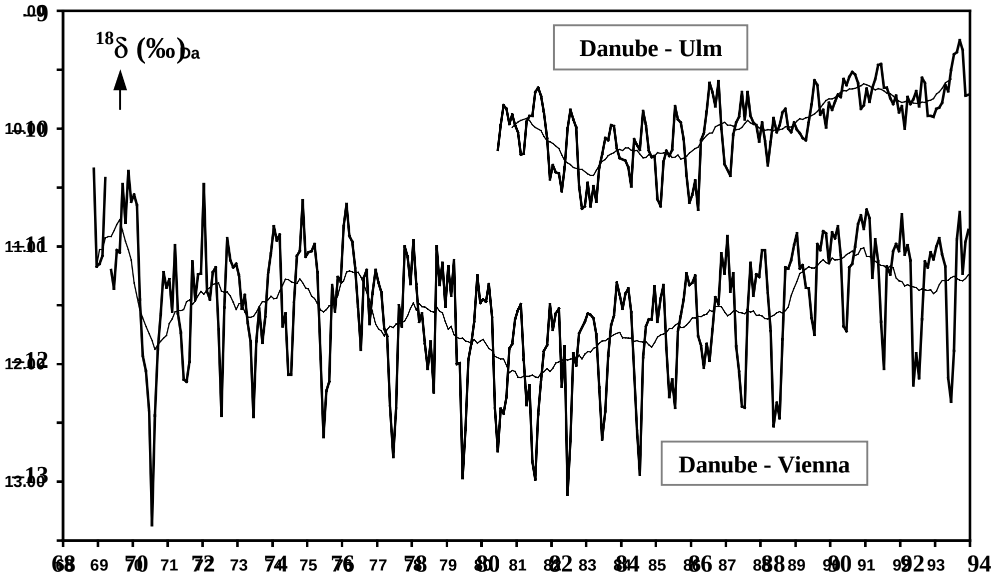

Fig.5.1 $^{18}\delta$ record for Danube river at Ulm (Germany) and Vienna (Austria), for the time period 1969 – 1994. Comparison of long-term trend curves of $^{18}\delta$, expressed as departures of the smoothed $^{18}\delta$ record from the long-term mean for the river Danube and for precipitation at Vienna. The two are shifted by one year (modified from Rank et al., 1998).

5.3 CLIMATIC CHANGES STORED IN LAKE SEDIMENTS

Lacustrine deposits are among the most valuable continental materials for palaeoclimatic reconstructions (Stuiver, 1970). They can provide high resolution, relatively continuous records of late Pleistocene/Holocene climatic changes. Lake sediments often contain authigenic carbonates and fossil shells whose oxygen isotopic composition is mainly controlled by that of the lake water and by temperature. From the preceding discussion it is apparent that $^{18}\delta$ and $^{2}\delta$ of open lakes, located at mid-latitudes and characterised by relatively fast water turnover, primarily respond to changes of the isotopic composition of precipitation over the lake basin, which in turn is temperature dependent. Consequently, the periods of cold and mild climate are reflected by minima and maxima in $\delta^{18}O$ of the deposited calcite (e.g. Siegenthaler et al., 1984; Goslar et al., 1995). For closed lakes, the isotopic composition of water is largely determined by evaporation and exchange with atmospheric moisture; dry periods, usually characterised by an increased ratio of evaporation to inflow, are marked by high $^{18}\delta$. In the tropics, $^{18}\delta$ of authigenic calcite deposited in lakes generally reflects the extent of evaporative enrichment of the lake water, which in turn is connected with the residence time of the water in a given lake system. Therefore, $^{18}\delta$ then predominantly reflects the changes in precipitation regime. In monsoon-controlled regions the isotopic composition of precipitation primarily responds to the amount of rainfall and, consequently, to the intensity of monsoon circulation. Records of $^{18}\delta$ and $^{2}\delta$ of ancient precipitation preserved in various continental archives located in such regions may thus provide important information about the extent and intensity of the major monsoon systems in the past (e.g. Morinaga et al., 1993; Lister et al., 1991).

Of particular importance for high resolution climatic reconstructions on continents are lacustrine archives that contain annually laminated sediments. Seasonally varying sedimentation patterns in some lakes may lead to the formation of varves, thus providing a chronological timescale of climatic proxies preserved in sediments, such as pollen and stable isotopes in authigenic carbonates and organic matter. In most cases such scales are floating i.e. they are not fixed on the calendar timescale although they can provide an annual resolution for various periods of time. Only in rare cases is the absolute calibration of floating chronologies possible, for instance through ^{14}C dating of terrestrial macrofossils preserved in such sediments (e.g. Hajdas et al., 1993; Goslar et al., 1995; Kitagawa and Van der Plicht, 1998).

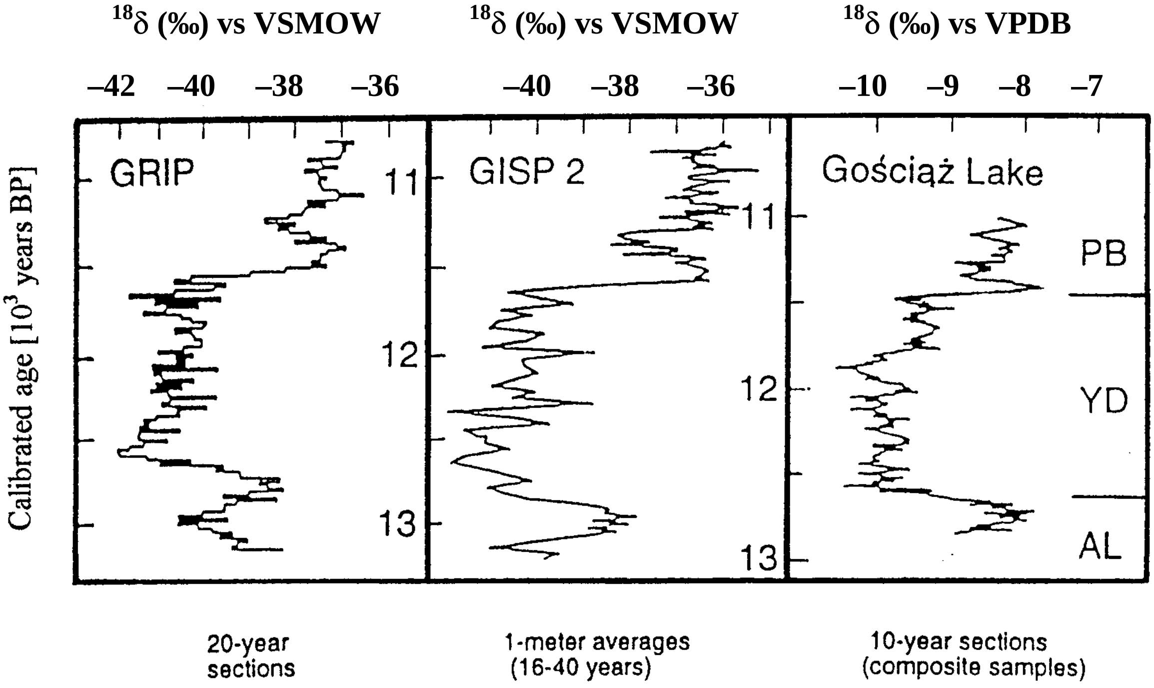

Fig.5.2 The Younger Dryas cold episode, as reflected in the $^{18}\delta$ data of the GISP 2 and GRIP deep ice cores drilled on the Summit of the Greenland ice sheet and in the $^{18}\delta$ of authigenic carbonate deposited in Lake Gosciaz, Central Poland (modified from Rozanski et al., 1997).

Any attempt to quantify palaeoclimatic information obtained from isotopic records preserved in lacustrine sediments should involve a comprehensive isotopic characterisation of the modern lake system from which the given record was retrieved. Such calibration study, including a water balance and the dynamics of the given system, will help to quantify the role of the different factors in the formation and preservation of the isotopic signal in lacustrine archives, including the ‘catchment effect’.

REFERENCES

Allison, G.B. and Leaney, F.W., 1982. Estimation of isotopic exchange parameters using constant-feed pans. J. Hydrol. 55: 151-161.

Amarasekera, N.A., Lee, R.F., Williams, E.R: and Eltahir, E.A.B., 1997. ENSO and the natural variability in the flow of tropical rivers. J. Hydrol. 200: 24-39.

Anati, D.A. and Gat, J.R., 1989. Restricted marine basins and marginal sea environments. In: Handbook of Environmental Isotope geochemistry, Volume 3, The Marine Environment A. (Fritz, P. and J. Ch. Fontes, eds.), Elsevier: 29-73..

Assouline, S., 1993. Estimation of lake hydrologic budget terms using simultaneous solution of water heat and salt balances and a Kalman filtering approach: Application to lake Kinneret. Water Res. Res. 29: 3041-3048.

Aucour, A.-M., Sheppard, S.M.F., Guyomar, O. and Wattelet, J., 1999. Use of ^{13}C to trace origin and cycling of inorganic carbon in the Rhône river system. Chem. Geol. 159: 87-105.

Baertschi, P., 1976. Absolute ^{18}O content of Standard mean Ocean Water. Earth and Planet. Sci. Lett. 31: 341-344.

Begemann, F. and Libby, W.F., 1957. Continental water balance, groundwater inventory and storage times, surface ocean mixing rates and world-wide water circulation patterns from cosmic ray and bomb tritium. Geochim. Cosmochim. Acta 12: 277 – 296.

Berner, E.K. and Berner, R.A., 1987. The Global Water Cycle: Geochemistry and Environment. Prentice Hall, Inc.

Broecker, W.S. and Walton, A., 1959. The geochemistry of ^{14}C in fresh-water systems. Geochim. Cosmochim. Acta 16: 15.

Brutsaert, W.H., 1982. Evaporation into the Atmosphere, D. Reidel, Dordrecht.

Buhl, D. Neuser, R.D., Richter, D.K., Riedel, D., Roberts, B., Strauss, H. And Veizer, J., 1991. Nature and Nurture: Environmental Isotope Story of the Rhine River. Naturwissenschaften 78: 337 – 346.

Burgman, J.O., Calles, B. and Westman, F., 1987. Conclusions from a ten-year study of the oxygen-18 in precipitation and runoff in Sweden. In; Isotope Techniques in Water Resources Development. Proc. IAEA Symp., Vienna: 579-590.

Cole, J., Rind., D., Jouzel, J., Webb, R.S. and Healy, W.S., 1999. Climatic controls on interannual variability of precipitation $\delta^{18}O$: The simulated influence of temperature, precipitation amount, and vapour source region. J. Geophys. Res. 104: 14,223-14,235.

Coplen, T.B., 1996. New guidelines for reporting stable hydrogen, carbon and oxygen isotope-ratio data. Geochim. Cosmochim. Acta 60: 3359-3360.

Craig, H., 1961a. Standards for reporting concentrations of deuterium and oxygen-18 in natural waters. Science 133: 1833-1834.

Craig, H., 1961b. Isotopic variations in meteoric waters. Science 133: 1702-1703.

Craig, H. and Gordon, L.I., 1965. Deuterium and oxygen-18 variations in the ocean and the marine atmosphere. In: Stable Isotopes in Oceanographic Studies and Paleotemperatures, E. Tongiorgi (Ed.), Lab. Geol. Nucl., Pisa: 1-122.

Craig, H., 1975. Lake Tanganyika geochemical and hydrographic study: 1973 Expedition, Scripps Institution of Oceanography, University of California, SIO Reference Series 75-5, La Jolla, California.

Dansgaard, W., 1964. Stable isotopes in precipitation. Tellus 16: 436-468.

De Wit, J.C., Van der Straaten, C.M. and Mook, W.G., 1980. Determination of the absolute D/H ratio of VSMOW and SLAP. Geostandards Newsletters 4: 33-36.

Dinçer, T., 1968. The use of oxygen-18 and deuterium concentrations in the water balance of lakes. Water Res. Res.: 1289-1306.

Dirican, A., Özaydin, V., Güler, S. and Demiröz, E., 1999. Dynamics of Van Lake using environmental isotopes and hydrochemical data. Proc. IAEA Int. Symposium on Isotope Techniques in Water Resources Development and Management, Vienna 1999. CD-ROM.

Eltahir, E.A.B., 1996. El Niño and the natural variability in the flow of the Nile river. Water Resources Research 32 (1): 131-137.

Epstein, S. and Mayeda, T. 1953. Variations of O^{18} content of waters from natural sources. Geochim. Cosmochim. Acta 4: 213-224.

Esser, N., 1980. Bombentritium – Zeitverhalten seit 1963 im Abfluss mitteleuropäischer Flüsse und kleiner hydrologischer Systeme. PhD thesis, University of Heidelberg, Germany.

Ferronski, V.I. and Brezgunov, V.S., 1989. In: Handbook of Environmental Isotope geochemistry, Volume 2, The Terrestrial Environment B. (Fritz, P. and J. Ch. Fontes, eds.), Elsevier, Amsterdam, New York: 1-27.

Fontes, J.Ch. and Gonfiantini, R., 1970. Composition isotopique et origine de la vapeur d'eau atmospherique dans la region du Lac Leman. Earth Planet. Sci. Lett. 7: 325-329.

Fontes, J.Ch., Boulange, B., Carmouze, J.P. and Florkowski, T., 1979. Preliminary oxygen-18 and deuterium study of the dynamics of Lake Titicaca. In: Isotopes in Lake Studies. International Atomic Energy Agency, Vienna, 145-150.

Fritz, P., 1981. River waters. In: Stable Isotope Hydrology: Deuterium and Oxygen-18 in the Water Cycle. Tech. Rep. Series. No. 210, IAEA, Vienna: 177-202.

Froehlich, K., Rozanski, K., Povinec, P., Oregioni, B. and Gastaud, J., 1999. Isotope studies in the Caspian Sea. The Science of the Total Environment 237/238: 419-427.

Froehlich, K., 2000. Evaluating the water balance of inland seas using isotopic tracers: the Caspian Sea experience. Hydrological Processes 14: 1371-1383.

Gaillardet, J., Dupré, B., Louvat, P. and Allègre, C.J., 1999. Global silicate weathering and CO_2 consumption rates deduced from the chemistry of large rivers. Chem. Geol. 159: 3-30.

Garrels, R.M., Mackenzie, F.T. and Hunt, C., 1975. Chemical cycles and the global environment. Kaufmann, Inc.

Gat, J.R. and Tzur, Y., 1967. Modification of the isotopic composition of rainfall by processes which occur before groundwater recharge. In: Proc. IAEA Symposium on Isotope Hydrology, IAEA, Vienna: 49-60.

Gat, J.R., 1970. Environmental isotope balance of Lake Tiberias. In: Isotopes in Hydrology 1970, IAEA, Vienna: 109-127.

Gat, J.R. and Bowser, C., 1991. The heavy isotope enrichment of water in coupled evaporative systems. In: Stable Isotope Geochemistry: A Tribute to Samuel Epstein, Spec. Publ. 3 of the Geochemical Society: 195-168.

Gat, J.R., 1995. Stable isotopes of fresh and saline lakes. In: Physics and Chemistry of Lakes (A.Lerman, D.M. Imboden and J.R. Gat, eds.). Springer-Verlag: 139-165.

Gat, J.R. and Lister, G.S., 1995. The catchment effect on the isotopic composition of lake waters; its importance in palaeolimnological interpretations. Paläoklimaforschung 15: 1-15.

Gat, J.R., 1996. Oxygen and hydrogen isotopes in the hydrological cycle. Ann. Rev. Earth Planet. Sci. 24: 225-262.

Gibson, J.J., Edwards, T.W.D. and Prowse, T.D., 1996. Development and validation of an isotopic method for estimating lake evaporation. Hydrological Processess 10: 1369-1382.

Gibson, J.J., Edwards, T.W.D. and Prowse, T.D., 1999. Pan-derived isotopic composition of atmospheric water vapour and its variability in northern Canada. J. Hydrol. 217: 55-74.

Gonfiantini, R., 1986. Environmental isotopes in lake studies. In: Handbook of Environmental Isotope geochemistry, Volume 2, The Terrestrial Environment B. (Fritz, P. and J. Ch. Fontes, eds.), Elsevier, Amsterdam, New York: 113-163.

Gonfiantini, R., Zuppi, G.M., Eccles, D.H. and Ferro, W., 1979. Isotope investigation of Lake Malawi. In: Isotopes in Lake Studies, IAEA, Vienna: 195-207.

Goslar, T., Arnold, M., Bard, E., Kuc, T., Pazdur, M.F., Ralska-Jasiewiczowa, M., Rozanski, K., Tisnerat, N., Walanus, A. Wicik, B. and Wieckowski, K., 1995. High concentration of atmospheric ^{14}C during the Younger Dryas cold episode. Nature 377: 414-417.

Hajdas, I., Ivy, S.D., Beer, J., Bonani, G., Imboden, D., Lotter, A.F., Sturm, M., and Suter, M., 1993. AMS radiocarbon dating and varve chronology of Lake Soppensee: 6000 to 12000 years BP. Clim. Dyn. 9: 107-116.

Hoffmann, G., and Heimann, M., 1993. Water tracers in the Echam General Circulation Model. In: Isotope Techniques in the Study of Past and Current Environmental Changes in the Hydrosphere and the Atmosphere, IAEA, Vienna: 3-15.

Hoffmann, G., Jouzel, J. and Masson, V., 2000. Stable water isotopes in atmospheric General Circulation Models. Hydrol. Processes 14: 1385-1406.

Horita, J., Wesolowski, D.J. and Cole, D.R., 1993. The activity-composition relationship of oxygen and hydrogen isotopes in aqueous salt solutions: I. Vapor-liquid water equilibration of single salt solutions from 50 to 100^{o}C. Geochim. Cosmochim. Acta 57: 2797-2817.

Horita, J. and Wesolowski, D.J., 1994. Liquid-vapor fractionation of oxygen and hydrogen isotopes of water from the freezing to the critical temperature. Geochim. Cosmochim. Acta 58: 3425-3437.

Hutchinson, G.E., 1957. A Treatise on Limnology, Vol.I, Wiley, New York.

IAEA, 2001. Estudios de fugas de embalses. Final Report of the Proj. RLA/8/016 (ARCAL XVIII), IAEA, Vienna, Isotope Hydrology Section.

Ikebuchi, S., Seki, M. and Ohtoh, A., 1988. Evaporation from Lake Biva. J. Hydrol. 102: 427-449.

Imboden, D.M. and Wüest, A., 1995. Mixing mechanisms in lakes. In: Physics and Chemistry of Lakes (A.Lerman, D.M. Imboden and J.R. Gat, eds.). Springer-Verlag: 83-139.

Jacob, H. and Sonntag, C., 1991. An 8-year record of the seasonal variations of ^{2}H and ^{18}O in atmospheric water vapour and precipitation at Heidelberg, Germany. Tellus 43B: 291-300.

Johnsen, S.J., Dansgaard, W. and White, J.W.C., 1989. The origin of Arctic precipitation under present and glacial conditions. Tellus 41B: 452-468.

Joussaume, S. and Jouzel, J., 1993. Paleoclimatic tracers: An investigation using an atmospheric general circulation model under ice age conditions. J. Geophys. Res. 96: 7495-7507.

Katz, B.G., Lee, T.M., Plummer, L.N., Busenberg, E., 1995. Chemical evolution of groundwater near a sinkhole lake, northern Florida, 1. Flow patterns, age of groundwater, and infuence of lake water leakage. Water Res. Res. 31: 1549-1564.

Kitagava, H., and Van der Plicht, J., 1998. Atmospheric radiocarbon calibration to 45000 years BP: Late Glacial fluctuations and cosmogenic isotope production. Science 279: 1187-1190.

Kohler, M.A., 1954. Lake and pan evaporation. In: Water-loss Investigations: Lake Hefner Studies. US Geol. Survey Prof. Paper No. 269: 127-148.

Krabbenhoft, D.P., Bowser, C.J., Anderson, M.P. and Valley, J.W., 1990a. Estimating groundwater exchange with lakes. 1. The stable isotope mass balance method. Water Resour. Res. 26: 2445-2453.

Krabbenhoft, D.P., Anderson, M.P. and Bowser, C.J.,1990b. Estimating groundwater exchange with lakes. 2. Calibration of a Three-Dimentional, Solute Transport to a Stable Isotope Plume. Water Resour. Res. 26: 2455-2462.

Krabbenhoft, D.P. and Webster, K.E., 1995. Transient hydrogeological controls on the chemistry of a seepage lake. Water Resour. Res. 31: 2295-2305.

Leibundgut, C., McDonnell, J. and Schultz, G. (Eds.), 1999. Integrated Methods in Catchment Hydrology – Tracer, Remote Sensing and New Hydrometric Techniques. IAHS Publication No. 258, IAHS Press, Institute of Hydrology, Wallingford, Oxfordshire, UK, ISBN 1-901502-01-5.

Lister, G.L., Kelts, K., Chen Ke Zao, Jun-Qing Yu and Nissen, F., 1991. Lake Qinghai, China: closed-basin lake levels and oxygen isotope record for ostracoda since the latest Pleistocene. Palaeogeog. Palaeoclim. Palaeoecol. 84: 141-162.

Majoube, M., 1971. Fractionnement en oxygéne-18 et en deuterium entre l’eau et la vapeur. J. Chim. Phys. 68: 1423-1436.

Maloszewski, P., Rauert, W., Stichler, W. and Herrmann, A., 1983. Application of flow models in an Alpine catchment area using tritium and deuterium. J. Hydrol. 66: 319-330.

McKenna, S.A., Ingraham, N.L., Jacobson, R.L. and Cochran, G.F., 1992. A Stable Isotopic Study of Bank Storage Mechanisms in the Truckee River Basin. J. Hydrol. 134: 203-219.

Merlivat, L. and Coantic, M., 1975. Study of mass transfer at the air-water interface by an isotopic method. J. Geophys. Res. 80: 3455-3464.

Merlivat, L., 1978. Molecular diffusivities of $H_2{}^{16}O$, $HD^{16}O$, $H_2{}^{16}O$ in gases. J. Chem. Phys. 69: 2864-2871.

Merlivat, L., and Jouzel, J., 1979. Global climatic interpretation of the deuterium –oxygen 18 relationship for precipitation. . J. Geophys. Res. 84: 5029-5033.

Meybeck, M., 1995. Global distribution of lakes. In: Physics and Chemistry of Lakes (A.Lerman, D.M. Imboden and J.R. Gat, eds). Springer-Verlag: 1-35.

Michel, R.L., 1992. Residence times in river basins as determined by analysis of long-term tritium records. J. Hydrol. 130: 367-378.

Mook, W.G., 1970. Stable carbon and oxygen isotopes of natural waters in the Netherlands. In: Proc. Isotope Hydrology, IAEA, Vienna: 163-189.

Mook, W.G., Groeneveld, D.J., Brouwn, A.E. and Van Ganswijk, A.J., 1974. Analysis of a run-off hydrograph by means of natural ^{18}O. In: Proc. Isotope Techniques in Groundwater Hydrology, IAEA, Vienna: 145-153.

Mook, W.G., 1982. The oxygen-18 content of rivers. Mitt. Geol.-Paläont. Inst. Univ. Hamburg, SCOPE/UNEP Sonderband 52: 565-570.

Mook, W.G. and Tan, F.C., 1991. Stable carbon isotopes in rivers and estuaries. In: Biogeochemistry of Major World Rivers (E.T.Degens, S.Kemoe and J.E.Richey, eds.). SCOPE Volume, John Wiley & Sons, London, New York: 245-264.

Morinaga, H., Itota, C., Isezaki, N., Goto, H., Yaskawa, K., Kusakabe, M., Liu, J. and Cong, S., 1993. Oxygen-18 and carbon-13 records for the past 14,000 years from lacustrine carbonates of Siling-Co lake in the Qinghai-Tibetan Plateau. Geophys. Res. Lett. 20: 2909-2912.

Négrel, P. and Lachassagne, P., 2000. Geochemistry of the Maroni River (French Guiana) during low water stage: implications for water-rock interaction and groundwater characteristics. J. Hydrol. 237: 212-233.

Nir, A. and Lewis, S., 1975. On tracer theory in geophysical systems in the steady and nonsteady state I.. Tellus 27: 372-383.

Oster, H., Sonntag, C. and Münnich, K.O., 1996. Groundwater age dating with chlorofluorocarbons, Water Res. Res. 32: 2989-3001.

Payne, B., 1970. Water balance of Lake Chala and its relation to groundwater from tritium and stable isotope data. J. Hydrol. 11: 47-58.

Peeters, F., Kipfer, R., Hohmann, R., Hofer, M., Imboden, D.M., Kodenev, G.G., and Khozder, T., 1997. Modeling transport rates in Lake Bajkal: Gas exchange and deep water reneval. Environ. Sci. Technol. 31: 2979-2982.

Peeters, F., Kipfer, R., Achermann, D., Hofer, M., Aeschbach-Hertig, W., Beyerle, U., Imboden, D.M., Rozanski, K. and Froehlich, K., 2000. Deep-Sea Research I, 47**:** 621-654.

Phillips, F.M., Person, M.A. and Muller, A.B., 1986. A numerical lumped-parameter model for simulating the isotopic evolution of closed-basin lakes. J. Hydrol. 85: 73-86.

Quay, P.D., Broecker, W.S., Hesslein, R.H. and Schindler, D.W., 1980. Vertical diffusion rates determined by tritium tracer experiments in the thermocline and hypolimnion of two lakes. Limn. Oceanogr. 25: 201-218.

Ramspacher, P., Zojer, H., Fröhlich, K. and Stichler, W., 1992. The recharge of late springs from a carbonate aquifer near Innsbruck, applying environmental tracers. In: Tracer Hydrology (Hötzl and Werner, eds.). Balkema, Rotterdam: 251-257.

Rank, D., Adler, A., Araguás-Araguás, L., Froehlich, K., Rozanski, K., Stichler, W., 1998. Hydrological parameters and climatic signals derived from long term tritium and stable isotope time series of the river Danube. In: Isotope Techniques in the Study of Environmental Change, International Atomic Energy Agency, Vienna, 191-205.

Redfield, A. and Friedman, I., 1965. Factors affecting the distribution of deuterium in ocean. In: Symposium on Marine Geochemistry. Univ. Rhode Isl. Occas. Publ. 3: 149-168.

Remeda, V.H., Cherry, J.A., Edwards, T.W.D., 1993. Oxygen isotope variations in clay aquitards in the western glaciated plains of North America. In: Isotope techniques in the Study of Past and Current Environmental Changes in the Hydrosphere and the Atmosphere, IAEA, Vienna: 381-395.

Robinson, R.A. and Stokes, R.U., 1959. Electrolyte Solutions. Butterworths, London (1959): 559 pp.

Roldão, J., Lopes, N., Stichler, W., and Zuber, A., 1989. Artificial and environmental tracers in the study of leakage under a dike of the Samuel reservoir, Porto Velho, Brazil. In: Isotope Hydrology Investigations in Latin America, IAEA, Vienna, TECDOC 502: 103-111.

Rozanski, K., Sonntag, C. and Münnich, K.O., 1982. Factors controlling stable isotope composition of modern European precipitation. Tellus 34: 142-150.

Rozanski, K., 1987. Oxygen-18 and Deuterium in Atmospheric Part of Hydrological Cycle. Sci. Bull. Univ. Mining & Metallurgy, No.1098, Krakow: 7-101.

Rozanski, K., Araguás-Araguás, L. and Gonfiantini, R., 1993. Isotopic patterns in modern global precipitation. In: Climate Change in Continental Isotopic Records, Geophysical Monograph 78, American Geophysical Union, 1-36.

Sacket, W.M. and Moore, W.S., 1966. Isotopic variations of dissolved inorganic carbon. Chem. Geol. 1: 323-328.

Schlosser, P., Shapiro, S.D., Stute, M., Aeschbach-Hertig, W., Plummer, N. and Busenberg, E., 1998. Tritium/^{3}He measurements in young groundwater. In: Proc. Isotope Techniques in the Study of Environmental Change, IAEA, Vienna: 165-189.

Schoch-Fischer, H., Rozanski, K., Jacob, H., Sonntag, C., Jouzel, J., Östlund, G. and Geyh, M.A., 1984. Hydrometeorological factors controlling the time variation of D, ^{18}O and ^{3}H in atmospheric water vapour and precipitation in the northern westwind belt. In: Isotope Hydrology 1983. Proc. IAEA Conf., Vienna: 3-31.

Schotterer, U., Froehlich, K., Stichler, W., Trimborn, P., 1993. Temporal variation of ^{18}O and deuterium excess in precipitation, river and spring waters in Alpine regions of Switzerland. In: Isotope Techniques in the Study of Past and Current Environmental Changes in the Hydrosphere and the Atmosphere. Proc. IAEA Symp., Vienna: 53-64.

Schrag, P.D., Hampt, G., Murray, D.W., 1996. Pore fluid constraints on the temperature and oxygen isotopic composition of the glacial ocean. Science 272: 1930-1932.

Sene, K.J., Gash, J.H.C. and McNeil, D.D., 1991. Evaporation from a tropical lake: comparison of theory with direct measurements. J. Hydrol. 127: 193-217.

Shackleton, N.J., 1987. Oxygen isotopes, ice volume and sea level. Quatern. Sci. Rev. 6: 183-190.

Siegenthaler, U. and Matter, H., 1983. Dependence of δ^{18}O and δD in precipitation on climate. In: Palaeoclimate and Palaeowaters: A Collection of Environmental Isotope Studies, IAEA, Vienna: 37-51.

Siegenthaler, U., Eicher, U. and H. Oeschger, 1984. Lake sediments as continental δ^{18}O records from the glacial/post-glacial transition. Annals of Glaciology 5: 149-152.

Simpson, H.J. and Herczeg, A.L., 1991. Stable Isotopes as an Indicator of Evaporation in the River Murray, Australia. Water Res. Resour., 27:1925-1935.

Simpson, H.J., Cane, M.A., Herczeg, A.L., Zebiak, S.E. and Simpson, J.F., 1993. Annual river discharge in South-eastern Australia related to El Nino-Southern Oscillation forecasts of sea surface temperatures. Water Resources Res. 29 (11): 3671-3680.

Sofer, Z. and Gat, J.R., 1972. Activities and concentrations of oxygen-18 in concentrated aqueous salt solutions: analytical and geophysical implications. Earth Planet. Sci. Lett. 15: 232-238.

Sofer, Z. and Gat, J.R., 1975. The isotope composition of evaporating brines: effect on the isotopic activity ratio in saline solutions. Earth Planet. Sci. Lett. 26: 179-186.

Solomon, D.K., Cook, P.G. and Sanford, W.E., 1998. Dissolved gases in subsurface hydrology. In: Isotope Tracers in Catchment Hydrology, (C. Kendall and J.J. McDonnell, eds.). Elsevier: 291-313.

Solomon, D.K. and Cook, P.G., 2000. ^{3}H and ^{3}He. In: Environmental Tracers in Subsurface Hydrology (P.G.Cook and A.L.Herzeg, eds.). Kluwer Academic Publishers, Dordrecht/Boston/London: 397-425.

Stauffer, R.E., 1985. Use of solute released tracers by weathering to estimate groundwater inflow to seepage lakes. Environ. Sci. Technol. 19: 405-411.

Stichler, W. and Herrmann, A., 1978. Verwendung von Sauerstoff-18-Messungen für hydrologische Bilanzierungen. Deutsche Gewässerkundliche Mitt. 22, Heft 1: 9-13.

Stichler, W., Maloszewski, P., Bertleff, B., Trapp, Ch., Watzel, R. and Weinsziehr, R., 1999. Modeling of lake – groundwater interaction based on environmental isotope data. Proc. IAEA Int. Symposium on Isotope Techniques in Water Resources Development and Management, Vienna 10-14 May, 1999: CD-ROM.

Stuiver, M., 1970. Oxygen and carbon isotope ratios of freshwater carbonates as climatic indicators. J. Geophys. Res. 75: 5247-5257.

Tan, F.C., 1989. Stable carbon isotopes in dissolved inorganic carbon in marine and estuarine environments. In: Handbook of Environmental Isotope Geochemistry, Vol.III: the Marine Environment A (P.Fritz and J.Ch.Fontes, eds.). Elsevier Science Publ. Amsterdam, New York: 171-190.

Torgersen, T., Top, Z., Clarke, W.B., Jenkins, W.J. and Broecker, W.S., 1977. A new method for physical limnology. Tritium-helium-3 ages: results from Lakes Erie, Huron and Ontario. Limnol. Oceanogr. 22: 181-193.

Torgersen, T., Clarke, W.B. and Jenkins, W.J., 1978. The tritium/helium-3 method in hydrology. In: Isotope Hydrology 1978, IAEA, Vienna: 917-930.

Truesdell, A.H., 1974. Oxygen isotope activities and concentrations in aqueous salt solutions at elevated temperatures: consequences for isotope geochemistry. Earth Planet. Sci. Lett. 23: 387-396.

Vaikmae, R., Kaup, E., Martma, T., Savitski, L., Vallner, L., 1999. Identification of glacial meltwater in the cambrian-vendian aquifer system (north Estonia) using isotope composition of groundwater. In: Isotope techniques in Water resources Development and Management. IAEA, Vienna: 189-190.

Vogt, H.J., 1978. Isotopentrennung bei der Verdünstung von Wasser. Thesis, Institute of Environmental Physics, University of Heidelberg.

Vrbka, P., Jacob., H., Froehlich, K. and Salih., M., 1993. Identification of Groundwater Recharge Sources in Northern Sudan by Environmental Isotopes. Journal of Environmental Hydrology 1 (4):98-125.

Ward, A.D. and Elliot, W.J., 1995. Environmental Hydrology, CRC Lewis Publishers.

Weiss, W. and Roether,W., 1975. Der Tritiumabfluss des Rheins 1961-1973. Deutsche Gewässerkundliche Mitteilungen 19: 1-5.

Weiss, W., 1979. Tritium and helium-3 studies in Lake Constance. In: Isotopes in Lake Studies, IAEA, Vienna: 227-231.

Yang, C., Telmer, K. and Veizer, J., 1996. Chemical dynamics of the St. Lawrence riverine system: $\delta^{18}O$, $\delta^{2}H$ and $\delta^{34}S$ and dissolved $^{87}Sr/^{86}Sr$. Geochim. Cosmochim. Acta 60: 851-866.

Yehdegho, B., Rozanski, K., Zojer, H. and Stichler, W., 1997. Interaction of dredging lakes with the adjacent groundwater field: an isotope study. J. Hydrol. 192: 247-270.

Yurtsever, Y., 1999. Use of environmental tritium to study catchment dynamics: case study from the Danube River basin. In: Leibundgut, C., McDonnell, J., Schultz, G. (Eds.), Integrated Methods in Catchment Hydrology – Tracer, Remote Sensing and New Hydrometric Techniques. IAHS Publication No. 258: 167-174.

Zimmermann, U., 1978. Isotopenhydrologie von Baggerseen, Steir. Beitr. Hydrogeol. 30: 139-167.

Zimmermann, U., 1979. Determination by stable isotopes of underground inflow and outflow and evaporation of young artificial groundwater lakes. In: Isotopes in Lake Studies, IAEA, Vienna: 87-94.

Zimmermann, U. and Ehhalt, D., 1970. The use of stable isotopes in the water balance of Lake Neusiedl – investigation on the reliability of the stable isotope method. In: Isotope Hydrology 1970. International Atomic Energy Agency, Vienna: 129-139.

Zuber, A., 1983. On the environmental isotope method for determining the water balance components of some lakes. J. Hydrol. 61: 409-427.

Zuber, A., 1986. Matchematical models for the interpretation of environmental radioisotopes in groundwater systems. In: Handbook of Environmental Isotope Geochemistry, (P. Fritz and J.Ch. Fontes, eds.), Volume 2, The Terrestrial Environment B., Elsevier Publ.Comp.: 1-55.

LITERATURE

H.Moser **W.Rauert**	**Isotopenmethoden in der Hydrologie** (1980) (in German language) ISBN 3-443-01012-1	Gebr. Borntraeger Berlin, Stuttgart
P.Fritz **J.Ch.Fontes**	**Handbook of Environmental Isotope** Publ. **Geochemistry** ISBN 0-444-41781-8	Elsevier Science Amsterdam, Oxford New York, Tokyo
	Vol.1. The Terrestrial Environment A (1980)	ISBN 0-444-41780-X
	Vol.2. The Terrestrial Environment B (1986)	ISBN 0-444-42225-0
	Vol.3. The Marine Environment A (1989)	ISBN 0-444-42764-3
F.J.Pearson e.a.	**Applied Isotope Hydrogeology**, a case study in Northern Switzerland (1991) ISBN 0-444-88983-3	Elsevier Science Publ. Amsterdam, Oxford, New York, Tokyo
I.Clark **P.Fritz**	**Environmental Isotopes in Hydrogeology** (1997) ISBN 1-56670-249-6	Lewis Publishers Boca Raton, New York
F.Gasse **Ch.Causse**	**Hydrology and Isotope Geochemistry** ISBN 2-7099-1377-1	Editions de l'Orstom Paris
W.Kaess	**Tracing in Hydrogeology** (1998) ISBN 3-443-01013-X	Balkema
C.Kendall **J.J.McDonnell**	**Isotopes in Catchment Hydrology** (1998) ISBN 0-444-50155-X	Elsevier/North Holland Publ.Comp. Amsterdam

E.Mazor	**Chemical and Isotopic Groundwater Hydrology – The applied approach** (1998) ISBN 0-8247-9803-1	Marcel Dekker Inc.
P.G.Cook **A.L.Herczeg** **(ed.)**	**Environmental Tracers in Subsurface Hydrology** (2000) ISBN 0-7923-7707-9	Kluwer Acad. Publ.
G.Friedlander **J.W.Kennedy** **E.S.Macias** **J.M.Miller**	**Nuclear and Radiochemistry** (1981) ISBN 0-471-86255-X	John Wiley & Sons New York, Chichester, Brisbane, Toronto
G.Faure	**Principles of Isotope Geology** (1986)	John Wiley & Sons
R.E. Criss	**Principles of Stable Isotope Distribution** ISBN 0-19-511775-1 (1999)	Oxford University Press

IAEA PUBLICATIONS

IAEA CONFERENCE PROCEEDINGS

1963 **Radioisotopes in Hydrology**, Tokyo, 5-9 March 1963, IAEA, Vienna, 459 pp. (STI/PUB/71) (out of print)

1967 **Isotopes in Hydrology**, Vienna, 14-18 November 1966, IAEA, Vienna, (in co-operation with IUGG), 740 pp. (STI/PUB/141) (out of print)

1970 **Isotope Hydrology**, Vienna, 6-13 March 1970, IAEA, Vienna, (in co-operation with UNESCO), 918 pp. (STI/PUB/255) (out of print)

1974 **Isotope Techniques in Groundwater Hydrology**, Vienna, 11-15 March 1974, IAEA, Vienna, 2 volumes: 504 and 500 pp. (STI/PUB/373) (out of print)

1979 **Isotope Hydrology** (in 2 volumes), Neuherberg, Germany, 19-23 June 1978, IAEA, Vienna, (in co-operation with UNESCO), 2 volumes of 984 pp. (STI/PUB/493) ISBN 92-0-040079-5 and ISBN 92-0-040179-1

1983 **Isotope Hydrology**, Vienna, 12-16 September 1983, IAEA, Vienna, (in co-operation with UNESCO), 873 pp. (STI/PUB/650) ISBN 92-0-040084-1

1987 **Isotope Techniques in Water Resources Development**, Vienna, 30 March-3 April 1987, IAEA, Vienna, (in co-operation with UNESCO), 815 pp. (STI/PUB/757) ISBN 92-0-040087-6

1992 **Isotope Techniques in Water Resources Development**, Vienna, 11-15 March 1991, IAEA, Vienna, (in co-operation with UNESCO), 790 pp.(STI/PUB/875) ISBN 92-0-000192-0

1993 **Isotope Techniques in the Study of Past and Current Environmental Changes in the Hydrosphere and the Atmosphere,** Vienna, 19-23 April 1993, IAEA, Vienna, 624 pp. (STI/PUB/908) ISBN 92-0-103293-5

1995 **Isotopes in Water Resources Management** (in 2 volumes), IAEA, Vienna, 20-24 March 1995, IAEA, Vienna, 2 volumes: 530 and 463 pp. (STI/PUB/970) ISBN 92-0-105595-1 and 92-0-100796-5

1998 **Isotope Techniques in the Study of Environmental Change**, Vienna, 14-18 April 1997, IAEA, Vienna, 932 pp. (STI/PUB/1024) ISBN 92-0-100598-9

1999 **Isotope Techniques in Water Resources Development and Management**, 10-14 May 1999, IAEA, Vienna, CDRom (IAEA-CSP-2/C) ISSN 1562-4153

SPECIAL IAEA SYMPOSIA

1967 **Radioactive Dating and Methods in Low-Level Counting,** Monaco, 2-10 March 1967, IAEA, Vienna, 744 pp. (STI/PUB/152) (out of print)

1979 **Behaviour of Tritium in the Environment,** San Fransisco, USA, 16-20 October 1978, 711 pp. (STI/PUB/498) ISBN 92-0-020079-6

1981 **Methods of Low-Level Counting and Spectrometry,** Berlin, Germany, 6-10 April 1981, IAEA, Vienna, 558 pp. (STI/PUB/592) (out of print)

IAEA REPORTS AND TECHNICAL DOCUMENTS (TECDOCS)

Environmental Isotope Data no.1 – no.10: World Survey of Isotope Concentration in Precipitation, Data from network of IAEA and WMO over period 1953-1991, published 1969-1994.

Interpretation of Environmental Isotope and Hydrochemical Data in Groundwater Hydrology, Proc. Adv. Group Meeting, Vienna, 27-31 January 1975, IAEA, Vienna, 1976, 230 pp. (STI/PUB/429) ISBN 92-0-141076-X

Isotopes in Lake Studies, Proc. Adv. Group Meeting, Vienna, 29 August-2 September 1977, IAEA, Vienna, 1979, 290 pp. ISBN 92-0-141179-0 (out of print)

Arid Zone Hydrology: Investigations with Isotope Techniques, Proc. Adv. Group Meeting, Vienna, 6-9 November 1978, IAEA, Vienna, 1980, 265 pp. (STI/PUB/547) ISBN 92-0-141180-4

Stable Isotope Standards and Intercalibration on Hydrology and Geochemistry, (R. Gonfiantini ed.), Report on Consultants' Meeting, Vienna, 8-10 September 1976, IAEA, Vienna, 1977.

Stable Isotope Hydrology Deuterium and Oxygen-18 in the Water Cycle, (J.R.Gat and R.Gonfiantini eds.), Monograph by Working Group, IAEA, Vienna, 1981, 340 pp. (STI/DOC/10/210)

Palaeoclimates and Palaeowaters: A Collection of Environmental Isotope Studies, Proc. Adv. Group Meeting, Vienna, 25-28 November 1980, IAEA, Vienna, 1981, 207 pp. (STI/PUB/621) ISBN 92-0-141083-2

Guidebook on Nuclear Techniques in Hydrology, by Working Group IAEA, Vienna, 1983, 439 pp. (STI/DOC/10/91/2)

Stable Isotope Reference Samples for Geochemical and Hydrological Investigations, (R. Gonfiantini ed.), Report by Advisory Group's Meeting, Vienna, 19-21 September 1983, IAEA, Vienna, 1984.

Stable and Radioactive Isotopes in the Study of the Unsaturated Soil Zone, Proc. Meeting on IAEA/GSF Progr., Vienna, 10-14 September 1984, IAEA, Vienna,1985, 184 pp. (TECDOC-357)

Isotope Techniques in the Study of the Hydrology of Fractured and Fissured Rocks, Proc. Adv. Group Meeting, Vienna, 17-21 November 1986, IAEA, Vienna, 1989, 306 pp. (STI/PUB/790)

Stable Isotope Reference Samples for Geochemical and Hydrological Investigations, Report on Consultants' Meeting, Vienna, 16-18 September 1985, edited by G. Hut, IAEA, Vienna, 1987.

Use of Artificial Tracers in Hydrology, Proc. Adv. Group Meeting, Vienna, 19-22 March 1990, IAEA, Vienna, 1990, 230 pp. (TECDOC-601)

C-14 Reference Materials for Radiocarbon Laboratories, (K. Rozanski, ed), Report on Consultants' Meeting, Vienna, 18-20 February 1981, IAEA, Vienna 1991.

Guidelines for Isotope Hydrology, Manuel for Operation of an Isotope Hydrology Laboratory IAEA, Vienna, 1999 (in prep.)

Isotopes of Noble Gases as Tracers in Environmental Studies, Report by Consultants' Meeting, Vienna, 29 May-2 June, 1989, IAEA, Vienna, 305 pp. (STU/PUB/859) (out of print) ISBN 92-0-100592-X

Statistical Treatment of Data on Environmental Isotopes in Precipitation, IAEA, Vienna, 1992, 781 pp. (STI/DOC/10/331)

Isotope and Geochemical Techniques applied to Geothermal Investigations, Proc. Res. Coord. Meeting, Vienna, 12-15 October 1993, IAEA, Vienna, 1995, 258 pp. (TECDOC-788)

Reference and Intercomparison Materials for Stable Isotopes of Light Elements, Proc. Cons. Meeting, Vienna, 1-3 December 1993, IAEA, Vienna, 1995. (TECDOC-825)

Manual on Mathematical Models in Hydrogeology, IAEA, Vienna, 1996, 107 pp. (TECDOC-910)

CONSTANTS

a	year = 3.1558×10^{7} s
amu	atomic mass unit = $1.660\ 54\times10^{-27}$ kg
c	velocity of light (in vacuum) = $2.997\ 925\times10^{8}$ $\mathrm{m{\cdot}s^{-1}}$
cal	calorie = 4.184 J
e	elementary/electron/proton charge = $1.602\ 18\times10^{-19}$ C
eV	electronvolt = $1.602\ 18\times10^{-19}$ J
g	acceleration of free fall = 9.806 65 $\mathrm{m{\cdot}s^{-2}}$
h	Planck constant = $6.626\ 08\times10^{-34}$ J·s
J	Joule = 0.2390 cal
k	Boltzmann constant = $1.380\ 54\times10^{-23}$ J/K
m_e	electron mass = $9.109\ 39\times10^{-31}$ kg
m_n	neutron mass = $1.674\ 93\times10^{-27}$ kg
m_p	proton mass = $1.672\ 62\times10^{-27}$ kg
M/E eq.	mass/energy equivalence: 1 amu ≡ 931.5 MeV
N_A	Avogadro constant = $6.022\ 14\times10^{23}$ $\mathrm{mol^{-1}}$
π	= 3.141 592 6535
R	gas constant = 8.314 51 $\mathrm{J{\cdot}K^{-1}{\cdot}mol^{-1}}$
T	thermodynamic temperature = t (^{0}C) + 273.15 K
V_m	molar volume (= 22.41 $\mathrm{L{\cdot}mole^{-1}}$ at STP)

SUBJECT INDEX